

UPPSALA
UNIVERSITET

UPTEC STS 14027
Examensarbete 30 hp
Augusti 2014

Design of an Alternative Frequency Controller for Hydropower Stations

Reducing the 60-second Floating in the Grid Frequency of the Nordic Power System

Camilla Odelbrink

UPPSALA
UNIVERSITET

Teknisk- naturvetenskaplig fakultet
UTH-enheten

Besöksadress:
Ångströmlaboratoriet
Lägerhyddsvägen 1
Hus 4, Plan 0

Postadress:
Box 536
751 21 Uppsala

Telefon:
018 – 471 30 03

Telefax:
018 – 471 30 00

Hemsida:
http://www.teknat.uu.se/student

Abstract

Design of an Alternative Frequency Controller for Hydropower Stations

Camilla Odelbrink

A periodic oscillation in the grid frequency of the Nordic power system has been observed. The oscillations, also denoted as a floating, have periods of about 60 to 90 seconds. The reason for the floating is not fully known, and the strength of the floating has been increasing during the last years. It is assumed that the floating causes an undesired wear of the systems frequency control equipment.

The aim of the study was to research the possibility of a new control structure in primary frequency controlling hydropower units. The purpose of the new modified control structure was to dampen the grid frequency floating. The modified design of the controller was conditioned to be implemented in a smaller fraction of all regulating hydropower stations in the Nordic power system. This smaller fraction has here been assumed to 10 %.

The new structure of the modified controller was designed as a leadlag-filter, where a shape was assumed as to give the filter high energy in the frequency range of focus. The parameters of the leadlag-filter were determined according to a set of criteria, including damping ability, stability margins and preconditions on the control signals from the modified system.

The study showed that a leadlag-filter could be constructed so that a periodic grid frequency floating with periods of 60-90 seconds would be significantly reduced in amplitude. The reduction of the floating did not necessarily require more generated power compared to the current system, though the modified plants did deliver most of the power. Both reduction of the amplitude of the floating and amount of required power depended on the amplitude and frequency of the disturbance causing the floating.

Handledare: Jonas Funkquist & Jonas Persson
Ämnesgranskare: Bengt Carlsson
Examinator: Elísabet Andrésdóttír
ISSN: 1650-8319, UPTEC STS14 027

Populärvetenskaplig sammanfattning

En periodisk svängning hos den nordiska nätfrekvensen har observerats och orsaken till svängningen är inte helt känt. Svängningens, även kallad svävning, periodtid ligger omkring 60 till 90 sekunder och det antas att denna svävning orsakar oönskat slitage utav frekvensreglerande apparatur. Frekvensreglerande verk består främst av vattenkraftsverk.

Studiens syfte var att undersöka möjligheten till en ny regulatorstruktur i primärreglerande vattenkraftsverk. Målsättningen för den nya regulatorstrukturen var att dämpa frekvenssvävningen mer än den nuvarande regulatorstrukturen gör. Den nya formen av reglering skulle implementeras i en mindre andel av alla primärreglerande vattenkraftsverk i norden. Denna andel antogs i studien till 10 %.

Den nya regulatorstrukturen var designad som ett leadlag-filter, ett vanligt förekommande filter inom klassisk reglerteknik. Filters parametrar ställdes in med hjälp av ett antal kriterier, såsom dämpningsförmåga och stabilitetsmarginal samt begränsningar gällande systemets styrsignaler.

Studien visade att leadlag-filtret kunde utformas så att en periodisk frekvenssvävning minskade avsevärt i amplitud. Mängden effekt som krävdes för att minska svävningens amplitud var inte nödvändigtvis större än den som det nuvarande systemet använder, dock kom större delen av effekt från andelen med den nya formen av reglering. Hur mycket effekt kom krävdes för att minska svävningens amplitud berodde både på amplitud och frekvens hos den störning som orsakade svävningen.

Acknowledgements

The work of my Master's Thesis would not have been possible without the help of others whom I would like to acknowledge.

I would like to express my deepest appreciation to Jonas Funkquist and Jonas Persson, my supervisors at Vattenfall. Your advice and assistance have been essential throughout this work. Together with the additional staff at Vattenfall R&D, you have all given me great support and encouragement.

I also wish to thank Bengt Carlsson, my supervisor at Uppsala University, for his enthusiasm regarding this project. His professional guidance has been of great value to me.

A special thanks to Linn Saarinen, whom with great generosity shared with me her own studies, time, and support, answering the many questions I presented to her.

I would also like to express my gratitude towards fellow master thesis students at Vattenfall R&D together with fellow student and dear friend Sara Johansson, for letting me continuously repeat the matters of my thesis.

Finally, I wish to thank my husband Emil and children Liam, Måns, and Nora for your endless love and support. What would I have done without you?

To all, my profoundest thank you.

Camilla Odelbrink
Uppsala, Sweden
June, 2014

Table of content

1 Introduction 1

1.1 Project Description 2

2 Previous Research 2

3 Background 3

3.1 Electrical Frequency 3

3.2 Frequency Control 4

3.2.1 Primary Frequency Control 4

3.2.2 Secondary Frequency Control 5

3.3 Hydropower 6

3.3.1 Hydropower as Frequency Control 6

4 Modelling and Control Design 7

4.1 System Model 7

4.1.1 Governor – the Current Frequency Controller 8

4.1.2 Model Parameters 10

4.2 System Model with Modified Control 12

4.2.1 Modified Frequency Controller 13

4.2.2 Modified Model Parameters 14

4.3 Method of Analysis 17

4.3.1 Frequency Domain Analysis 17

4.3.2 Time Domain analysis 20

4.3.3 Robustness Analysis 20

4.3.4 Course of Controller Design and Performance analysis 21

5 Simulations and Results 22

5.1 Simulations with the Current Control 23

5.1.1 Frequency Domain 23

5.1.2 Time Domain 27

5.2 Simulations with the Modified Control 28

5.2.1 Frequency Domain 28

5.2.2 Time Domain 35

6 Discussion 41

7 Conclusions 42

8 Suggestions for Future Work 43

References 44

Appendices

		Number of pages
APPENDIX A	System Model Parameters	2
APPENDIX B	Simulink Models	1
APPENDIX C	Compiled Data Excel files	1
APPENDIX D	Additional Analysis Results EP0	2
APPENDIX E	Analysis Results EP1	6
APPENDIX F	Analysis Results EP2	6
APPENDIX G	Analysis Results EP3	6

1 Introduction

As illustrated in Figure 1-1, a slow floating in the grid frequency is often observed, where the reason for the floating is not fully understood. The term floating is used to denote a periodic oscillation of the grid frequency. The floating has a period of about 60 to 90 seconds and the strength of the floating is increasing by the year. Since deviations in the grid frequency will cause the primary frequency control generators to activate, it is assumed that the floating causes an undesired wear of the systems equipment. Primary frequency control generators are mainly hydropower generators [21].

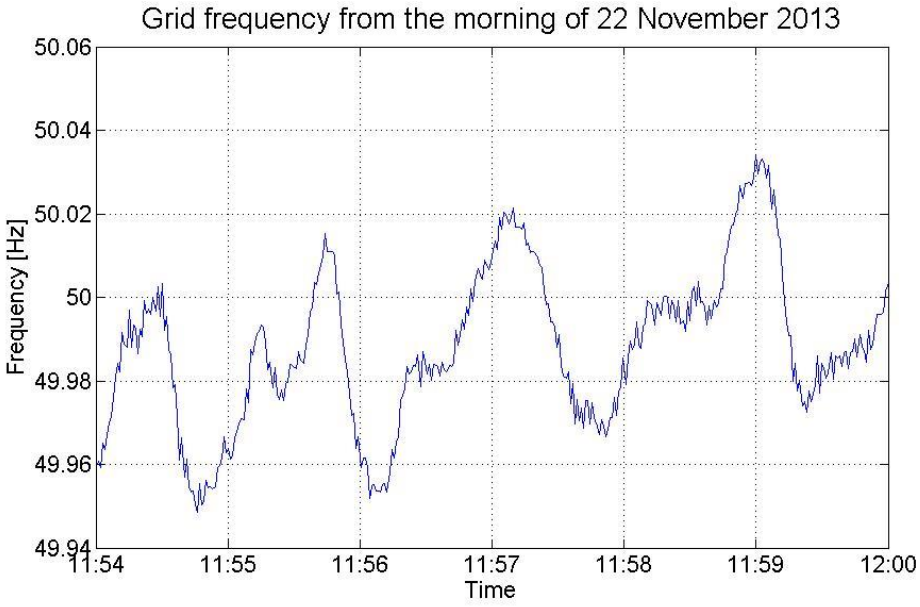


Figure 1-1: Five minutes of the Nordic power grid frequency from the morning of 22 November 2013.

It has also been observed how the general frequency quality (going under 49.9 or over 50.1 Hz) has deteriorated during the same time period that the floating has increased. This can be viewed as being connected and therefore it is believed that the frequency floating is deteriorating the overall frequency quality [1].

Previous studies have shown that load disturbances, power variations, with a *periodic oscillation* will generate relative large frequency deviations, even if the power amplitude is quite small. Therefore it can be assumed that a periodic frequency floating negatively contributes to the unbalance of the grid frequency [11].

As the grid frequency floating may result in the primary frequency control being used unduly and thereby increasing the wear of the controlling units, it would be beneficiary to find a way of damping the floating. If a new form of controlling were to be implemented, could this possibly decrease the floating? What could that new controlling structure be, and how much would the floating be reduced?

1.1 Project Description

The aim of the study was to investigate the possibility of a new control structure in primary frequency controlling hydropower units. The purpose of the new modified control structure was to dampen the grid frequency floating with time periods of about 60 to 90 seconds. By decreasing the floating, the wear of primary frequency controlling units is assumed to be reduced and the quality of the grid frequency increased. The modified design of controller was conditioned to be implemented in a smaller fraction of all regulating hydropower stations in the Nordic power system.

2 Previous Research

In a report from Fingrid, the Finnish equivalent to Swedish Svenska Kraftnät, the nature of the 60-second frequency floating in the Nordic power system is studied [17]. The study uses data from the years of 2008 to 2011, but the results focus mainly on 2011. The report states that it is clear that the frequency floating increases the time outside the normal frequency band of 49.9-50.1 Hz, which in turn impairs the quality of the grid frequency and increases the need for frequency control power. It also states that the frequency floating has slightly been increasing from 2008 to 2011 [17].

By filtering grid frequency data, different characteristics and trends were distinguished. Yearly variations were identified that shows how the amount of floating is higher during the summer months, with exception of the month of July. It is also stated that there is a relation between the amount of oscillations and energy production. When the production is high, during the winter months, the amounts of oscillations are lower and the other way around, the amounts of oscillations are higher when the production is low. Weekly variations shows slightly higher amount of oscillation during weekdays and smaller amounts during the weekends. No evident variations due to day and night time could be identified, though a clear increase of floating during change of hour is observed. During change of hour sudden drops or rises in the grid frequency is common, due to balance control [17], [12].

The period of the floating varies without any clear trend for the year, week or day. The median of the period is about 50-55 seconds and the majority of periods lies within 40-80 seconds [17].

In 2011 the median of the amplitude of the oscillations were 0.02-0.0225 Hz and the majority of the amplitudes were in the area of 0.015-0.030 Hz. There is a clear connection between amounts of oscillations and the amplitude of the oscillations. When there is a higher amount of oscillations, the amplitudes of the oscillations are also higher [17].

Several experiments have been performed with the purpose of studying the 60-second floating in the Nordic systems grid frequency. One of these experiments was performed in the Messaure power station on October 30-31 2013. Two power units were used to generate a sinusoidal power signal, with period time 40 s, 60 s, and 100 s, that was fed into the grid. The amplitude of the signal lay between 38 MW and 72 MW. The responding grid frequency was periodic with amplitude between 18 to 32 mHz [1].

The purpose of the test was to study the dynamics of the system, such as the turbine and the controller. The findings of the tests include the fact that rather small periodic power oscillations will create rather big periodic frequency oscillations [1]. Other results from the test include confirming the theories connected to hydropower units, where theory and the measurements show agreement [20].

In 2008 an oscillation problem was observed in the power system in Colombia. Unlike the oscillations in the Nordic power systems, these where low frequency periodic oscillations of about 0.06 Hz, or 17 s period time. In this case a hydro power plant that was contributing to the frequency oscillations could be located. In the study of the oscillations it was established that the models used for analysis of the plants were inadequate and that the parametric settings used needed to be adjusted. Measurements were performed to create new models and new parametric settings were tested to reduce the low frequency disturbance. The study stated that especially the integrating time constant had an effect on the oscillations and by increasing this, the frequency stability was improved [4].

3 Background

To fully understand the phenomena described in the previous sections, several concepts are in need of clarification. In this chapter a brief background on electrical frequency, frequency control and hydropower is given.

3.1 Electrical Frequency

Every synchronous system has an electrical frequency linked to the oscillations of the alternating current (AC) transmitting through the system. A synchronous system is defined as a system where every producer and consumer is connected through transformers and AC lines. Within the synchronous system there is a balance of the electrical frequency as the frequency is, on average, the same throughout the system [18].

Frequency balance is connected to power balance, where power balance means that produced and consumed power corresponds. When produced power is equal to consumed power including losses, the electrical frequency will be kept constant. If the production exceeds or is less than the consumption, the frequency will start to deviate. When the production is lower than the consumption the frequency will drop, and the other way around the frequency will rise as the production exceeds consumption [18]. A highly fluctuating frequency with a large deviation from the nominal value may cause damage and is not acceptable, and therefore the frequency must be kept stable [3]. Frequency is stabilized through frequency control. Different power systems regulate the frequency in different ways.

The Swedish electrical grid is connected with Norway, Finland and (east) Denmark and forms a joint synchronous system, the Nordic power system. The nominal frequency in the Nordic system is 50.0 Hz [7].

3.2 Frequency Control

In a power plant the generator converts mechanical energy to electrical energy. Within a generator there are a number of regulators with different assignments. One of these regulators operates the turbine, adjusting the flow of mechanical energy to a desired level. This process can be connected such that the flow of mechanical energy produces a frequency corresponding to the set limits. This is called frequency control. In the Nordic power system those set limits are 49.9-50.1 Hz and the transmission system operators (TSO's) in each country are responsible for the balance of the frequency. Svenska Kraftnät is the Swedish TSO and has the responsibility for production and consumption balance. This is achieved by purchasing frequency control power from producers [3],[24].

The rotating component in a generator is called a rotor. At stationary operating mode the rotor rotates with a number of revolutions that corresponds to the power grids electrical frequency. If the consumption of electrical power exceeds the production, the rotor will slow down as more energy is taken out of the generator. This is how stored kinetic energy is used to replace the shortfall in the grid. The stored energy, which is due to inertia in the machines, is however limited. When the rotor speed is reduced the frequency will fall and therefore more energy will be produced to cancel the reduction and regain balance of the frequency. In the Nordic power system this is done by two steps, primary and secondary frequency control [3].

3.2.1 Primary Frequency Control

Primary frequency control has the ability to respond to sudden changes in the power consumption and/or production. As described above, balance between production and consumption in the power grid will give a balanced grid frequency. The balance is maintained as energy is taken from the stored reserves in the synchronous machines. Through an increased consumption, taking more electrical energy out of the generator than mechanical energy is supplied by the turbine, the acceleration of the generators rotor descends resulting in a decrease in the electrical frequency. As frequency drops production is increased which is done through primary frequency control [18].

The increase of production is relative to the so called *regulation strength*, R. The regulation strength is the slope of the frequency versus production-curve. In other words, how big the power plants pull is when the frequency falls. The unit for R is MW/Hz as it tells how much power will be produced relative the frequency deviation. The same is valid for the other way around, when production exceeds consumption and the grid frequency increases the production will decrease relative to R. The relation for difference in produced power through primary frequency control and the grid frequency is

$$\Delta p = -R \cdot \Delta f \tag{1}$$

where Δp is the change in power production and Δf is the frequency deviation. The negative sign represents that negative frequency deviation will result in an increased power production [9].

To be able to produce power for primary frequency control one must have a reserve that can be activated when needed, that is when the frequency varies. For normal operation this is called FCR-N (Frequency Containment Reserves, Normal) and shall be at least ±600 MW in the Nordic power system. The primary frequency regulation is designed to react to sudden changes in the grid frequency within normal operating limits. These limits are 49.9-50.1 Hz and therefore a frequency deviation within ±0.1 Hz will activate the FCR-N. This reserve is activated according to the regulation strength. With a 0.1 Hz frequency deviation, 63 % of the regulating strength should be activated within 60 seconds and 100 % within 3 minutes. With a reserve of 600 MW for a frequency deviation of 0.1 Hz the regulation strength in the Nordic power system will be 6000 MW/Hz [6], [18].

Plants involved in the regulation will vary how much they will regulate at a frequency deviation depending on the setting of *EP*. The EP mode will determine how much of the machines' rated power that will be produced for regulation in %/Hz. There are four different EP modes: EP0, EP1, EP2, and EP3. EP0 delivers 20% of rated power per deviating Hz, EP1 delivers 50%/Hz, EP2 100%/Hz, and EP3 200%/Hz [21]. More on EP modes can be found in section 4.1.1.

As long as the frequency is decreasing the production will increase until balance is regained and a new stationary position is reached. Primary frequency control results in a new stationary position of the frequency that differs from the nominal value, a steady state error. This is due to that primary frequency control is executed by a P-controller, see section 4.1.1. Therefore additional power must be added so that the frequency reaches its set-point value of 50 Hz. This is done by *secondary frequency control* [18].

3.2.2 Secondary Frequency Control

Primary frequency control is activated when there is an unbalance between produced and consumed power as measured by the grid frequency. When primary frequency control has been activated the frequency will have a new steady-state level that differs from its nominal value of 50.0 Hz. There is also the issue of depleted reserves to handle new instabilities which is managed by secondary frequency control. The aim of secondary frequency control is thus to restore the frequency to its nominal value after a deviation and replace the used primary reserve if a new frequency drop will happen [18]. Secondary frequency control has other purposes as well, but as this report first and foremost deals with primary frequency control, other uses will fall outside the aim of this report. This is also the case for other types of control, and therefore the reader should be advised that the control mentioned in the rest of this report refers to primary frequency control, if nothing else is explicitly stated.

To summarize, if the consumption increases or the production decreases the frequency will fall when the stored kinetic energy in the rotating masses is used instead. As a response, the primary frequency control will be activated and stabilize the frequency to a new steady-state level. If that level differs from the nominal value, the secondary frequency control will be activated to restore the frequency level [18].

3.3 Hydropower

Hydropower is produced from water by letting flowing water pass through a turbine. The turbine will rotate as a reaction to the flowing water, and by connecting the turbine to a generator; the kinetic energy can be used to produce electrical energy. By storing the water in large dams, the outtake of power can be regulated [25].

Figure 3-1 shows an illustration of a hydropower plant layout. The dams keep the water in a reservoir to create needed falling height, called head. The water passes through the waterways setting the turbine in motion. The rotation of the turbine is turned into electrical energy by the generator, and then the voltage is regulated by the transformer to an appropriate level for the power grid [25].

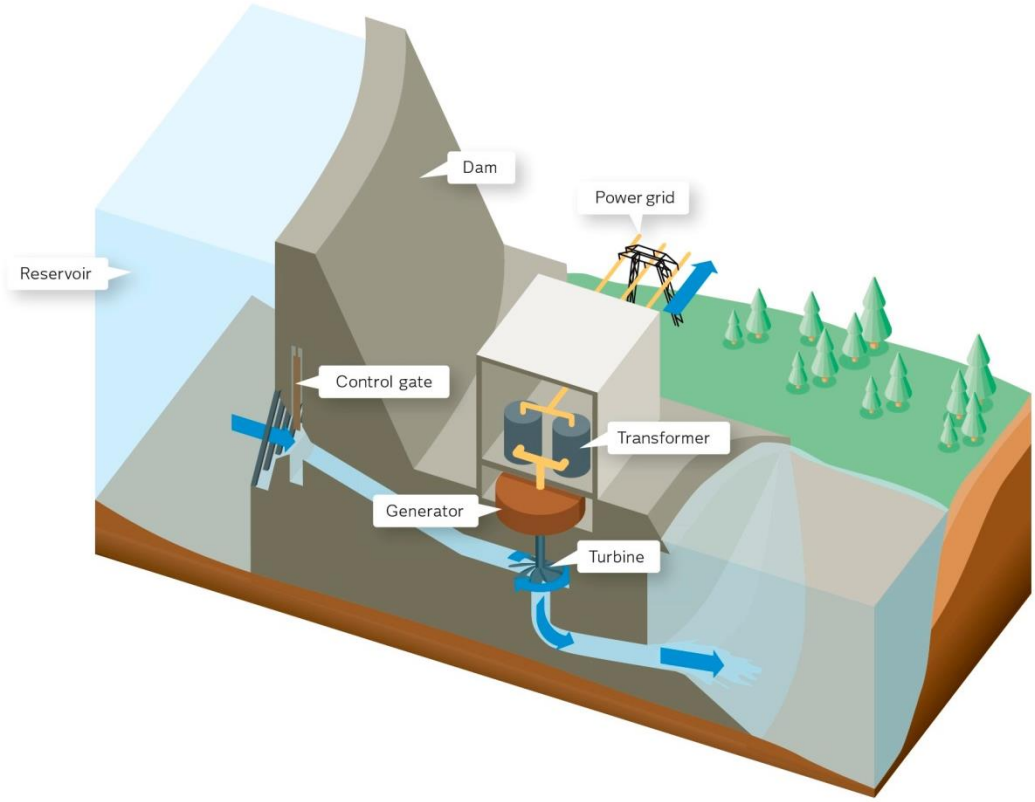


Figure 3-1: Layout of a hydropower plant. Image source: Vattenfall's media bank.

Every power plant is unique in the sense that the water flow to the reservoir, size of reservoir, head, waterways and other circumstances differs. There are also different turbine types used, depending on size of head [16].

3.3.1 Hydropower as Frequency Control

In the Nordic power system mostly hydropower is used as regulating power [6]. Hydropower plants are used for frequency regulation which is controlled by a governor. The governor, also called controller, shall maintain the grid frequency and the balance between consumed and produced power, as discussed in section 3.2 [16]. In this study, frequency controllers of hydropower plants active in primary frequency control are of interest.

A hydropower facility consists of, in simplified terms, a governor as well as a plant. The governor is the controlling unit which takes the frequency variation, Δf, as input and the output is a control signal Y of how the vane openings in the water ways of the turbine much change to remove the frequency variations. This control signal is then the input to the plant where the action is carried out: the vane openings shift, the selected amount of water flows through the turbine and power is thereby generated. This power in turn is fed to the grid where it is consumed. If the amount of power generated does not meets the amount of power consumed the grid frequency will fluctuate. The frequency deviation will be used as an input signal to the governor and the regulation continues [16].

4 Modelling and Control Design

The following sections have the purpose of defining the systems of interest, how they are modelled and how the design of the new controller is performed. First the current system model with all its units is described followed by the modified model and thereafter the method of analysis.

4.1 System Model

The system of interest for this report is defined as consisting of hydropower facilities active in the primary frequency control and the Nordic power grid. All these hydropower stations in the Nordic power system are represented as one unit. The different facilities may have different characteristics, such as different time constants, different water ways, and so on, but for this work they are all considered identical. The consequences of this simplification are addressed later in the report.

Figure 4-1shows a representation of the system. f_{ref} is the reference frequency, which in the Nordic power system is 50 Hz. The reference frequency minus the actual grid frequency f tells how much the frequency is differing, Δf. The control signal Y indicates how much the vane openings in the plant will change (unit percent). The output of the plant, P, is real power which goes into the grid and results in the grid frequency, f. The grid in Figure 4-1 represents the entire Nordic power grid with all its connected components.

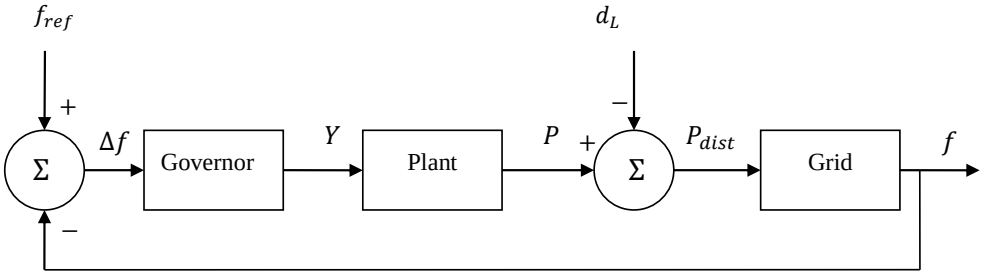


Figure 4-1: System model.

The power consumption in the grid is an input to the system that cannot be controlled and is therefore considered a disturbance signal. Consequently, a load disturbance d_L is added to the model.

Each block in the system model is described by transfer functions that have been defined to represent the relation between input and output.

The grid takes power as input and delivers frequency as output. This relationship is described by the following transfer function

$$G_{Grid}(s) = \frac{1}{M \cdot s + D} \tag{2}$$

where M refers to the grids inertia and D, which acts as a small damping constant, refers to the frequency dependence of the component parts in the grid [8].

The plant, which takes guide vane opening in percent as input and delivers power as output, is expressed as

$$G_{Plant}(s) = \frac{-T_w \cdot s + 1}{\frac{T_w}{2} \cdot s + 1} \tag{3}$$

The time constant T_w is related to the time it takes for the water to move through the waterways of the plant. As is apparent by the transfer function above, equation (3), this is of non-minimum phase, as the zero is in the right half plane. This represents the fact that after the guide vane opening is increased to produce more power, it initially delivers a lower amount of power before the desired amount can be reached. This is due to lowered pressures and water accelerations [8], [19], [20].

4.1.1 Governor – the Current Frequency Controller

The governor-block in Figure 4-1 represents the frequency controller of the hydropower plant with some internal characteristics such as delay and permanent speed droop. The structure of the controller that is used in Swedish hydropower plants today is partly of PI-type. A PI-controller consist of a proportional (P) and a integrating (I) part, hence the name PI. The controller as well as internal delay and a feedback of the EP, droop, are parts of the governor-block which is visualized in Figure 4-2.

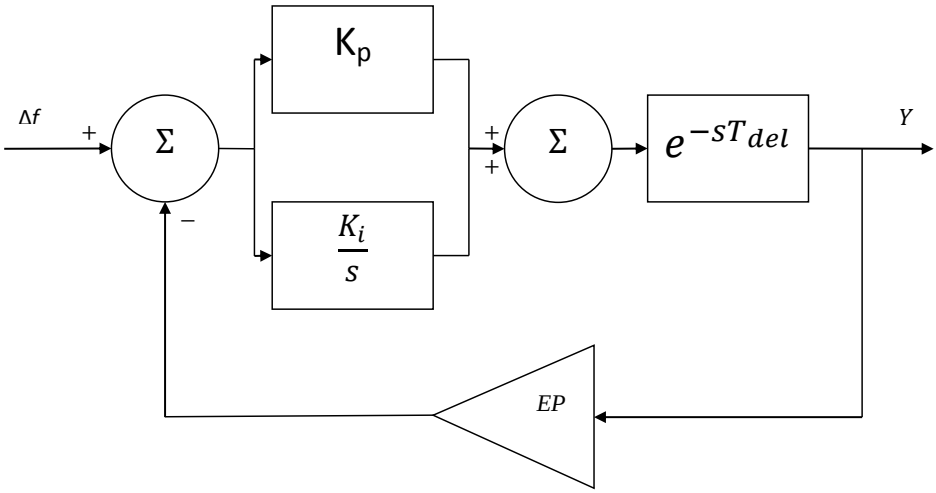


Figure 4-2: The system controller. The controller is partly of PI-type with the addition of a feedback of the EP as well as a time delay.

A **PI-controller** consists of the sum of two parts with a proportional and an integrative term. The ideal PI-controller is describe with the following equation:

$$u(t) = K_P e(t) + K_I \int_0^t e(\tau) d\tau \tag{4}$$

where

K_P: proportional gain

K_I: integral gain

$e(t)$: the error between reference and output signal

The proportional term uses the error to construct the control signal to linearly correct the output. As the proportional part of the controller is driven by the error in the feedback-loop (difference between the reference signal and the output signal), a steady state error will occur [10].

The integral term is proportional to the integral of the error and will therefor eliminate the steady state error [10]. In this case though, due to droop and delay, this is not a true PI-controller. With no pure integration a steady state error will remain - hence the need for secondary frequency control.

Due to the hydraulic and mechanical devices that convert the opening control signal Y to actual opening, there is a delay in the system. This is modelled by a **delay function** with a time delay T_{del} [19], [20]. This delay represents all the mechanical devises in the plant and how they delay the signal as it moves through this part of the system.

Droop is the feedback loop with **EP** as gain. EP is the inverse of the regulation strength in percent of rated power, unit [Hz/%]. For the four different EP modes mentioned in

section 3.2.1, the percentage increase or decrease of for example 20%/Hz in EP0 corresponds to an EP value of 0.05 Hz/%.

As the total of regulating strength in the Nordic power system should amount to at least 600 MW for normal operating state, the sum of regulating machines that are needed depends on which EP-settings are being used. The EP mode is set for each single machine [6]. As the simplified model of the system that is used in this report assumes all regulating machines to be one, using for example the EP3-mode would mean that all machines are regulating at full speed. If this was to be the case, not all regulating machines would be in use. Instead, a fraction of all machines would be used to deliver the regulating strength of 600MW. Therefore a **fraction** block is added to the model of the system. This block is visible in Figure 4-3. The fraction depends on the chosen EP mode.

4.1.2 Model Parameters

The model defined above is per unit-based. The per unit-system is a way of simplifying power system calculations, where power quantities are related to a base and expressed in per unit of that base. The per unit-value of a quantity is calculated as

$$per\ unit\ quantity = \frac{actual\ value\ of\ quantity}{base\ value\ of\ quantity} \tag{5}$$

where the actual quantity and the base value has a quantity related unit and the per unit quantity is dimensionless [9].

All quantities and parameters related to the basic model of the system is summarized and presented in Appendix A with standard values and bases. A more detailed explanation of the standard values and definitions of the bases follow below.

The frequency related signals in the above model, Figure 4-1, such as f, Δf, and f_{ref} have unit Hz and the base value is the nominal frequency of 50 Hz. The control signal Y (guide vane opening) has unit percent and base value is thus 100 in order be transformed to per unit.

Different **power quantities** such as produced power P and load disturbance d_L in Figure 4-1 have unit MW and the base is related to rated power of the system. Rated power in this case is the available power in the system or the regulation strength, which in turn will depend on the grid frequency as well as the EP-mode of the system. Regulation strength is 600MW/0.1Hz or 6000MW/Hz at frequency 50Hz and the EP-mode is set to EP0 in per unit. The EP-mode will differ, but this is handled with the EP-dependent fraction mentioned above and the base is instead kept constant as $FCR\text{-}N \cdot f \cdot ep0 = 6000 \cdot 50 \cdot 0.1\ \left[\frac{MW}{Hz} \cdot Hz\right]$ [14].

The grids inertia *M* in equation (2) is calculated as

$$M = 2 \cdot S \cdot H\ [MWs] \tag{6}$$

where S is the total apparent power, unit $[MVA]$, in the grid and H is the equivalent inertia constant, unit $\left[\frac{MWs}{MVA}\right]$, of the grid. The inertia will differ depending on high versus low load in the grid. For the nominal case a medium load has been estimated giving an inertia $M = 60000 \cdot 4.5 \cdot 2\ [MWs]$ [15]. With the powerbase defined above the per unit-value of M equals $18\ s$.

The load-damping factor D in the grid shows how the load in the grid depends on the frequency as $D = \frac{\Delta P}{\Delta f}$. If the load respectively frequency variations are given in percent the load-damping factor will be in per unit, where a typical value is $D = 1.0$ [13].

The two **time constants T_w and T_{del}** depends on the characteristics of the different plants. Typical values for T_w lies between 0.5-2 seconds, depending on lengths of waterways and so on [8]. Therefore an average value of $T_w = \frac{0.5+2}{2} = 1.25s$ was assumed. The delay time constant T_{del} was set to 0.3s as this is a common delay time [19], [20].

The nominal values of the parameters mentioned above are summarized in Table 4-1 below.

Table 4-1: Nominal values of plant and grid model parameters.

Parameter	**Nominal value [pu]**
M	$18\ s$
D	1
T_w	$1.25\ s$
T_{del}	$0.3\ s$

The EP of the controller can have four different values depending on how much of the plants rated power should be delivered, that is the plants regulation strength in percent. As the EP is the inverse of the regulation strength, the base is defined as the inverse of the base values for the regulating strength, $\left(\frac{100}{50}\right)^{-1}$ with unit $\left[\left(\frac{\%}{Hz}\right)^{-1}\right]$. The four different EP-modes are presented in Table 4-2 below [19],[21].

Table 4-2: The values of the different EP-modes are given by the inverse of the regulating strength. Division with the above defined base gives the per unit-value.

Mode	**Regulating strength** $\left[\frac{\%}{Hz}\right]$	**EP value** $\left[\frac{Hz}{\%}\right]$	**EP value, per unit**
EP0	20	0.05	0.1
EP1	50	0.02	0.04
EP2	100	0.01	0.02
EP3	200	0.005	0.01

The parameters of the controller, K_p and K_i, varies with the choice of EP-mode. K_i also depends the equivalent time constant T_i that must have a maximum value of 60 s, where $K_i = \frac{1}{ep \cdot T_i}$. Also the amount of regulating machines differs with the EP-mode, as discussed in section 4.1.1, resulting in an *EP-fraction*. The EP dependent parameters and their values are presented in Table 4-3 below [23],[19].

Table 4-3: Control parameter values.

Mode	K_p **[pu]**	K_i $[s^{-1}]$	$EP\text{-}fraction$ **[pu]**
EP0	1	1/6	1
EP1	1	1/2.4	0.4
EP2	1	1/1.2	0.2
EP3	2	1/0.6	0.11

4.2 System Model with Modified Control

The aim of the project has been to modify the frequency controller of some hydropower plants in order to reduce the recurring frequency floating in the Nordic power grid. This modification was to be employed in a smaller proportion of the regulating plants in the Nordic power system.

To generate a model of the new system, the current model of the system, visible in Figure 4-1, has been augmented with an extra regulating branch with a modified governor structure, as seen in Figure 4-3. The upper branch represents the plants that regulates in the conventional way and works in the same way as the current model described above. As some of the total amount of regulation plants were to be used for the new form of regulation, a scaling factor has been introduced. This scaling factor is visible in Figure 4-3 as two gain blocks called *part* and *1-part*. The sum of this scaling

factor will always add up to one, and the size of the part will decide how many percent, in per unit, of the regulating plants that will be active in the modified form of regulation. The remaining plants, of size 1-part, will regulate in the conventional way.

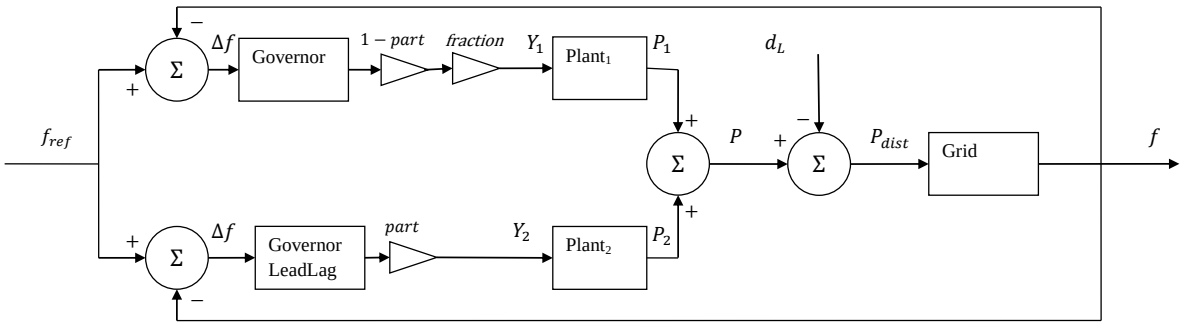


Figure 4-3: System with the new controller added. The upper branch is regulating in the conventional way, while the lower branch uses a modified governor made up of a lead-lag filter.

In the new system there is also the addition of the *fraction block* mentioned in section 4.1.2. The size of this block depends in the EP-mode of choice, according to Table 4-3.

The different signals in the new system have the same physical function as in the basic case, though with the addition of an extra control signal, Y_2, and an additional flow of power P_2 that, together with the power P_1 produced in the conventional plants, is fed into the grid. The blocks representing the grid and the conventional governor are identical with the current model, see section 4.1. The plant-blocks have the same structure, but differ in parametric values. This is discussed further in section 4.2.2.

4.2.1 Modified Frequency Controller

For the design of the new added controller a lead-lag structure was implemented. The lead-compensator is given by equation (7) and the lag-compensator is given by equation (8) [10].

$$F_{lead} = K \cdot \frac{\tau_D s + 1}{\beta \tau_D s + 1} \tag{7}$$

$$F_{lag} = \frac{\tau_I s + 1}{\tau_I s + \gamma} \tag{8}$$

For the modelling, a time delay block was also added representing the delay time from the control signal to the actual response of the plant. The modelling design of the new controller is figured in Figure 4-4.

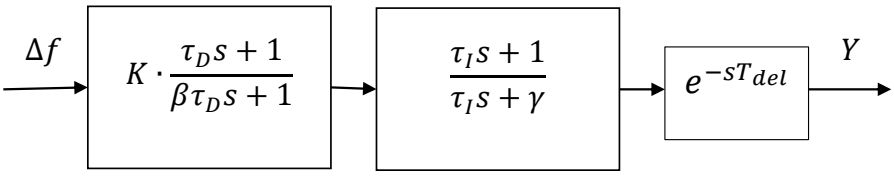


Figure 4-4: Structure of the modified controller.

4.2.2 Modified Model Parameters

In the new model of the system there are two sets of blocks representing the plants. The two blocks have the same structure as described in Equation (3), though the value of the parameter T_w differs. In the basic case, an average of 1.25 s was assumed as a typical value as T_w varies between 0.5 s to 2 s making the plants faster or slower in their processes. In the proposal of a modified regulation in a smaller portion of the regulating plants, it is not farfetched to assume that more rapidly plants would be selected for this purpose. Consequently, two new parameters were introduced: $T_{w_{slow}}$ and $T_{w_{fast}}$, where the first was given a value of 2 s and the latter a value of 0.5 s. When replacing T_w in Equation (3) with one of the two new parameters, a slow or a fast plant is generated. In the model of the new system, Figure 4-3, Plant_1 is assumed to be comprised of slow plants and Plant_2 of fast plants.

The delay time T_{del} of the modified controller was assumed to be the same as the one of the basic controller. As this is due to mechanical devices and such that react to the control signal this should not differ when the controller design is modified.

A smaller fraction of all frequency controlling plants was, according to the project description, to be active in the new form of control. The actual amount of plants for the modified control was not specified, but 10 % of active plants were assumed to be reasonable. In per unit, the scaling factor $part$ was therefore set to 0.1, and its counterpart $1 - part$ to 0.9.

The nominal values of the parameters of the new model are summarized in Table 4-4.

Table 4-4: Nominal values of the additional parameters in the new model. The unit is in per unit.

Parameter	**Nominal value [pu]**
$T_{w_{slow}}$	2 s
$T_{w_{fast}}$	0.5 s
T_{del}	0.3 s
$part$	0.1
$1 - part$	0.9

The leadlag-structure of the new controller has five new parameters: K, τ_D, β, τ_I, and γ. A typical appearance of a lead-filter in a magnitude Bode plot is figured in Figure 4-5 and a typical lag-filter in Figure 4-6. The relationship between the filters characteristics and the above mentioned parameters can be seen in these figures [10].

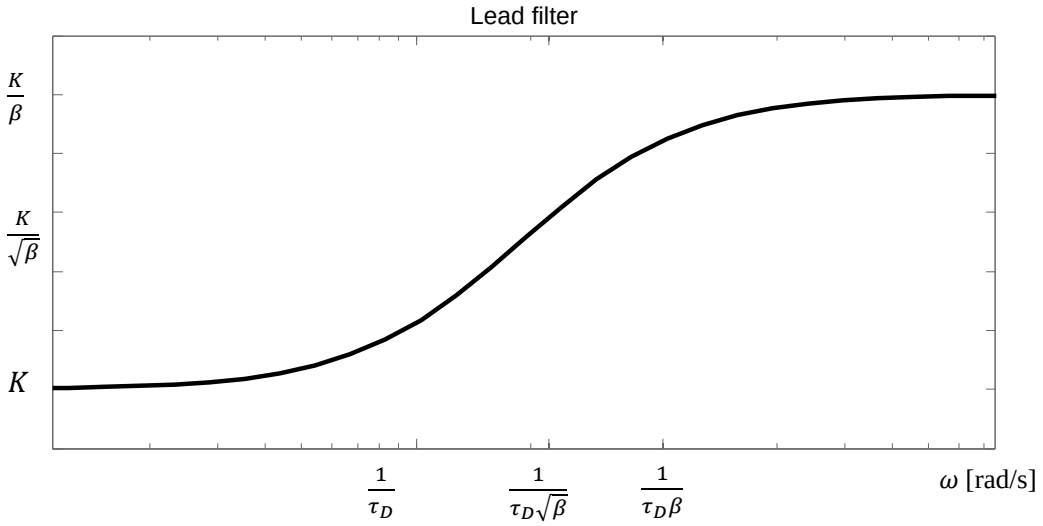


Figure 4-5: Typical appearance of a lead-filter.

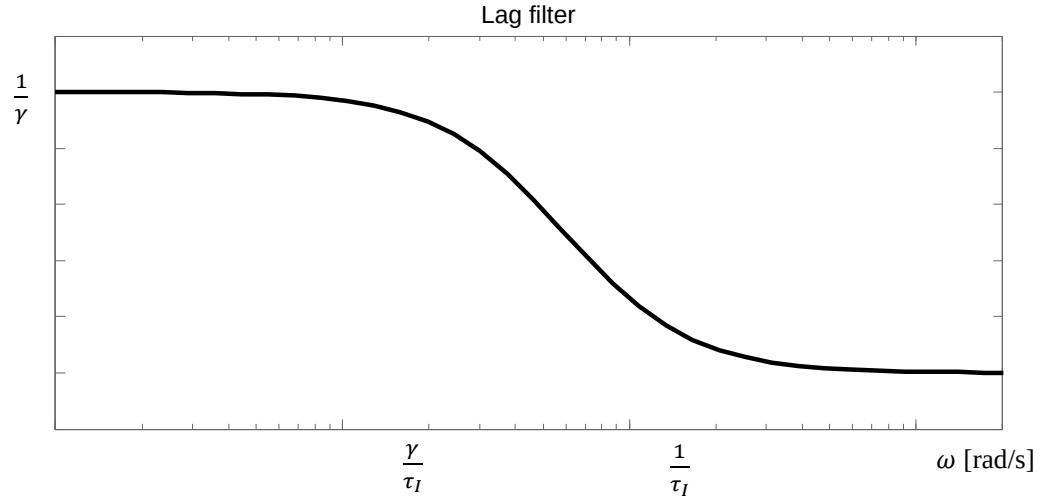


Figure 4-6: Typical appearance of a lag-filter.

As the aim of the modified controller is to damp load disturbances with energy content in a certain frequency range, a first notion was made that the leadlag-controller should focus on that range. Therefore an assumption of a shape for the leadlag-filter was made according to Figure 4-7.

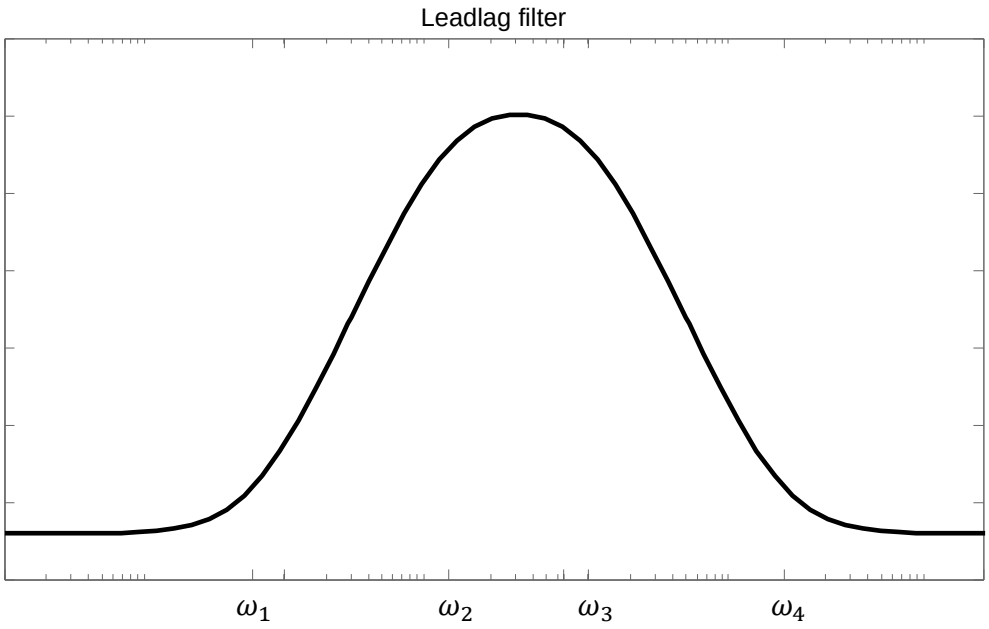


Figure 4-7: Desired appearance of the leadlag-filter.

To design the new controller, instead of determining the above mentioned five leadlag-parameters, the known relationship of the filters characteristics and the parameters were put to use and could thereby be defined according to frequencies as follows:

$$\omega_1 = \frac{1}{\tau_D} \tag{9}$$

$$\omega_2 = \frac{1}{\tau_D \beta} \tag{10}$$

$$\omega_3 = \frac{\gamma}{\tau_I} \tag{11}$$

$$\omega_4 = \frac{1}{\tau_I} \tag{12}$$

The gain of the controller, K, becomes

$$K = \frac{\sqrt{\beta}}{|G|} \tag{13}$$

where $|G|$ is the system to be controlled [10]. To achieve a controller of the shape seen in Figure 4-7 it is also clear that

$$\frac{K}{\beta} = \frac{1}{\gamma} \tag{14}$$

To determine the five unknown leadlag-parameters it was thus enough to determine the first three frequencies ω_1, ω_2, and ω_3 making equation (12) obsolete. To narrow down five unknown parameters in to a combination of only three was important to simplify the design process.

Starting points for the three unknown frequencies were set to $\omega_1 = 0.006$, $\omega_2 = 0.15$, and $\omega_3 = 1.5$. These were then varied both up and down so that five possible settings for each frequency were attained, according to Table 4-5. With five possible setting for three different frequencies, 125 (5^3) different cases were created and tested by simulations, see section 5.2.

Table 4-5: Variation of the frequencies used to determine the leadlag-parameters. Each frequency was given five different variations making the total amount of 125 cases.

Frequency					
$\boldsymbol{\omega_1}$	0.002	0.004	0.006	0.008	0.01
$\boldsymbol{\omega_2}$	0.05	0.1	0.15	0.2	0.25
$\boldsymbol{\omega_3}$	0.5	1	1.5	2	2.5

4.3 Method of Analysis

The study to determine the leadlag-parameters and evaluate the performance of the modified design is performed in several steps. The method of analysis is described in the following sections.

4.3.1 Frequency Domain Analysis

Analyses in the frequency domain are useful to understand the dynamics of a system and how it responses to input with different frequency contents. For the sake of this project, several aspects have been studied in the frequency domain where instruments as Bode plots and concepts like bandwidth and phase margin have been utilized as performance measures.

Bode Plots

A bode plot is a representation of a system's magnitude and phase as a function of frequency. Usually the magnitude is given in decibel, the phase in degrees and the frequency in radians per second, though the units can be chosen differently to illustrate different aspects. In this study, the magnitude is most commonly given in absolute values, the phase in degrees and the frequency in Hz. From a bode plot one can obtain information about the systems dynamics. The Bode plot illustrates how the system responds from input to output [10].

In this report Bode plots are mainly treated as a mean of examining how inputs amplify outputs depending on frequency. First and foremost Bode plots displaying magnitude *from the load disturbance-signal d_L to the grid frequency f*, see Figure 4-3, are used. These types of plots demonstrate which frequencies in the load disturbance that will amplify, or not amplify, the output frequency. The control is designed to smoothen out the highs and lows in the grid frequency that results from load disturbances. This also implies that Bode plots, demonstrating gain from disturbance signal to grid frequency, should in a perfect regulating sense show no peaks. To reduce the grid frequency floating, it is thus of great importance to enhance the regulating abilities in this area. To evaluate how well the modified system regulates this type of disturbances a ***damping factor*** is introduced. This damping factor will tell how peaks in the Bode plot is reduced when comparing the current system to the new and modified. This is the first of several criteria established to determine the performance of the new regulation and, ultimately, the damping of the slow floating in the grid frequency. The definition of the damping factor as well as the other criteria is presented in the section Performance Criteria below.

Furthermore it is important to confirm that the new type of regulation do not demand excessive amounts of regulating power. This is often a tradeoff that needs to be done. An increase in regulating power will most likely be necessary to dampen the floating, at least in the plants that are dedicated to perform the new method of regulation. For this purpose it is important to observe how inputs affect the control signals Y_1 and Y_2, see Figure 4-3, as these control how much power that is generated. When constructing a controller that provides a system with a good damping factor, one must make sure that any peaks in the Bode plots showing magnitude from the load disturbance signal and the control signals are not too large. This would mean that the controller reacts with a high amount of power for load disturbances with frequencies for where the top lies. This constitutes the second criteria where *peaks in the magnitude-Bode plots from load disturbance to control signals should be held at a minimum.*

Another aspect is the case of measurement noise, denoted as n. The grid frequency is fed back into the system by a feedback loop, as seen in Figure 4-3, so that the controllers can react to frequency deviations. If these deviations are a result of measurement noise, and not actual fluctuations in the grid frequency, it is not desired that the controllers react with unnecessary power. The reaction to measurement noise needs to be kept at a minimum and it is important that measurement noise gives moderate response from the controllers. This is handled in the same way as with the relation between load disturbance and control signals. *Peaks in the magnitude-Bode plots from measurement noise to control signals should be held at a minimum.*

The feedback signal is sampled when it is taken as input to the controller. When a signal is sampled it is inevitable that information is lost, such as frequencies higher than some frequency ω. According to the Sampling theorem, see [26], this frequency is the *nyquist frequency* ω_N which is defined as $\omega_s/2$ and where ω_s is the sampling frequency [10],[26]. The sampling frequency of a hydropower controller is approximately 25 Hz [5]. The consequence of this is that signals with energy levels in the frequency area beyond ω_N will not be taken into the controller, and therefore not processed. So, if a

peak, in any of the Bode plots examined as mentioned above, is present at a frequency larger than ω_N this peak could be considered as irrelevant.

Bode plots can also be used to determine the bandwidth and phase margin.

Bandwidth

The bandwidth frequency ω_B can be explained as the upper frequency of a frequency range of a signal where the input signal has a significant impact on the output. The bandwidth can in other words be interpreted as stretching from steady state level, where $\omega = 0$, to $\omega = \omega_B$. The bandwidth frequency can be identified in the Bode plot as the frequency ω where the magnitude goes below $1/\sqrt{2}$ (-3 dB) the first time [22].

Bandwidth gives information about the systems speed. In general, a smaller bandwidth represents a slower system with larger rise times. On the contrary, a large bandwidth corresponds to a faster system with smaller rise times [22]. The speed of a regulated system impacts the robustness of that system, where the fastness of the system makes it more sensitive to noise.

When considering how the control signals in the system responds to load disturbances it is unwanted with a high sensitivity to noise. Control signals that react too much to the disturbances are an issue that must be taken into account. Hence another criterion is defined, where a controller design should not give an excessive bandwidth from the disturbance signal to the control signals. In other words, *the bandwidths from d_L to Y_1 and Y_2 should be held at minimum*.

Phase Margin

The phase margin φ_m indicates how far the phase in the open-loop Bode plot can be shifted before instability of the closed loop system occurs. φ_m is defined as the distance between the phase graph and -180°, for the frequency where the magnitude graph equals 1 (0 dB).

$$\varphi_m = \arg G_o(i\omega_c) - (-180°) \tag{15}$$

where G_o is the open-loop system and ω_c is the frequency for which $\left|G_o(i\omega_{c)}\right| = 1$. The unit of φ_m is the same as for the phase curve. This definition is however only valid if the amplitude curve crosses 1 and is decreasing in that location [10].

The phase margin is in other words a measurement of the closed loop stability. A common rule of thumb for the phase margin is that it should not be less than 30° [22]. This was used as the final criteria: to assure a stable closed-loop system, *the phase margin should not descend below 30°*.

Performance Criteria

The performance of the modified form of regulating was assessed according to a set of criteria in the frequency domain. These are put together in Table 4-6 as follows:

Table 4-6: Performance criteria for the modified form of regulation, their definitions and the aim of the criteria.

Criteria	**Definition**	**Aim**
Damping factor	$1 - \frac{\max(Gain\ curve_{dL \to f, new\ system})}{\max(Gain\ curve_{dL \to f, basic\ system})}$	Maximize
Max gain: load disturbance to control signals	$\max\left(Gain\ curve_{dL \to Y_i}\right), \quad i = 1,2$	Minimize
Max gain: measurement noise to control signals	$\max\left(Gain\ curve_{n \to Y_i}\right), \quad i = 1,2$	Minimize
Bandwidth: load disturbance to control signals	$\omega_{B_{dL \to Y_i}}, \quad i = 1,2$	Minimize
Phase margin: reference signal to output frequency (closed loop stability)	φ_m for the open loop system from f_{ref} to f.	$> 30°$

4.3.2 Time Domain analysis

For time simulations the models were implemented in the MATLAB toolbox Simulink. The Simulink-models can be found in Appendix B.

By generating a disturbance signal used as input to the model of the system, a response in the time domain is produced. This tells how the system responds to different forms of signals. As the aim of the project was to modify the regulation to damp the floating which has a period of about 30-90 seconds, three sinusoidal disturbance signals were generated. Each signal had an amplitude of 50 MW and the frequency of the signals were $1/30$, $1/60$, respectively $1/90$ Hz. These signals were used as inputs to the current model of the system, see Figure 4-1 and Figure B-1 Appendix B, as well as the modified model, see Figure 4-3 and Figure B-2 Appendix B. Thereby the different responses to the disturbance signals could be compared, and the damping-ability of the modified model relative the current model could be assessed.

The time simulations were used to evaluate and ensure the performance of the new control that had been generated according to the set criteria, see the section Performance Criteria below. In addition, the time simulation plots were used as an illustrative way of demonstrating the modified systems response in comparison with the current system.

As only the frequency deviation from the nominal value was of interest for the modelling, the reference frequency f_{ref} was set to zero for time simulations.

4.3.3 Robustness Analysis

As a model of a system is never more than just a model, and rarely the true system, it is important that the model is robust. Robust, in this case, means that the model has some

robustness with respect to modeling errors. Will the system still be stable and perform as desired even if some of the parameters are varied?

To test the models robustness three system parameters were varied: the inertia M of the grid, the frequency dependence D of the grid and the delay time T_{del} of the plants.

The inertia of the grid M will vary with the loads connected to the grid. A nominal case of medium load was chosen, see section 4.1.2, and a low load and a high load case was applied for the robustness tests. The low load case has an estimated inertia of $M = 2 \cdot 50000 \cdot 4.0\ [MWs]$ and the high load case has an estimated inertia of $M = 2 \cdot 80000 \cdot 4.5\ [MWs]$ according to Equation (6) [15]. With the base defined in section 4.1.2 the per unit values are $13.3\ s$ for the low load case and $24\ s$ for the high load case. In percentage of the nominal value of $18\ s$ the low load corresponds to about 74 % and the high load of about 133 %.

The nominal value of the frequency dependency of the grid D and the delay time T_{del} are uncertain in the sense that possible variations are unknown. A variation of $\pm 25\%$ was therefore assumed giving values according to Table 4-7:

Table 4-7: Parameter variations for the robustness cases.

Parameter	**Nominal value [pu]**	**Variation low**		**Variation high**	
		%	**[pu]**	**%**	**[pu]**
M	$18s$	74	$13.3s$	133	$24s$
D	1	75	0.75	125	1.25
T_{del}	$0.3s$	75	$0.225s$	125	0.375

During the robustness tests one parameter at a time was varied and the others were kept at their nominal value.

4.3.4 Course of Controller Design and Performance analysis

Determining the leadlag-parameter settings for the new controller was done in an iterative manner, where the performances were assessed according to the criteria. When analyzing appropriate leadlag-parameter settings, the following steps were followed for each EP-mode:

1. Starting values for the unknown parameters was chosen and then varied so that multiple cases were formed and tested, see section 4.2.2. The variations of leadlag-parameters were used to generate systems for both the nominal cases and the robust test-cases.

2. The resulting systems from the choices of parameters were first evaluated according to damping factor and stability. Any choices of parameters that lead to a system with negative damping factor (no improvement compared to the current

model) or negative phase margin (unstable system) was excluded from further evaluation.

3. The results from the remaining systems with their related sets of leadlag-parameters were then compiled in Excel sheets. These sheets were designed as figured in Table 4-8 for the nominal case and all of the robustness cases respectively. The complete results from this part can be found in Appendix C.

4. The different parameter cases were then sorted with respect to the damping factor for the nominal case, from the highest damping factor to the lowest. The sorted data was then used to generate plots with the purpose of deciding on a possible choice of parameter-settings that gave favorable results according to the set criteria.

5. The selected set of parameters was then subjected to further investigation, including time simulations, to ensure results.

Table 4-8: Example of some of the compiled data generated with EP-mode 0. This was done for each possible combination of chosen leadlag-parameters and for all four EP-modes. The structure was used for the nominal case as well as the robustness cases. The example displays data from the nominal case. Any combination of leadlag-parameters that resulted in negative damping factor and/or negative phase margin was excluded from the data before the compilation.

Leadlag-parameter combination	Damping factor [%]	Bandwidth dL to Y1	Bandwidth dL to Y2	Max dL to Y1	Max dL to Y2	Max n to Y1	Max n to Y2	Phase margin
w1=0.002, w2=0.25, w3=2	82.5553	0.1030	112.0441	0.7346	1.0572	0.0235	0.6927	12.0418
w1=0.002, w2=0.25, w3=2.5	82.5493	0.1031	120.0916	0.7346	1.0600	0.0230	0.7565	12.1813
w1=0.006, w2=0.15, w3=0.5	53.9890	0.3585	23.9040	0.9164	1.3397	0.5688	1.0033	0.6411
w1=0.006, w2=0.15, w3=1	53.2852	0.3636	31.6490	0.9260	1.3926	0.7389	1.0431	0.8356

5 Simulations and Results

As the basic governor-parameters differ with the EP-mode, it is assumed that the setting for the lead-lag parameters can be adjusted according to EP-mode. Therefore the four different EP-modes will be handled as four different cases when evaluating appropriate leadlag-settings.

First an analysis of the current systems characteristics according to the criteria is presented. Thereafter follows the work of establishing appropriate leadlag-parameter settings for the modified system and analyzing the results of these choices. An analysis in the frequency domain was firstly performed and followed by the time domain.

5.1 Simulations with the Current Control

The findings of the current system simulations were used as baseline for the following analysis of the new, modified design. Thus when analyzing the performance of the modified controlled system this was done in relation to the current system, also referred to as *the basic system*.

5.1.1 Frequency Domain

How the current system is affected by disturbance signals is of great importance and the analysis of this was one of the key issues for this project. Figure 5-1 shows the Bode plot of the basic system from the disturbance signal d_L to the grid frequency f, or more accurate the frequency deviation from its reference value. There are four curves representing the four different EP-modes. The upper plot shows the magnitude curves, and the lower shows the phase curves. As is obvious from Figure 5-1, the gain has a peak for a frequency range of about 0.005 to 0.05 Hz, which increases slightly with EP-mode. The maximum peak for all four curves appears around a frequency of roughly 0.016Hz, which corresponds to a period time of ~60 seconds. Clearly the basic system has poor damping in the frequency area that is related to the floating in the grid. In other words, load disturbances of frequencies in the range mentioned above will not be reduced as efficient as disturbances of other frequencies. Hence this is the goal of the modified control. This is directly connected to the criteria of the damping factor, where the damping factor will tell how well the peak in the Bode plot is reduced.

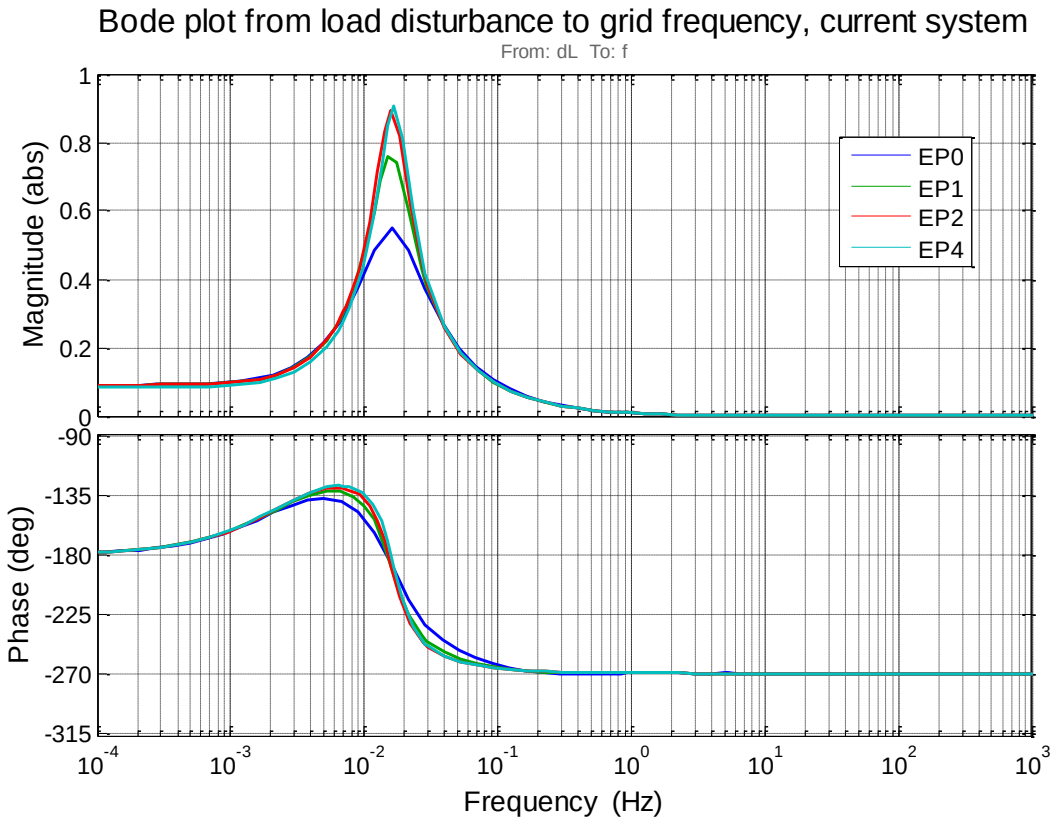


Figure 5-1: Bode plot from the load disturbance d_L to the grid frequency f for the different EP-modes for the current system. The upper plot displays the gain and the lower plot the phase.

Moreover it is clear from the magnitude plot in Figure 5-1 that the steady state-level does not approach zero, instead there is a steady state control error. This is due to the reasons discussed in section 3.2.2.

In Figure 5-1it was observed how a disturbance signal affects the output frequency. Figure 5-2 shows how a disturbance signal affects the magnitude of the control signal Y, the output of the controller in the system. As discussed in section 4.1, this control signal specifies how the guide vane openings should adjust their positions so that the desired power can be generated. In Figure 5-2 there are peaks for the four different EP-modes in approximately the same frequency area as in Figure 5-1. These maximum peaks as well as the bandwidth frequency of these basic systems were used as base when evaluating the modified systems, resulting in the maximum peaks and the bandwidths of the basic systems having a value of 1 pu. This made the assessment of the modified system related to the current system.

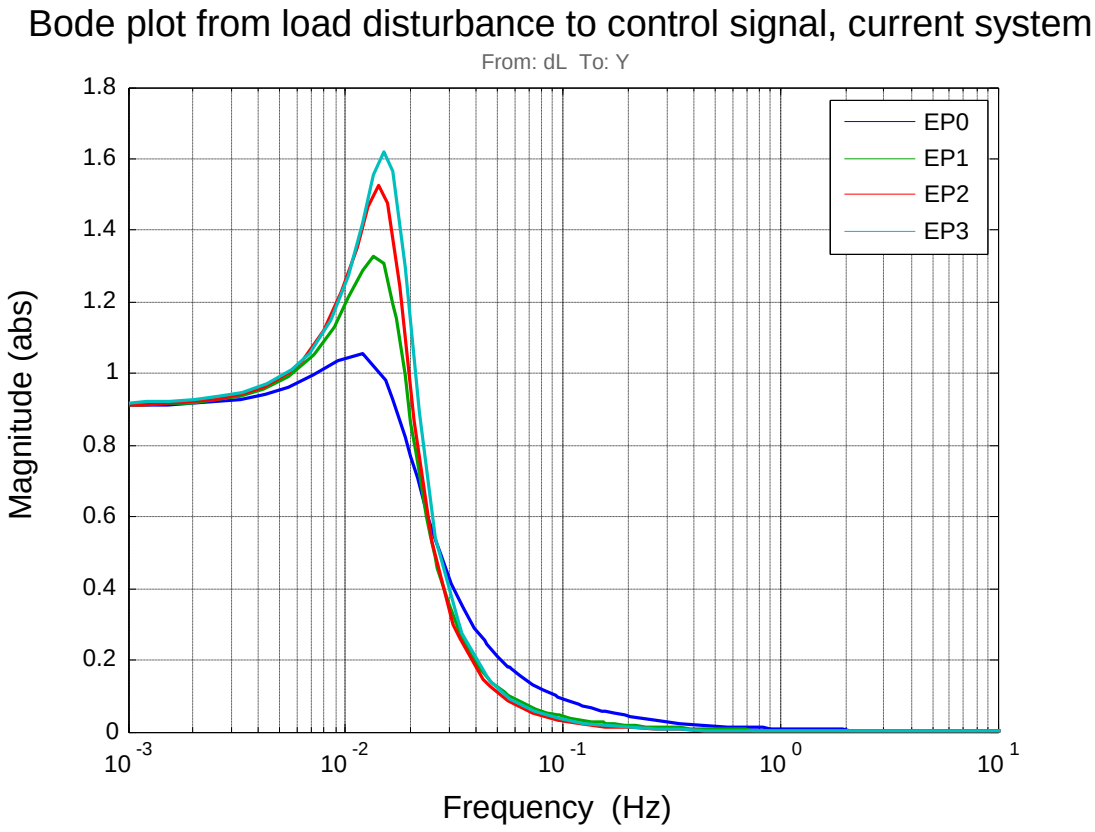


Figure 5-2: Bode plot showing gain from load disturbance d_L to the control signal Y for the current signal.

Figure 5-3 shows the magnitude Bode plot of the control signal response from the measurement noise n. The peaks shows a similar behaviour as in the previous magnitude plots in Figure 5-1 and Figure 5-2, only with a much higher gain with a maximum ranging from about 2 to 3.3. As with the bandwidth and maximum peaks from the load disturbance d_L to the control signal Y, the basic cases for maximum peaks from the measurement noise n to the control signal Y were used as base values.

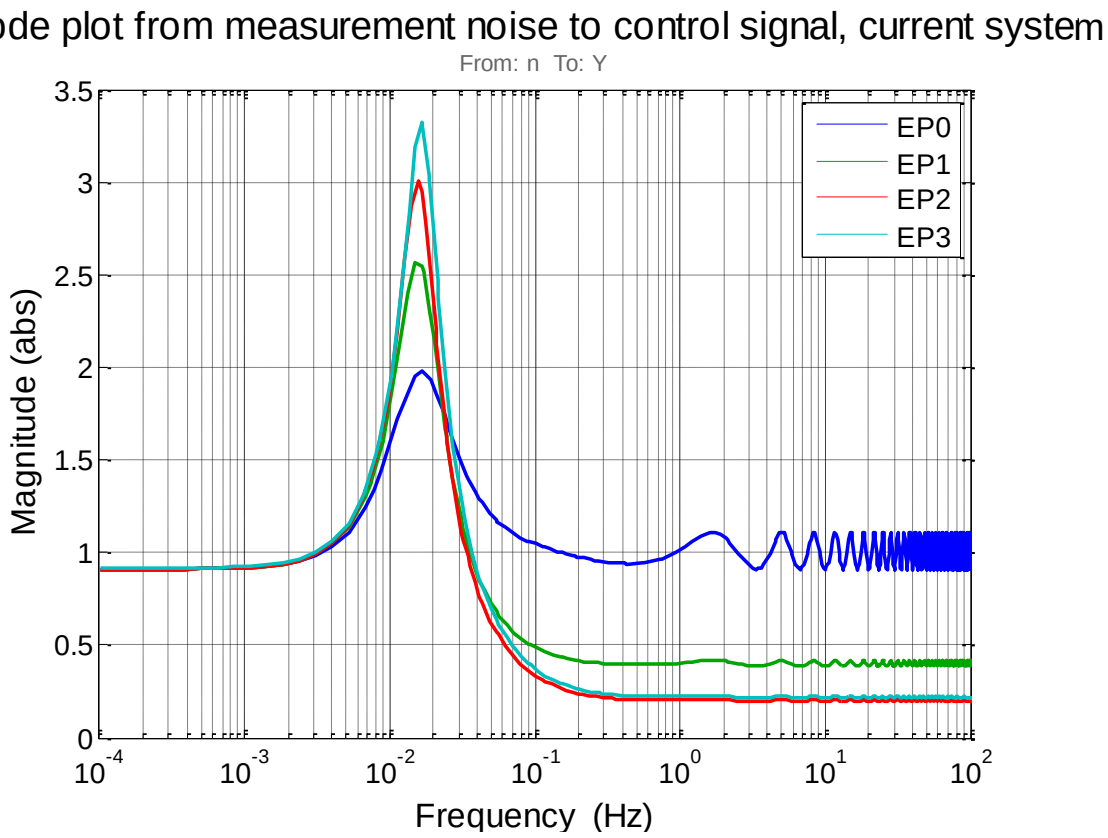


Figure 5-3: Bode plot showing gain from measurement noise n to the control signal Y for the current signal.

The actual values of the maximum peaks, the bandwidths and the phase margins of the four base cases with different EP-modes are presented in Table 5-1. The per unit values of these measures, except for the phase margin, are 1 pu.

Table 5-1: Analysis results for the criteria-quantities, current system.

	$max_{dL \to Y}$ [abs]	$max_{n \to Y}$ [abs]	$\omega_{B_{dL \to Y}}$ [rad/s]	φ_m [°]
EP0	1.0549	1.9814	0.1432	58.8512
EP1	1.3280	2.5768	0.1439	44.2558
EP2	1.5240	3.0046	0.1459	38.4766
EP3	1.6190	3.3188	0.1539	36.1657

As seen in Table 5-1, the maximum peaks as well as the bandwidths increases with the EP-mode. The phase margin decreases with increasing EP-mode, making the margin for stability less.

The peaks in the figures above are all within the frequency limits discussed in section 4.3.1, Bode Plots, and therefore all the peaks are considered as relevant.

5.1.2 Time Domain

By creating a disturbance signal, the time domain response of the basic system could be observed. To be able to examine the characteristics of interest for this study, the signals used has been sinus signals with frequencies varied between 1/30 Hz, 1/60 Hz, and 1/90 Hz. The amplitude was 50 MW, as this was deemed as a reasonable size that would give visible and clear response in the grid frequency. The response of the grid frequency as well as the control signal *Y* and the generated power (unit MW) for the four EP-modes are displayed in Figure 5-4. The upper plot contains the grid frequency response and the lower plot contains both the control signals (dashed lines) as well as the generated power (solid line). Increasing EP-mode will result in larger control signals as well as higher amounts of generated power. The grid frequency deviation will also increase with the EP-mode.

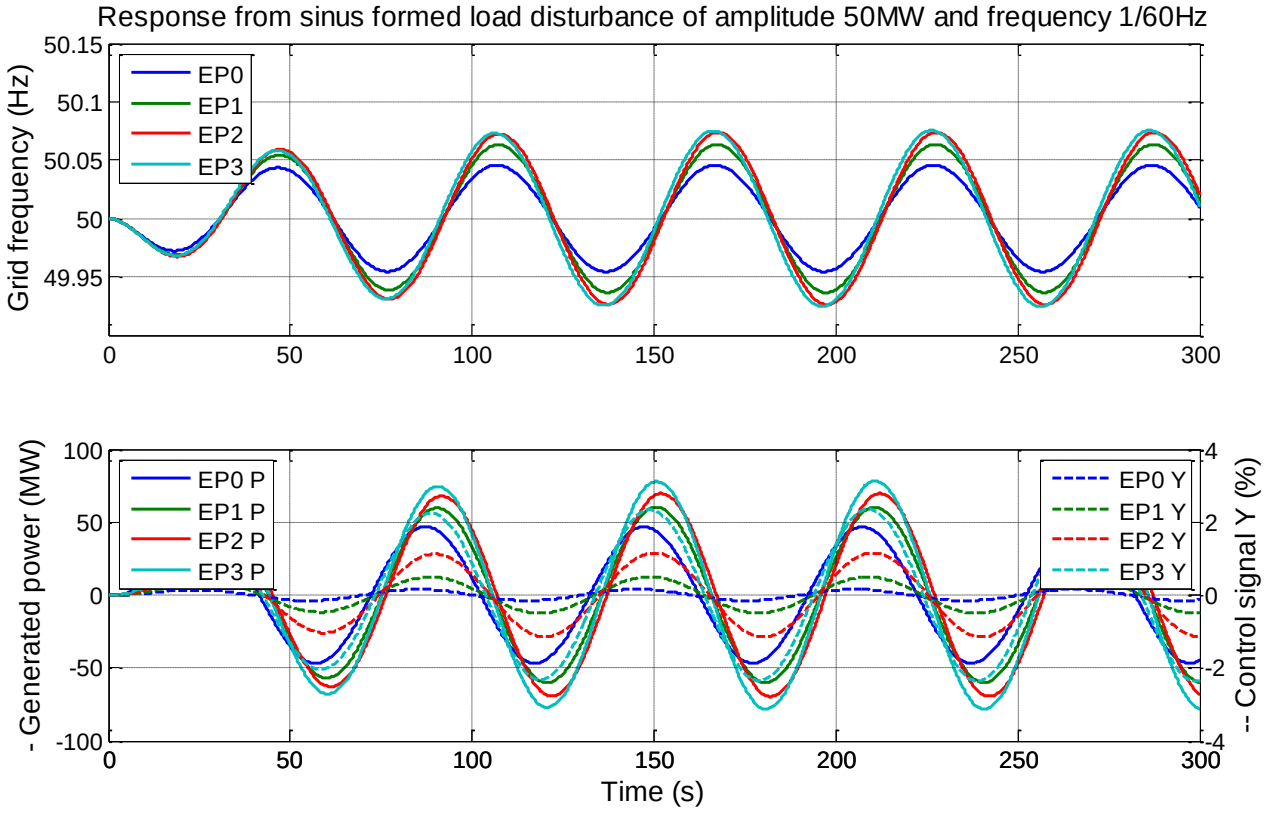


Figure 5-4: One example of a time simulation with a load disturbance with amplitude 50 MW and frequency 1/60 Hz. The upper plot is showing the grid frequency response for the different EP-modes. The lower plot, which has two axes, displays the generated power, solid line left axis, and the control signal, dashed line right axis.

The time simulations for the basic cases were used for comparison with the modified system in the following sections.

5.2 Simulations with the Modified Control

The new model of the system was simulated with 125 (5^3) leadlag-parameter variations, see section 4.2.2. In order to establish appropriate parameter settings according to the set criteria in Table 4-6, and regarding robustness according to Table 4-7, the simulations for both the nominal case as well as the robustness cases were made in parallel. Thereafter leadlag-parameters could be selected and subjected to further investigation.

5.2.1 Frequency Domain

Data was created and collected for each EP-mode in Excel files, see Appendix C. Next the data was sorted with respect to damping factor of the nominal case, from highest to lowest value. Suitable signals were then selected to be displayed and used as a first step in the selection process. These signals were the damping factors, the bandwidths from the load disturbance d_L to the control signal Y_2 from the modified controller, the maximum peaks from d_L to Y_2, and the maximum peaks from the measurement noise n to Y_2 for the nominal case and the robustness cases. These signals were selected as they were considered most critical. The remaining signals were put to use in the second step, when a first selection of leadlag-parameters had been made.

For each EP-mode plots were generated displaying the signals considered as most critical. The first example with EP-mode EP0 is seen in Figure 5-5, showing two plots. In the upper plot the solid lines are graphs of the damping factor where the different colors represent the different cases of nominal and robustness settings according to the legend. The legend is valid for both upper and lower plots. The dashed lines in the upper plot are graphs of the bandwidth from d_L to Y_2. In the lower plot the solid lines are graphs of the maximum gains from d_L to Y_2 and the dashed lines are of maximum gains from the measurement noise n to Y_2. Note that the lower plot is plotted with two y-axes where the left side is related to the solid lines and the right side to the dashed lines. The x-axes in the upper and lower plots are linked in the sense that for example point 5 in the upper plot is the same as point 5 in the lower plot. The points in the x-axes represent the different leadlag-parameter combinations and for EP0, as seen in Figure 5-5, 48 combinations of the initial 125 gave results with both positive damping factor and positive phase margin.

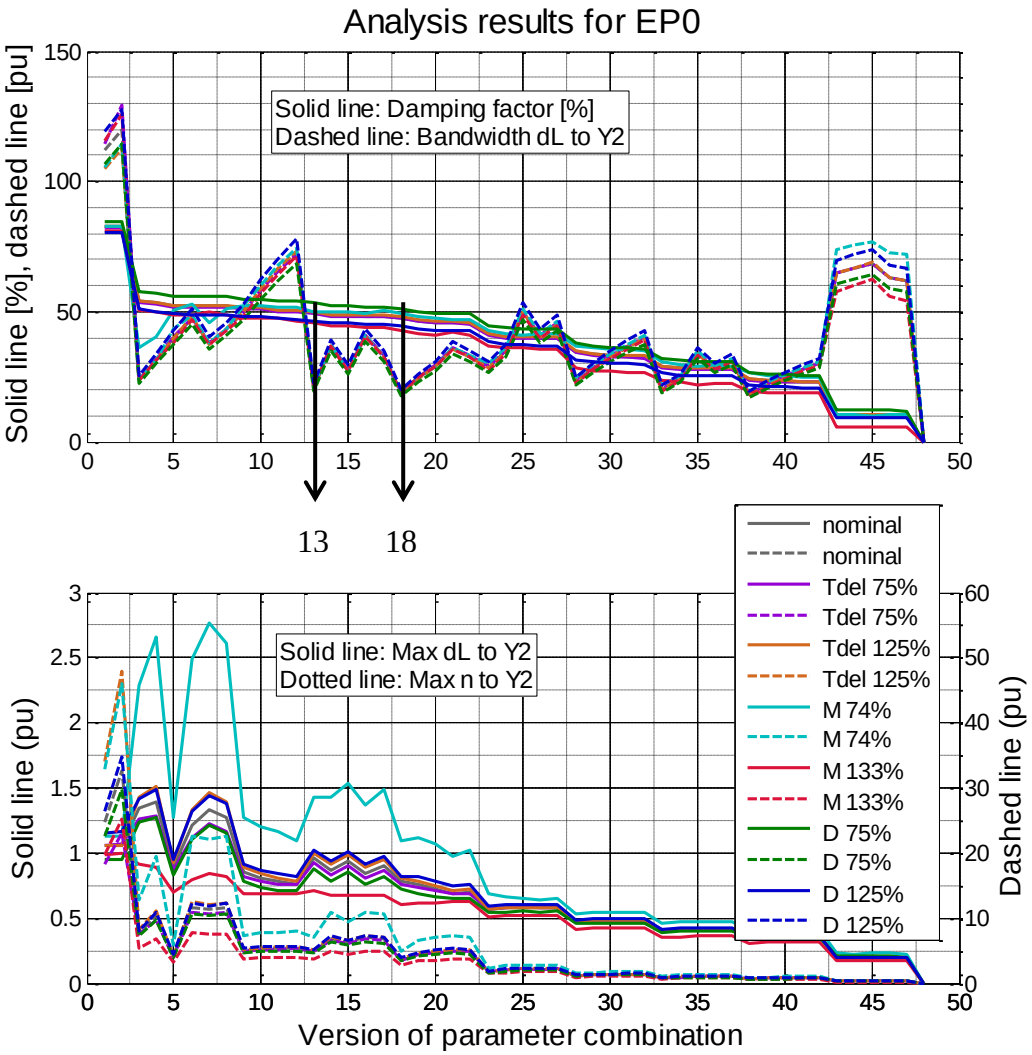


Figure 5-5: Results from simulations using EP-mode EP0. The solid lines in the upper subplot are graphs of the damping factor and the dashed lines are graphs of the bandwidth from the load disturbance d_L to the control signal Y_2 from the leadlag-controller.

The solid lines in the lower subplot are related to the left y-axis and are graphs of the max peaks from d_L to Y_2. The dashed lines are related to the right y-axis and are graphs of maximum peaks from the measurement noise n to Y_2. The legend belongs to both subplots and what case the different line colors represents.

According to the set criteria, see Table 4-6, the damping factors should be maximized while the other signals should be kept at a minimum. By inspecting the results in Figure 5-5, two different leadlag-parameter combinations were selected where the tradeoffs between the criteria were deemed as reasonable. These points were point 13 and point 18, as these were considered as relatively similar in the first step of selection. In the next step, the complete individual data of point 13 and 18 with information from all signals were examined. These results are presented in Figure 5-6 to Figure 5-9.

Figure 5-6 shows the damping factor, left plot, and the phase margin, right plot. The damping factor should be maximized and the phase margin should be kept above 30° according to the criteria. The left plot shows that point 13 is a better choice out of respect to damping ability. On the other hand the right plot shows that the stability margin for point 13 comes quite close to the limit of 30° for one of the robustness cases. This was for the low grid load case, where the inertia of the load in the grid only comes to 74 % of the nominal case with medium load.

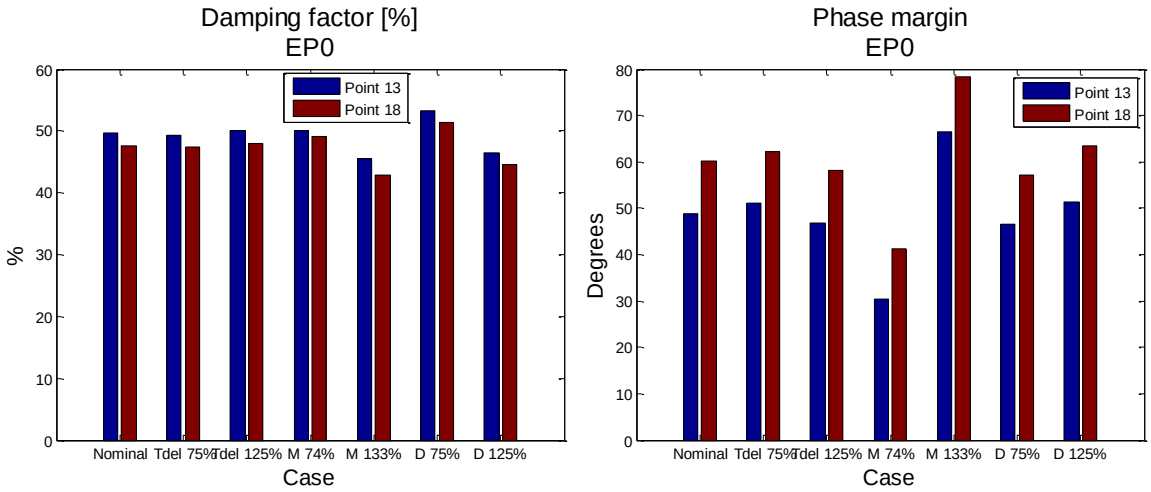


Figure 5-6: Damping factor and phase margin for the two selected points for EP0.

Figure 5-7 shows the bandwidth from the load disturbance d_L to the two control signals Y_1, left plot, and Y_2, right plot. According to the criteria the bandwidth should be kept at a minimum. The two points minimizes one control signal each, but as the bandwidth to control signal Y_2 is of greater magnitude point 18 is seen as a better choice.

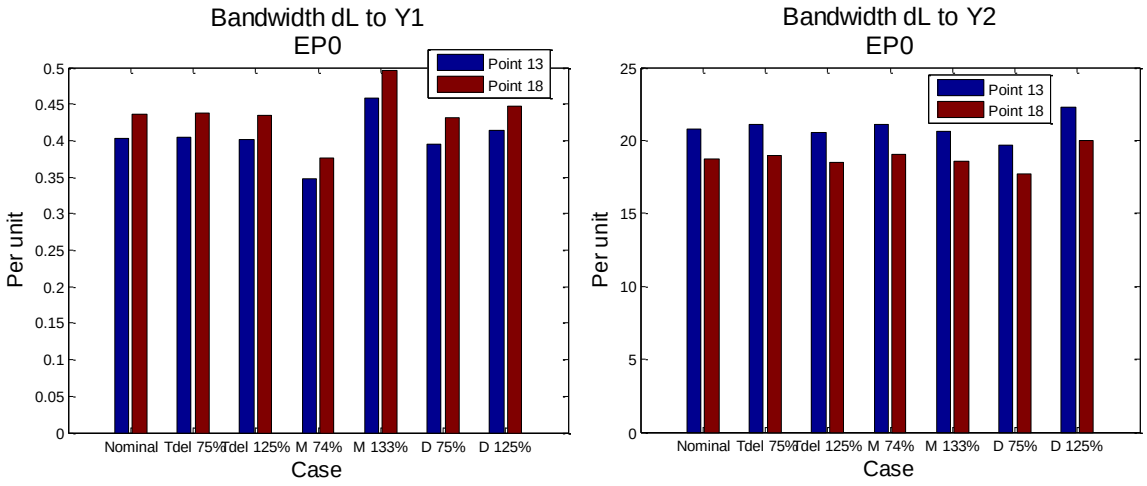


Figure 5-7: Bandwidth from load disturbance to conventional control signal Y_1, left plot, and to modified control signal Y_2, right plot. The values are in per unit.

Figure 5-8 shows the maximum gains from the load disturbance to the two control signals. The peaks in the gains should be minimized according to the set criteria. Point 18 gives smaller maximum gains for both control signals.

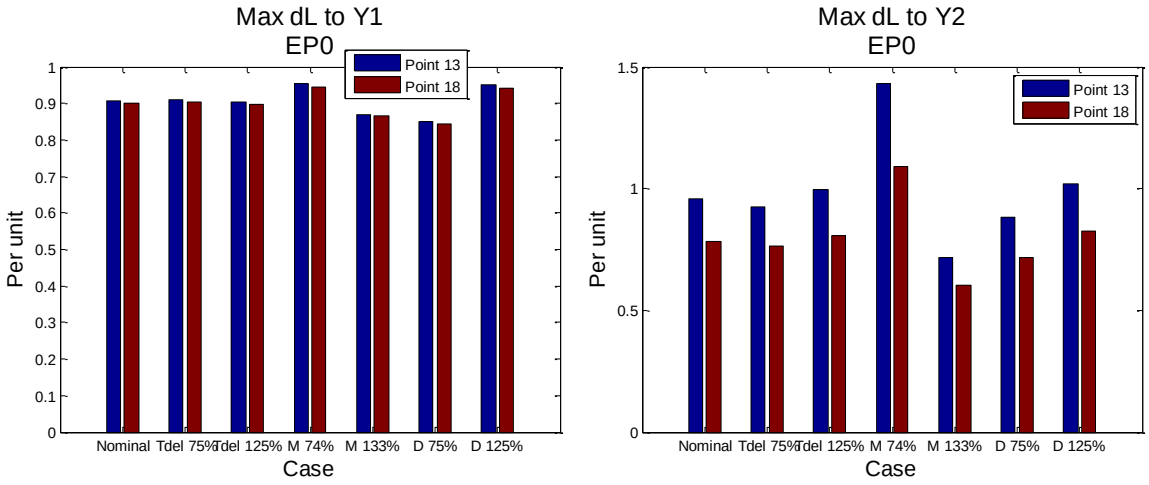


Figure 5-8: Max gain from load disturbance to conventional control signal Y_1, left plot, and to modified control signal Y_2, right plot. All values are in per unit.

Figure 5-9 shows the maximum gains from the measurement noise to the control signals. These should also be minimized according to the criteria, and point 18 gives smaller maximum gains for both control signals.

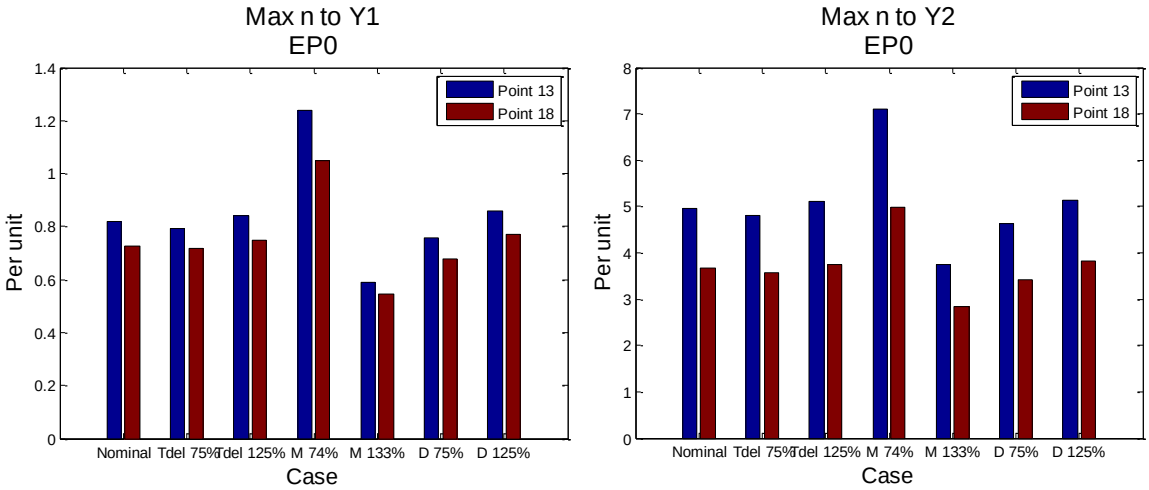


Figure 5-9: Max gain from measurement noise n to conventional control signal Y_1, left plot, and to modified control signal Y_2, right plot. All values are in per unit.

As all results in Figure 5-7 to Figure 5-9 are per unit values, with the current system as baseline, values below 1 means that the modified alternative is lower than the current one. In the same way, per unit-values above 1 are results higher than the current systems. Results equaling 1 would give the exact same results as the current system does.

When comparing the data of point 13 and 18 it is clear that point 13 offers a higher damping ability but at a higher cost in the form of bandwidth and maximum peaks for the control signal Y_2 from the modified branch and also a lower phase margin. When weighing the results of the two points, it was decided that the difference in damping factor was not sufficient enough but instead the bandwidth, peaks, and stability margins were considered as more crucial. Therefore point 18 was considered as the best choice for this case. The results displayed in Figure 5-6 to Figure 5-9 are summarized in Table D-1 and Table D-2 in Appendix D. The leadlag-parameter settings of the selected point 18 are presented in Appendix D, Table D-3.

For the following EP-modes, the selection process of appropriate leadlag-parameters was done in the same way as for EP-mode 0. The results from EP1 can be found in Appendix E, EP2 in Appendix F, and EP3 in Appendix G.

Collected Results

For all four EP-modes appropriate parameter settings were selected giving their performances according to the set criteria. All leadlag-parameters, as well as the *average* results from the nominal and the robustness cases according to set criteria are summarized in Table 5-2.

Table 5-2: Chosen parametric settings and results for the set criteria as average of nominal and robustness cases.

	EP0	**EP1**	**EP2**	**EP3**	
$\boldsymbol{K}$	0.5405	0.6470	0.6638	0.6034	Leadlag-parameters
$\boldsymbol{\beta}$	0.0667	0.0667	0.0667	0.0667	
$\boldsymbol{\tau_D}$	100	100	100	100	
$\boldsymbol{\tau_I}$	0.2467	0.2061	0.2009	0.2210	
$\boldsymbol{\gamma}$	0.1233	0.1030	0.1004	0.1105	
Damping factor [%]	47.27	63.27	68.19	66.27	Criteria performances
$\boldsymbol{\omega_{B_{dL\rightarrow Y_1}}}$ **[pu]**	0.44	0.41	0.41	0.44	
$\boldsymbol{\omega_{B_{dL\rightarrow Y_2}}}$ **[pu]**	18.76	18.40	18.13	18.14	
$\boldsymbol{max_{dL\rightarrow Y_1}}$ **[pu]**	0.90	0.74	0.65	0.65	
$\boldsymbol{max_{dL\rightarrow Y_2}}$ **[pu]**	0.80	0.87	0.79	0.62	
$\boldsymbol{max_{n\rightarrow Y_1}}$ **[pu]**	0.75	0.45	0.39	0.40	
$\boldsymbol{max_{n\rightarrow Y_2}}$ **[pu]**	3.72	4.42	3.97	2.73	
$\boldsymbol{\varphi_m}$ **[°]**	60.14	49.30	49.20	57.97	

The results in Table 5-2 are the average results for the nominal and robustness cases for each EP-mode. In the following plots, the nominal cases for the modified controlled system are presented.

Figure 5-10 shows gain and phase from load disturbance to grid frequency for all EP-modes. The solid lines are the current systems and the dashed lines shows the modified systems with the determined parameters from Table 5-2. It is clear that the peak in the gain is significantly reduced with the modified system.

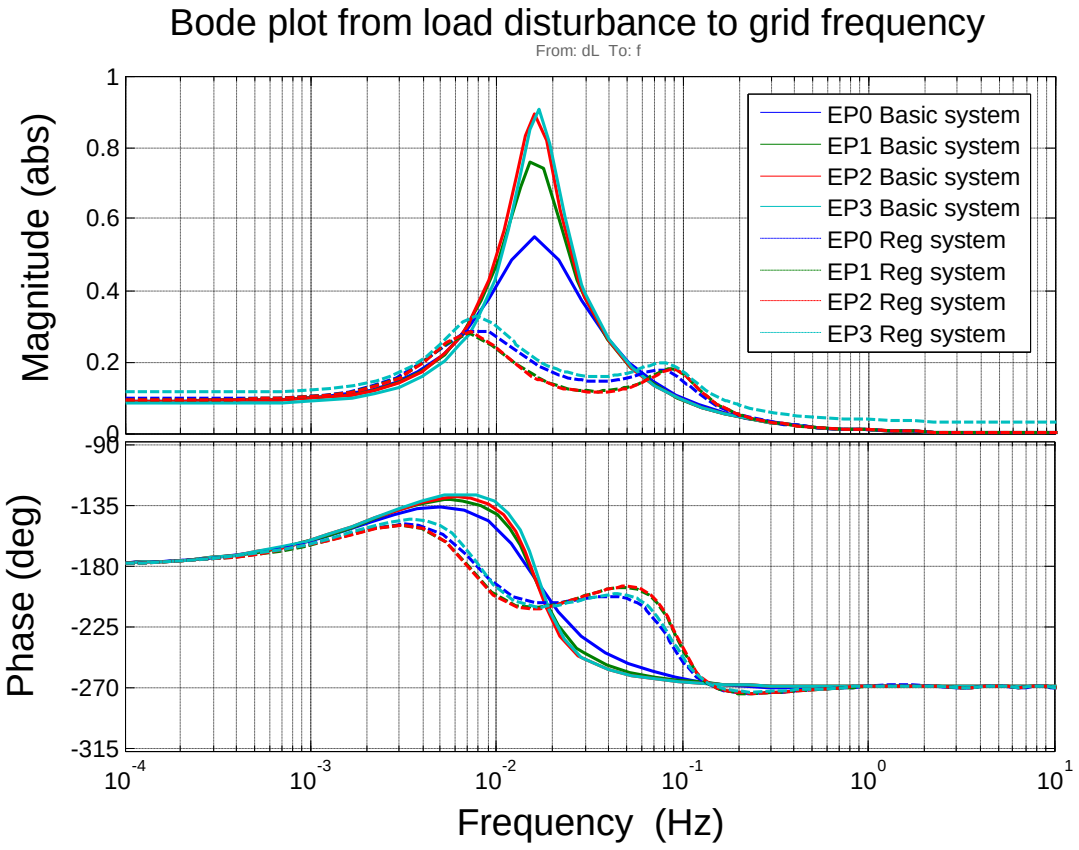


Figure 5-10: Gain and phase from load disturbance d_L to the grid frequency f for the nominal case for each EP-mode. The solid lines represents the current system and the dashed lines the modified system.

In Figure 5-11 the gain from the load disturbance to the different control signals in the systems are displayed. Each EP-mode has its own plot where the blue line represents the current system, which has one controller and one control signal Y. The modified system has two control signals where the green line represents the control signal from the conventional controller Y_1 and the red line represents the control signal from the modified controller Y_2. The plots shows that the peaks are reduced for both control signals Y_1 and Y_2 in the modified system, whilst the bandwidth is increased Y_2 and reduced for Y_1, compared to the current system.

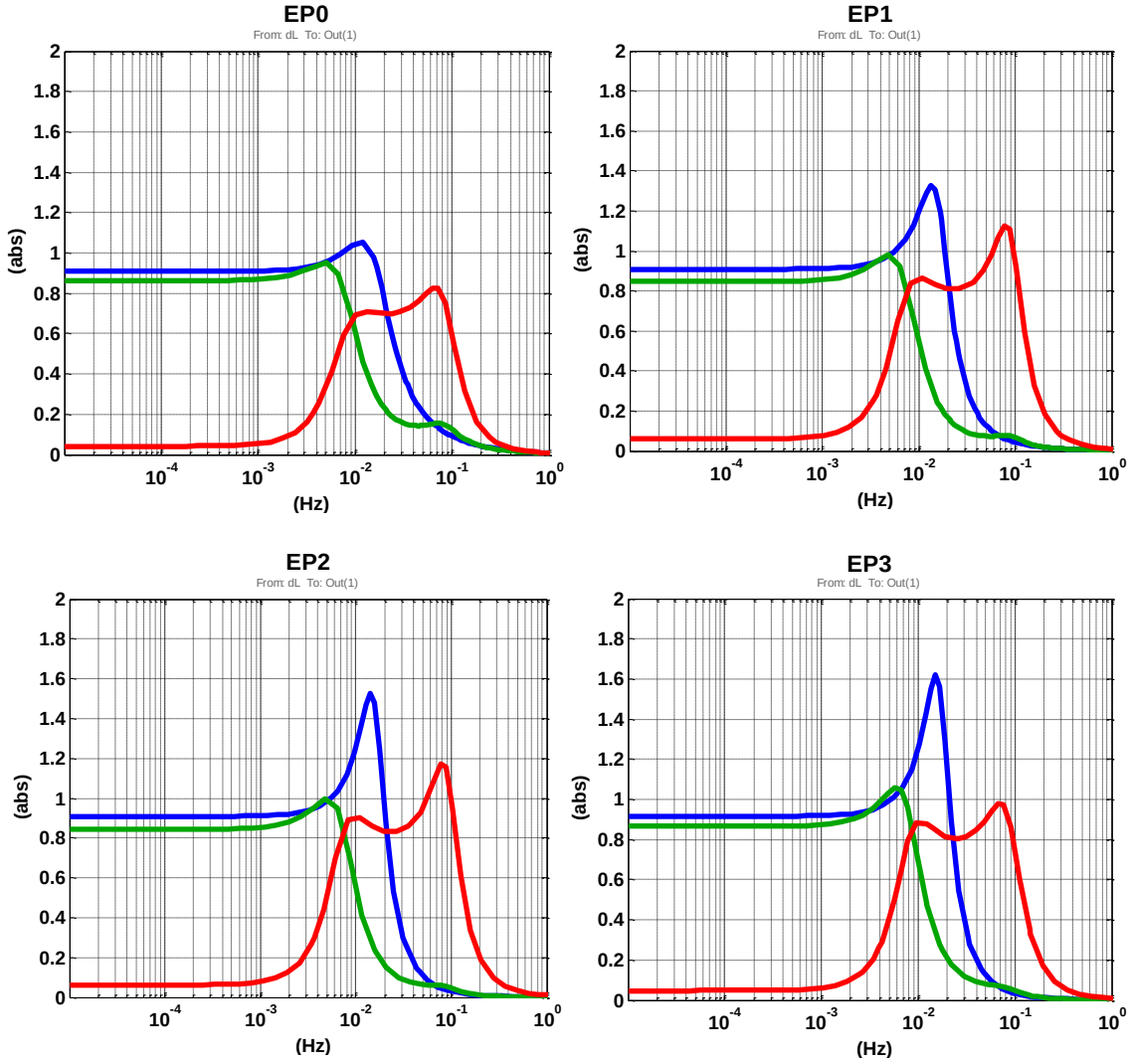


Figure 5-11: The plots are displaying the gain Bode plot from the load disturbance d_L to the control signals. The blue line is the control signal Y in the current system, the green line is the control signal Y_1 from the conventional controller in the modified system, and the red line is the control signal Y_2 from the modified controller in the modified system. Each plot represents one EP-mode each and parameter settings are the nominal case.

Figure 5-12 is divided into four plots, one for each EP-mode. The plots show the gain from the measurement noise n to the control signals. As in Figure 5-11 above, the blue line represents the control signal Y in the current system, while the green line is the control signal Y_1 from the conventional controllers in the modified system and the red represents the control signal Y_2 from the modified control. The plots show how the size of the peaks depends on EP-mode, peaking for EP-mode 2.

From Figure 5-11 and Figure 5-12 it is clear that the maximum gains from the load disturbance to the control signal Y_2 is reduced in the modified system compared to the current, whereas the maximum gain from the measurement noise to control signal Y_2 is

enlarged. This is related to the increase in bandwidth mentioned earlier, where a larger bandwidth gives a faster system which responds more to measurement noise.

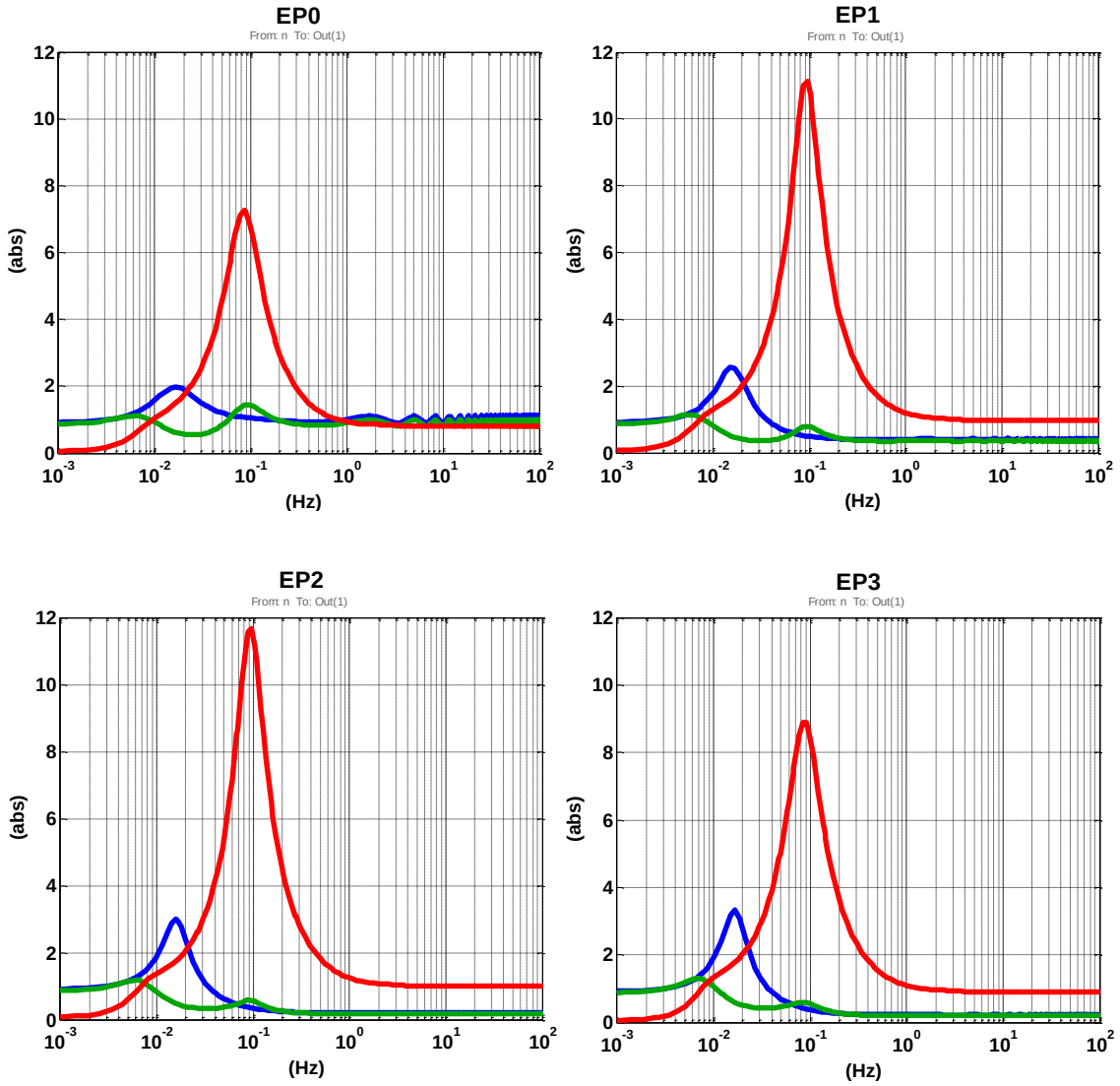


Figure 5-12: The plots are displaying the gain Bode plot from the measurement noise n to the control signals. The blue line is the control signal Y in the current system, the green line is the control signal Y_1 from the conventional controller in the modified system, and the red line is the control signal Y_2 from the modified controller in the modified system. Each plot represents one EP-mode each and parameter settings are the nominal case.

5.2.2 Time Domain

Using the parametric settings for the leadlag-parameters as decided in the previous section, a design for the leadlag-filter had been achieved for each EP-mode. To confirm the positive results achieved in the frequency domain and to validate the chosen settings, an analysis in the time domain was performed. The time domain analysis was done for the nominal cases for each EP-mode.

The disturbance signal used to excite the system in the time domain was sinusoidal with an amplitude of 50 MW and with frequencies varying between 1/30 Hz, 1/60 Hz, and 1/90 Hz. For each EP-mode a plot for every frequency was generated where the grid frequency response was compared for the current and the modified system. Furthermore, the generated power as well as the control signal (guide vane opening) were also plotted to visualize the actual work performed by the plants. As the current system, see Figure 4-1, only consists of one controller and plant unit, there is only one power signal P and one control signal Y. For the modified system, see Figure 4-3, there are two branches with one controller and one plant unit each. To visualize their individual work, the plots shows the amount of power P_1 and control signal Y_1 produced from the conventional branch and the power P_2 and control signal Y_2 produced from the modified branch.

Now follows three figures with the above mentioned plots for EP-mode 0. The figures contains 1-by-2 subplots where the grid frequency response for each case is presented in the top plot and the power and control signal responses are presented in the lower plot. Corresponding plots for the other EP-modes can be found in Appendix E, Appendix F, and Appendix G.

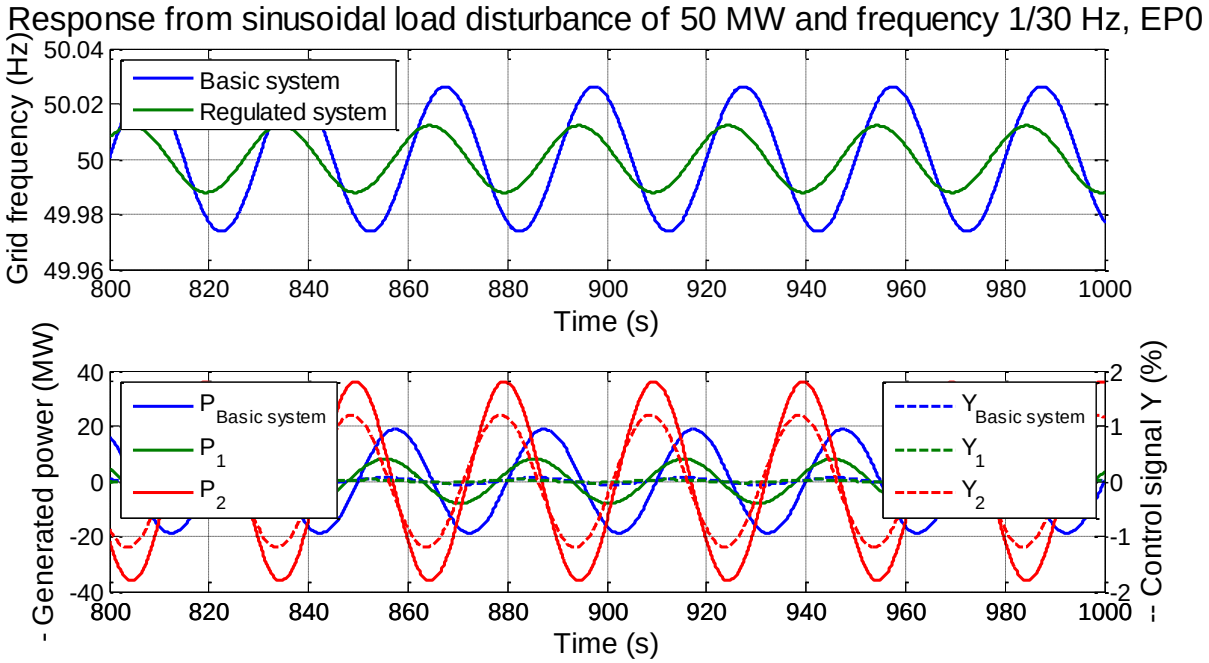


Figure 5-13: Time simulation response when system excited with sinusoidal load disturbance of amplitude 50 MW and frequency 1/30 Hz. The upper plot displays the grid frequency response and the lower plot the generated power, solid line left axis, and control signals, dashed lines right axis.

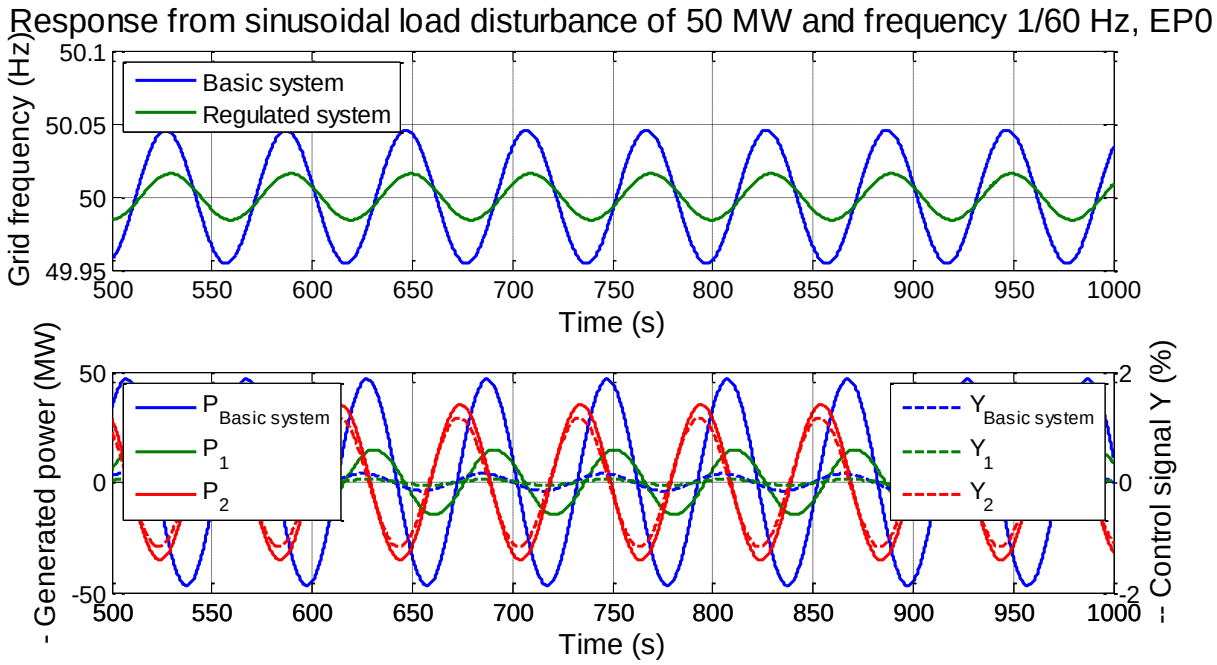


Figure 5-14: Time simulation response when system excited with sinusoidal load disturbance of amplitude 50 MW and frequency 1/60 Hz. The upper plot displays the grid frequency response and the lower plot the generated power, solid line left axis, and control signals, dashed lines right axis.

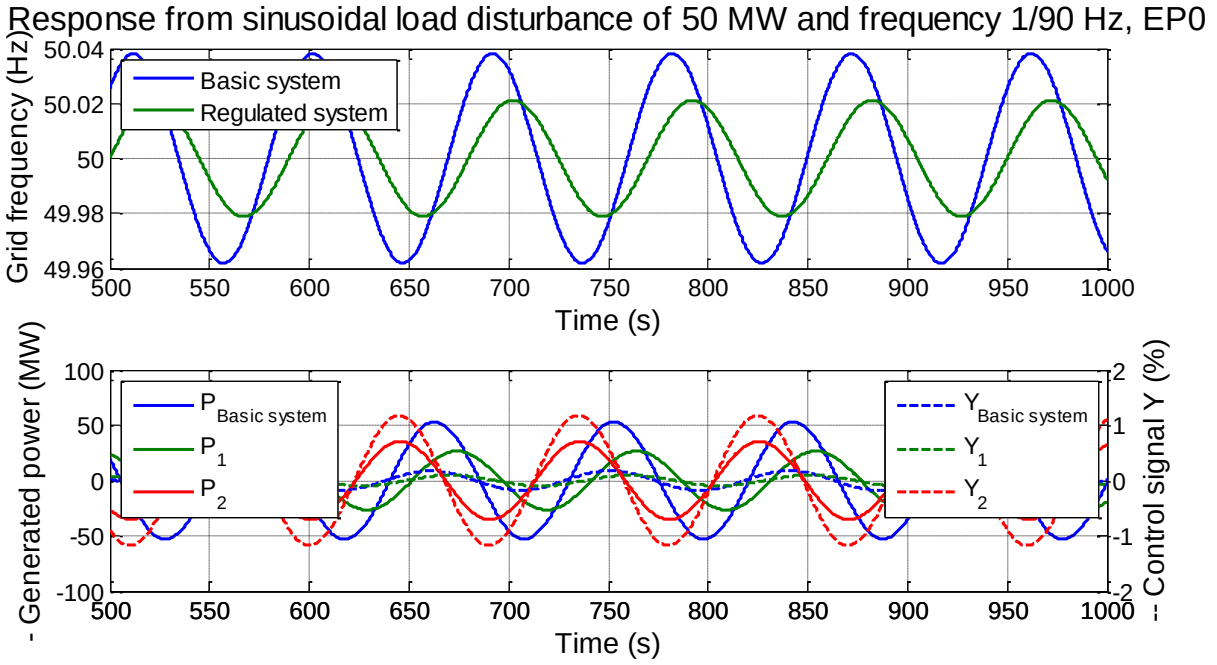


Figure 5-15: Time simulation response when system excited with sinusoidal load disturbance of amplitude 50 MW and frequency 1/90 Hz. The upper plot displays the grid frequency response and the lower plot the generated power, solid line left axis, and control signals, dashed lines right axis.

Collected Results

As can be seen in the above plots the amplitude of the grid frequency oscillations are significantly reduced with the modified system. This results holds for all EP-modes as can be seen in Appendix E, Appendix F, and Appendix G. The amplitude reduction and amount of work required differs some for the different cases. To visualize this, the maximum grid frequency deviation, the maximum power generated, and the maximum control signals for each tested disturbance signal-frequency and EP-mode are displayed in Table 5-3 and correspondingly Figure 5-16 to Figure 5-18. The maximum values are steady state values and corresponds to the peaks of the sinus-curves in the plots above.

Table 5-3: Maximum values in steady state. In the modified system 90 % of the controlling plants are of conventional type and 10 % of the controlling plants are of modified type. The data in the table are displayed in plots below.

Frequency of disturbance signal	**Quantity**	**System/Method of regulation**	**Signal**	**EP0**	**EP1**	**EP2**	**EP3**	
1/30 Hz	Maximum deviation [Hz]	Current	Δf	0.0263	0.0270	0.0270	0.0278	Figure 5-16, left
		New	Δf	0.0121	0.0098	0.0095	0.0111	
	Maximum power generated [MW]	Current	P	18.7949	14.2222	13.3904	15.1279	Figure 5-16, middle
		Conventional (90 %)	P_1	8.0786	4.7981	4.3890	5.6270	
		Modified (10 %)	P_2	36.0639	41.6141	42.6526	41.0909	
	Maximum control signal (guide vane opening) [%]	Current	Y	0.0611	0.1156	0.2178	0.4473	Figure 5-16, right
		Conventional (90 %)	Y_1	0.0282	0.0419	0.0766	0.1786	
		Modified (10 %)	Y_2	1.1974	1.3816	1.4160	1.3643	
1/60 Hz	Maximum deviation [Hz]	Current	Δf	0.0456	0.0634	0.0737	0.0754	Figure 5-17, left
		New	Δf	0.0158	0.0129	0.0126	0.0150	
	Maximum power generated [MW]	Current	P	46.7239	60.0036	69.5082	78.1939	Figure 5-17, middle
		Conventional (90 %)	P_1	14.7378	11.0785	10.8092	14.1392	
		Modified (10 %)	P_2	35.1593	41.0339	42.2958	41.5699	
	Maximum	Current	Y	0.1548	0.4969	1.1512	2.3546	Figu re

	control signal (guide vane opening) [%]	Conventional (90 %)	Y_1	0.0537	0.1010	0.1970	0.4685	
		Modified (10 %)	Y_2	1.1708	1.3664	1.4085	1.3843	
1/90 Hz	Maximum deviation [Hz]	Current	Δf	0.0381	0.0457	0.0487	0.0443	Figure 5-18, left
		New	Δf	0.0211	0.0181	0.0179	0.0214	
	Maximum power generated [MW]	Current	P	52.8844	62.7111	67.3764	67.3345	Figure 5-18, middle
		Conventional (90 %)	P_1	26.5325	22.4106	22.4003	29.4065	
		Modified (10 %)	P_2	35.2042	43.1639	45.0405	44.4245	
	Maximum control signal (guide vane opening) [%]	Current	Y	0.1758	0.5211	1.1198	2.0347	Figure 5-18, right
		Conventional (90 %)	Y_1	0.0976	0.2060	0.4118	0.9830	
		Modified (10 %)	Y_2	1.1729	1.4382	1.5007	1.4802	

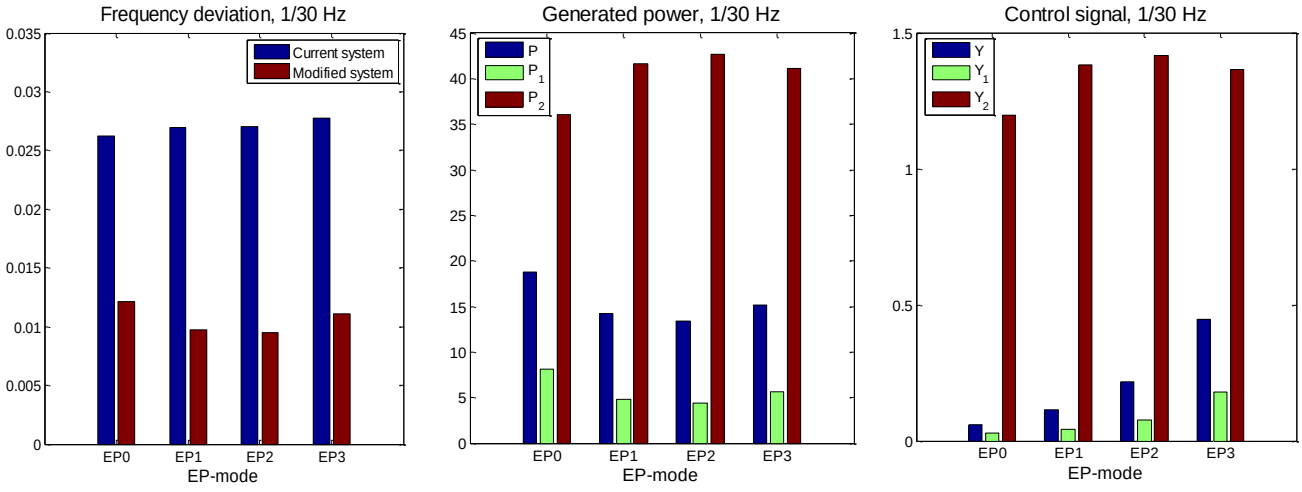


Figure 5-16: Disturbance signal with frequency 1/30 Hz. Left plot: Grid frequency deviation (Hz). Middle plot: Generated power (MW). Right plot: Control signals, guide vane opening (%).

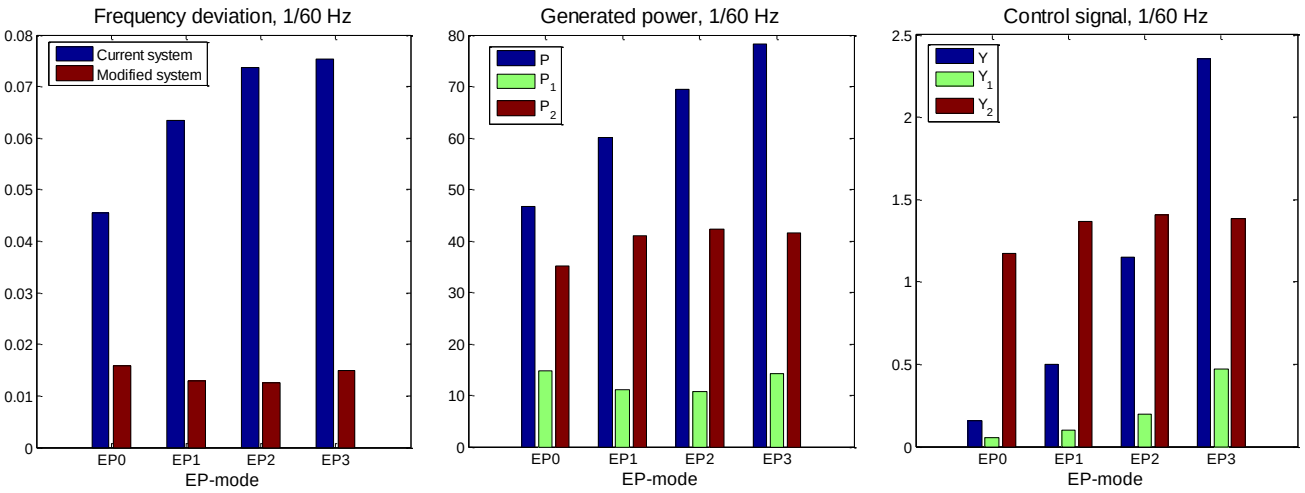


Figure 5-17: Disturbance signal with frequency 1/60 Hz. Left plot: Grid frequency deviation (Hz). Middle plot: Generated power (MW). Right plot: Control signals, guide vane opening (%).

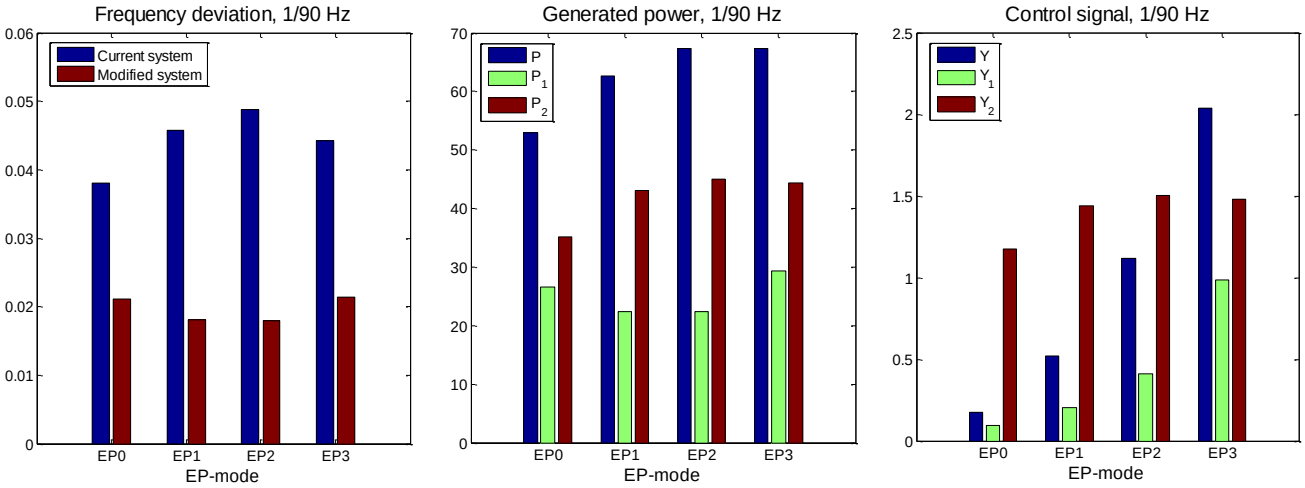


Figure 5-18: Disturbance signal with frequency 1/90 Hz. Left plot: Grid frequency deviation (Hz). Middle plot: Generated power (MW). Right plot: Control signals, guide vane opening (%).

The left plots in the above figures show that the grid frequency deviation is highest in the current system when the load disturbance is of frequency 1/60 Hz, while the modified system reduces the deviation and brings it down to a level of about 0.01-0.02 Hz for all frequency cases. The deviation in the current system are also more varying depending on EP-mode, while the modified system keeps the deviation on a more stable level for the different EP-modes.

Moreover, the middle plots in the above figures show how much power that is generated to reduce the sinusoidal load disturbance. From the plots it is clear that the modified form of control takes over a lot of the work from the conventional controller. However, depending on the frequency of the load disturbance the amount of power generated from

the modified controlled plant differs. Compared to the generated power from the current system, the modified system delivers less power when the disturbance frequency is of 1/60 or 1/90 Hz, while the 1/30 Hz-case demands a higher amount of power.

The right plots in the figures above visualises how much the guide vane openings must shift, in percent, according to the control signals. Since the amount of plants working according to the modified form of control only amounts to 10 % of the regulating plants, it is not surprising that the size of this opening shift is higher for these cases than for the other 90 % in the modified system. This is especially clear in the 1/30 Hz-case when more power is produced. In the current system the EP3-mode is the one that requires the largest shift in the guide vane openings, which is off course a result of the higher EP-mode (more MW per ΔHz) and the smaller fraction of active plants.

6 Discussion

There have been several assumptions and simplifications made in this work, one of them being the notion that all frequency regulating plants in the system are identical. This assumption does not take into account the different waterways, turbine types, size of head for each plant, and much more. As all regulating plants are taken into account in the system definition of this study, this could be considered as a valid assumption seen as an average of the plants characteristics. Though in separate, individual plants, these aspects might have a larger impact on the final result.

Nevertheless, the analysis of the basic system shows that the characteristic of the current system is such that disturbances with frequencies around 1/60 Hz are poorly damped in relation to other frequencies. This does very well explain why this form of periodic floating is present in the grid frequency as signals of this types is preserved to a higher extend when travelling through the system.

The study shows that by modifying the control structure of some of the controlling plants in the system, the mentioned floating in the grid frequency can be significantly reduced. There are though some issues related to the results of this modification to consider, which the following discussion will address.

With the addition of a modified form of control, the burden on the conventional form of control is reduced. This, however, comes with a cost, where the plants with the modified form of control will be run in a more forceful way increasing the movement of the guide vanes and production of power quite extensively. If this is a desirable or undesirable behavior falls outside the aim of this study, but poses an interesting issue. Is it better to run a few plants harsher and decrease the burden of the majority of plants or is it better to even out the burden? The work could probably be divided more evenly between the plants if the proportion of control method was redistributed from the 10 % to 90 % that was assumed for this report.

The fact that the modified controller does more work is a result of a higher bandwidth. The higher bandwidth implies that the modification does provide a larger frequency area where the controller has a bigger impact on the output. It also means that the system is faster, which is visible in the time-simulations where the modified system responds with generated power before the current and conventional plants does. But, as discussed in

section 4.3.1 under Bandwidth, a higher bandwidth and a faster system makes it more sensitive to noise. This can be seen in the results as the peaks in measurement noise-plots are up to almost four times higher in the modified controller compared to the current controller. Hence, the modified system has a higher sensitivity to noise in this specific frequency area. If measurement noise is present in this frequency range this could potentially pose a problem. This stresses the importance of knowledge of the feedback signal and, if needed, appropriate filtering of this signal to minimize the presence of noise.

When examining the results from the time domain analysis, it is clear that the modified controller is most efficient when the sinusoidal load disturbance has a frequency of 1/60 Hz or 1/90 Hz. As this was one of the targets set for the modified controller, to dampen frequency floating of these frequencies, it is recognized that the chosen structure and parametric settings are beneficial for this specific issue. Sinusoidal disturbances with frequencies 1/30 Hz demands a higher amount of power compared to the other cases, making the solution less efficient but still valid as the amplitude of the floating is dampened.

As can be seen in the frequency domain analysis, see Figure 5-10, the modified systems have a small “bump” for frequencies around 0.1 Hz where the damping will actually be less than for the current system. If there is a high amount of load disturbances in that frequency area this could possibly present a problem. Load disturbances of these frequencies will be enhanced using the modified system, compared to the current system. Although, the enhancement is much smaller than the one that the current system is performing on load disturbances of frequencies around 1/60 Hz today.

As observed in previous research, see [17], when there is a higher amount of oscillations, the amplitude of the oscillations are also higher. The causal sequence of this correlation is not known, but the connection is there and it is not farfetched to assume that by influencing the amplitude of the floating, the amount of oscillations might also be affected. As there is also a connection between the amount of oscillations and the time outside the normal frequency band, there is reason to believe that the amplitude of the oscillations might affect the quality of the grid frequency. If the amount of oscillations could be decreased due to decreased amplitude this could in turn lead to higher grid frequency quality.

As has also been observed in previous research, the grid frequency floating is more evident during the summer months when the power production is lower. This issue is also visible in the results produced in this study, where the robustness cases with low grid inertia gives lower damping and less stability. When the inertia in the grid is low, the grid frequency balance is more delicate.

7 Conclusions

The modified system offers the ability to reduce grid frequency floating with frequencies around 1/60-1/90 Hz. Depending on the size and frequency of the disturbance causing the floating, different amounts of power will be needed to counter the grid frequency deviation. For the frequencies of 1/60-1/90 Hz, the modified control will be most efficient offering high damping at a, comparably, lower power production.

However, the modified system is significantly more sensitive to measurement noise than the current system, which must be taken into account. Though these kinds of tradeoffs, in this case between damping ability and noise sensitivity, are not uncommon in control problems and there is often the issue of weighing pros and cons against each other.

8 Suggestions for Future Work

There are several aspects that have not been taken into consideration in this study that might pose interesting perspectives. Furthermore, there are possibilities of further development of the modified controller structure. The following are some of these aspects:

- Do time domain simulations for the perturbed cases, using the parametric settings from the robustness cases to study the time domain response. An expansion of the robustness cases where several parameters are changed at the same time could also be motivated.
- Vary the amount of modified regulating plants. In this study the division was set so that 10 % were regulating in the modified way, but what will the results be if just 1 or 2 % are modified or perhaps a much larger amount or even 100 %?
- If the modified controller were put into series with the current controller, perhaps in all regulating plants, how would this affect the results?
- Taking into consideration that the Norwegian frequency controlling hydropower plants in the Nordic Power system differs from the Swedish counterparts. By diversifying the different conventional plants in the modified model of the system, what would the outcome be?
- One should keep in mind that the choice of parametric values in this report is based on a modelled system. An implementation to a real system will probably require more work and testing to tune the parameters to desired results. What would this implementation look like?

References

1. Agneholm, E., 2010: Frekvenspendlingar i det nordiska kraftsystemet. Report number U-EAg-10-006-4B, Gothia Power.
2. Agneholm, E., 2014: Analysis of Full-Scale test 2013-10-30. Report number U-EAg-11-014-44A, Gothia Power.
3. Andersson, G., 1999: *Kraftsystemets dynamik och stabilitet, En introduktion*. Elektriska energisystem KTH, kompendium. Stockholm: Universitetsservice US AB.
4. Arango, O. J., Sanchez, H. M., Wilson, D.H., 2010: *Low Frequency Oscillations in the Colombian Power System – Identification and Remedial Actions*. Cigre 2010.
5. Bladh, J., Senior R&D Engineer at Power Technology, Sustainable Energy Projects, Vattenfall AB. Email contact, 2014-05-20.
6. Bojrup, M., Petersson, A., Agneholm, E., 2013: Utnyttjande av styrbara laster för systemdrifttjänster. Potential i kraftsystemet. Report number 13:58, Elforsk.
7. European Network of Transmission System Operators for Electricity: *Regional Groups*. https://www.entsoe.eu/about-entso-e/system-operations/regional-groups/ (2014-05-08)
8. Ghandari, M., 2013: *Stability of Power Systems, An introduction*. Electrical Power Systems KTH, compendium.
9. Glover, J., Sarma, M., Overbye, T., 2012: *Power System Analysis and Design*. Fifth edition. Stamford: Cengage Learning.
10. Glad, T. & Lung, L., 2006: *Reglerteknik, Grundläggande teori*. Lund: Studentlitteratur.
11. Hemmingsson, M., 2014: Analysis of Full-Scale test 2013-10-30. Report number U-EAg-11-014-44A, Gothia Power.
12. Hjalmarsson, L., Söder, L., Forsberg, K., Springfeldt, P.E., 2001: Systemtjänster. Report number 01:36, Elforsk.
13. Kundur, P., 1994: Power System Stability and Control. The McGraw-Hill Companies, Inc.
14. Lexholm, M., 2012: Measures to mitigate the frequency oscillations with a period of 60-90 seconds in the Nordic synchronous system, Linear Analysis. Report number U-EAg-12-009-4B, Gothia Power.
15. Lindahl, S., 2012: Mathematical models, Bode plots, step responses, and eigenvalues in automatic frequency control. Report number U-EAg-10-006-08D, Gothia Power.
16. Lundin, U., 2013: *Hydropower booklet – Technology and system*. Swedish hydropower center. Division for Electricity, Department of Engineering Sciences, Uppsala University.
17. Mäkelä, J., 2012: Oscillation of the frequency in the Nordic power system analysis. Report, Fingrid Oyj.
18. Nee, H.P., Leksell, M., Söder, L., Östlund, S., 2002: *Kompendium i Eleffektsystem*. Elektrotekniska system KTH, compendium. Stockholm: Universitetsservice US AB.
19. Norrlund, P. & Spiegelberg, E., 2014: Frequency control measurements at Letsi. Report Number U 13:103, Vattenfall.

20. Norrlund, P. & Spiegelberg, E., 2014: Frequency control measurements at Messaure hydro power plant. Report number U 13:104, Vattenfall.
21. Person, J., Frisk, A., Stenberg, L., 2011: Identification of frequency response in the Nordel system. Report Number U 10:183, Vattenfall.
22. Skogestad, S. & Postlethwaite, I., 2005: *Multivariable Feedback Control, Analysis and design. Second edition*. Chichester: John Wiley & Sons Ltd.
23. Svenska Kraftnät, 2012: Regler för upphandling och rapportering av primärreglering FNR och FDR. Faktablad 2012 08 01 Svenska Kraftnät.
24. Svenska Kraftnät, 2014: *Systemansvar*. http://www.svk.se/Om-oss/Var-verksamhet/Systemansvar/ (2014-05-09)
25. Vattenfall, 2013: *Så fungerar vattenkraft*. http://corporate.vattenfall.se/om-energi/el-och-varmeproduktion/vattenkraft/sa-fungerar-vattenkraft/ (2014-06-05)
26. Åström, K. & Wittenmark, B., 1990: *Computer-Controlled Systems, Theory and Design*. Second edition. Englewood Cliffs: Prentice-Hall, Inc.

APPENDIX A: System Model Parameters

All system model parameters, both current and modified, are compiled in Table A-1. The parameters are presented with their physical function, base value, nominal value, and per unit value when relevant. To read more about the model parameters and the models as such, see chapter 4.

Table A-1: System model parameters, definitions, base values, nominal values, and per unit values when relevant.

Parameter	**Physical function**	**Base value**	**Nominal value**	**Per unit value**
$\Delta f\ [Hz]$	Delta frequency	50	-	-
$f_{ref}\ [Hz]$	Reference frequency	50	50	1
$f\ [Hz]$	Grid frequency	50	-	-
Y [%]	Guide vane opening	100	-	-
$d_L\ [MW]$	Load disturbance	$\frac{600}{0.1} \cdot 50 \cdot 0.1$	-	-
M [MWs]	Grids inertia	$\frac{600}{0.1} \cdot 50 \cdot 0.1$	270000	$18s$
D	Grids frequency dependency	-	1	1
T_w [s]	Time constant related to waterways, etcetera.	-	$0.5 - 2\ s$	$\frac{0.5+2}{2} = 1.25s$
$T_{w_{slow}}$ [s]	Time constant related to waterways, etcetera. Slow plants.	-	$0.5\ s$	$0.5\ s$
$T_{w_{fast}}$ [s]	Time constant related to waterways, etcetera. Fast plants.	-	$2\ s$	$2\ s$
T_{del}	Time delay plant	-	$0.3\ s$	$0.3\ s$
$ep0\ \left[\left(\frac{\%}{Hz}\right)^{-1}\right]$	Droop with regulating strength of 20%/Hz	$\left(\frac{100}{50}\right)^{-1}$	0.05	0.1
$ep1\ \left[\left(\frac{\%}{Hz}\right)^{-1}\right]$	Droop with regulating strength of 50%/Hz	$\left(\frac{100}{50}\right)^{-1}$	0.02	0.04

$ep2\ \left[\left(\frac{\%}{Hz}\right)^{-1}\right]$	Droop with regulating strength of 100%/Hz	$\left(\frac{100}{50}\right)^{-1}$	0.01		0.02
$ep3\ \left[\left(\frac{\%}{Hz}\right)^{-1}\right]$	Droop with regulating strength of 200%/Hz	$\left(\frac{100}{50}\right)^{-1}$	0.005		0.01
K_p	Proportional gain (depends on EP-mode)	-	EP0	-	1
			EP1	-	1
			EP2	-	1
			EP3	-	2
K_i	Integral gain (depends on EP-mode)	-	EP0	-	1/6
			EP1	-	1/2.4
			EP2	-	1/1.2
			EP3	-	1/0.6
$Ep - fraction$ [%]	Proportion of regulating plants (depends on EP-mode)	100	EP0	100	1
			EP1	40	0.4
			EP2	20	0.2
			EP3	11	0.11
$part$ [%]	Proportion of regulating plants using the modified controller	100	10		0.1
$1 - part$ [%]	Proportion of regulating plants using the conventional controller	100	90		0.9

APPENDIX B: Simulink Models

The system models were constructed in the MATLAB toolbox Simulink, version 7.9 (R2012a). Figure B-1 corresponds to the current system model and Figure B-2 corresponds to the modified system model.

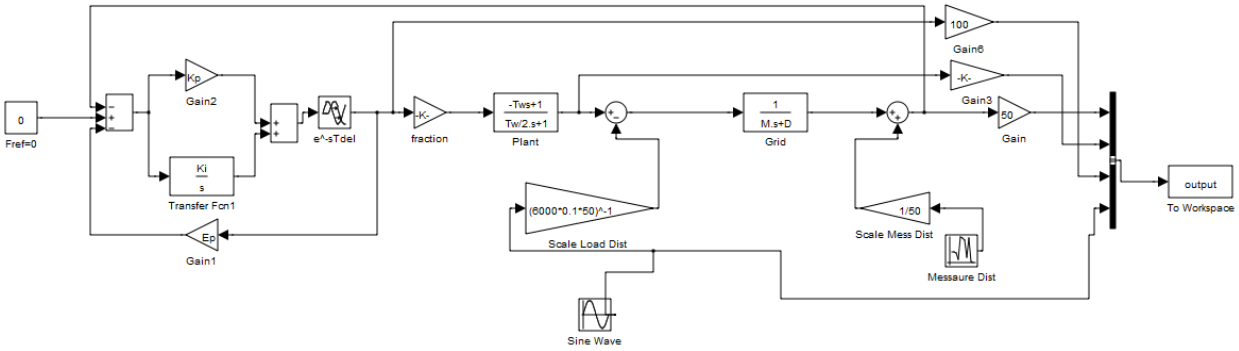


Figure B-1: Simulink model current system.

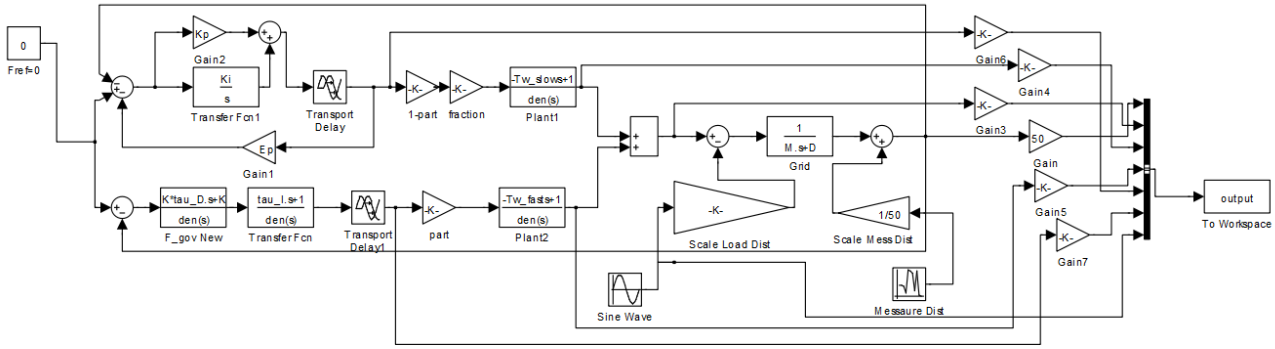


Figure B-2: Simulink model modified system.

APPENDIX C: Compiled Data Excel files

The generated data from the nominal and the robustness cases are compiled into Excel files which can be found by the following link below. To read about how the data was generated, see section 4.3.4.

Compiled data

APPENDIX D: Additional Analysis Results EP0

Additional results from the analysis of EP-mode 0.

Frequency domain EP0

The bar plots visible in Figure 5-6 to Figure 5-9 are derived from the data compiled in Table D-1 and Table D-2.

Table D-1: EP0-mode. Data according to set criteria for point 13.

Point 13 (EP0)								
Case	**Damping factor [%]**	$\omega_{B_{dL\rightarrow Y_1}}$ **[pu]**	$\omega_{B_{dL\rightarrow Y_2}}$ **[pu]**	$max_{dL\rightarrow Y_1}$ **[pu]**	$max_{dL\rightarrow Y_2}$ **[pu]**	$max_{n\rightarrow Y_1}$ **[pu]**	$max_{n\rightarrow Y_2}$ **[pu]**	φ_m **[°]**
Nominal	49.67	0.40	20.81	0.91	0.96	0.82	4.95	48.88
T_{del} **75%**	49.38	0.40	21.10	0.91	0.93	0.79	4.81	51.06
T_{del} **125%**	49.97	0.40	20.53	0.90	1.00	0.84	5.10	46.69
***M* 74%**	50.06	0.35	21.12	0.95	1.43	1.24	7.12	30.45
***M* 133%**	45.49	0.46	20.66	0.87	0.72	0.59	3.74	66.50
***D* 75%**	53.27	0.40	19.66	0.85	0.88	0.76	4.64	46.44
***D* 125%**	46.52	0.41	22.25	0.95	1.02	0.86	5.14	51.32
Average	**49.19**	**0.40**	**20.88**	**0.91**	**0.99**	**0.84**	**5.07**	**48.76**

Table D-2: EP0-mode. Data according to set criteria for point 18.

Point 18 (EP0)								
Case	**Damping factor [%]**	$\omega_{B_{dL\rightarrow Y_1}}$ **[pu]**	$\omega_{B_{dL\rightarrow Y_2}}$ **[pu]**	$max_{dL\rightarrow Y_1}$ **[pu]**	$max_{dL\rightarrow Y_2}$ **[pu]**	$max_{n\rightarrow Y_1}$ **[pu]**	$max_{n\rightarrow Y_2}$ **[pu]**	φ_m **[°]**
Nominal	47.70	0.44	18.71	0.90	0.78	0.73	3.66	60.25
T_{del} **75%**	47.39	0.44	18.95	0.90	0.76	0.72	3.58	62.21
T_{del} **125%**	48.00	0.43	18.47	0.90	0.81	0.75	3.76	58.29
***M* 74%**	49.11	0.38	19.01	0.94	1.09	1.05	4.99	41.19
***M* 133%**	42.84	0.50	18.54	0.87	0.60	0.55	2.83	78.47
***D* 75%**	51.34	0.43	17.68	0.84	0.72	0.68	3.41	57.26
***D* 125%**	44.52	0.45	20.00	0.94	0.82	0.77	3.83	63.35
Average	**47.27**	**0.44**	**18.76**	**0.90**	**0.80**	**0.75**	**3.72**	**60.14**

The leadlag-parameters for the chosen point 18 are presented in Table D-3.

Table D-3: EP0-mode. Leadlag-parameter settings for selected point.

Parameter (EP0)	**Point 18**
$\boldsymbol{\omega_1}$	0.01
$\boldsymbol{\omega_2}$	0.15
$\boldsymbol{\omega_3}$	0.50
$\boldsymbol{K}$	0.5405
$\boldsymbol{\beta}$	0.0667
$\boldsymbol{\tau_D}$	100
$\boldsymbol{\tau_I}$	0.2467
$\boldsymbol{\gamma}$	0.1233

APPENDIX E: Analysis Results EP1

Frequency domain EP1

Figure E-1 shows the results for the EP1-mode, where the upper plot in the figure displays the damping factor, solid line, and the bandwidth from d_L to Y_2, dashed line. The lower plot displays the graphs for max peaks from d_L to Y_2, solid line, and maximum peaks from the measurement noise n to Y_2, dashed lines. Note that the lower plot has two y-axes.

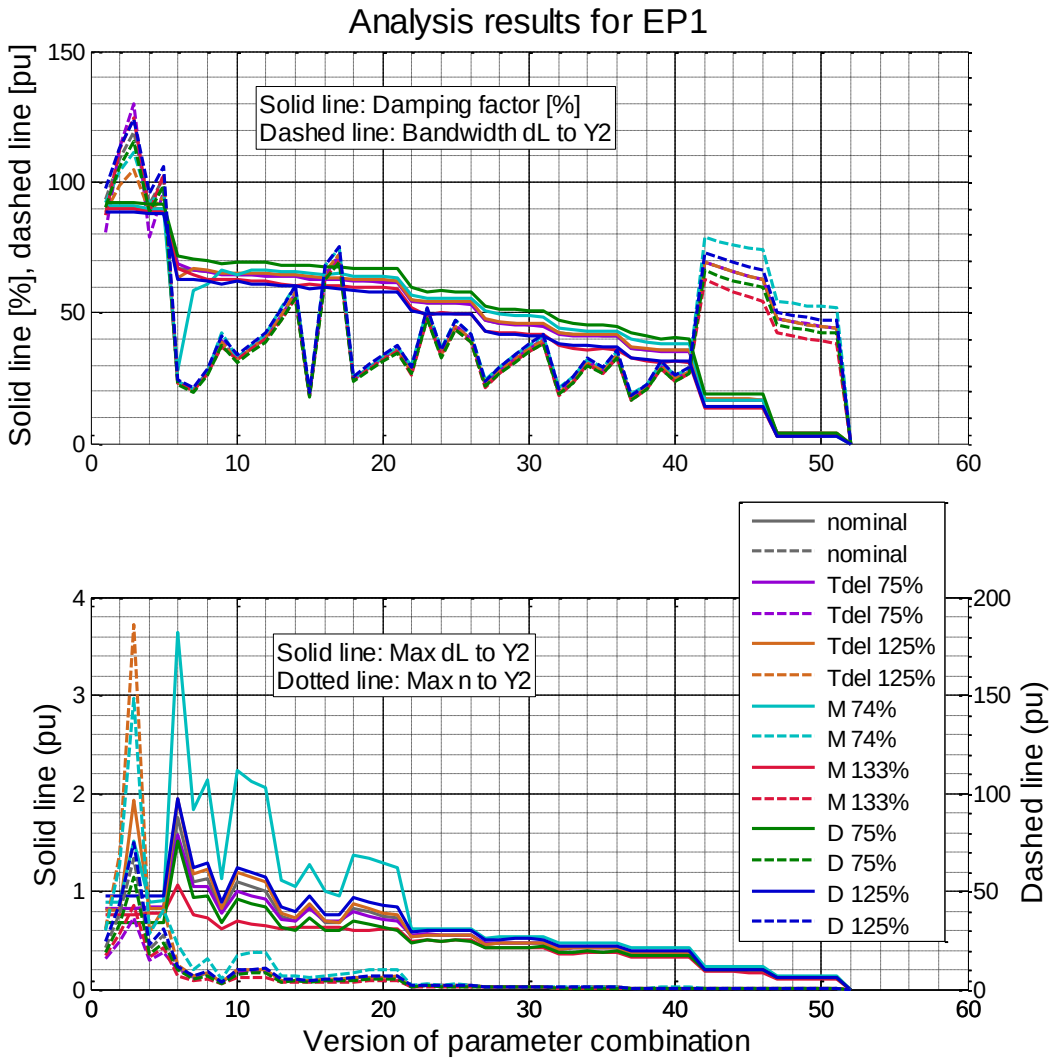


Figure E-1: Results from simulations using EP-mode EP1. The solid lines in the upper subplot are graphs of the damping factor and the dashed lines are graphs of the bandwidth from the load disturbance d_L to the control signal Y_2 from the leadlag-controller. The solid lines in the lower subplot are related to the left y-axis and are graphs of the max peaks from d_L to Y_2.

The dashed lines are related to the right y-axis and are graphs of maximum peaks from the measurement noise n to Y_2. The legend belongs to both subplots and what case the different line colors represents.

To maximize the damping factor and minimize the other criteria two sets of leadlag-parameters were chosen for the example with EP-mode 1, point 7 and point 15.

The complete individual data of point 7 and 15 are presented in Figure E-2 to Figure E-5 respectively Table E-1 and Table E-2.

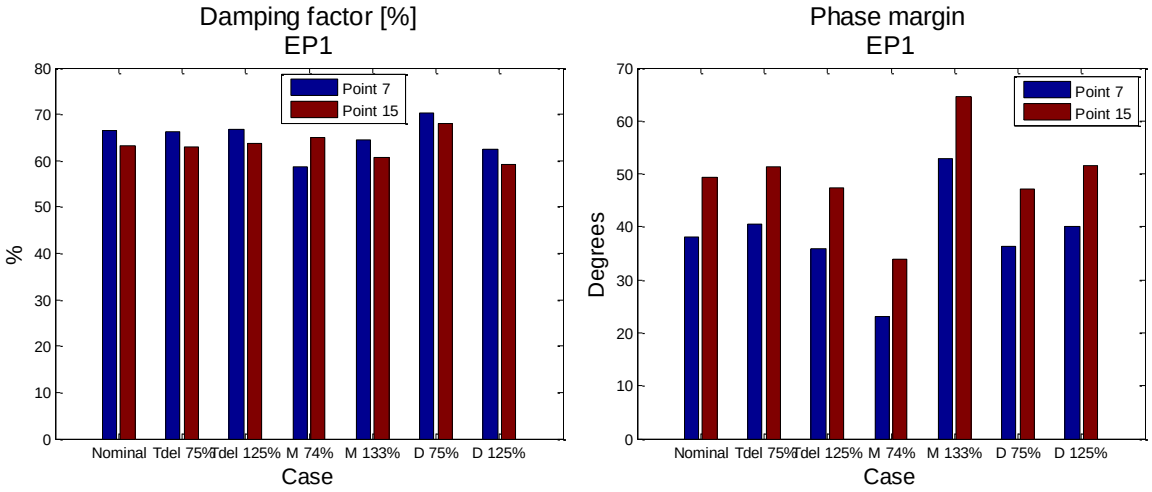


Figure E-2: Damping factor and phase margin for the two selected points for EP1.

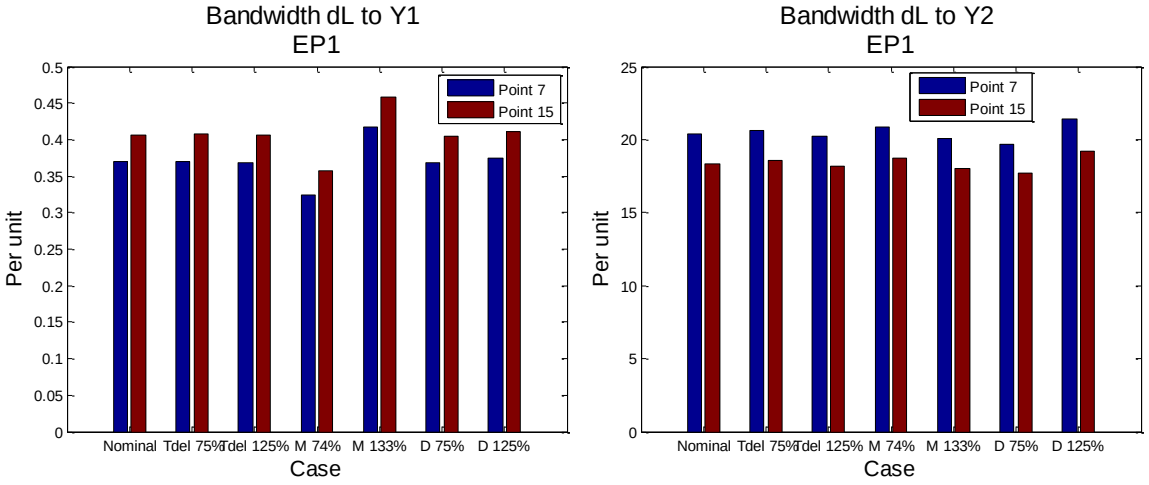


Figure E-3: Bandwidth from load disturbance to conventional control signal Y_1, left plot, and to modified control signal Y_2, right plot. Values are in per unit.

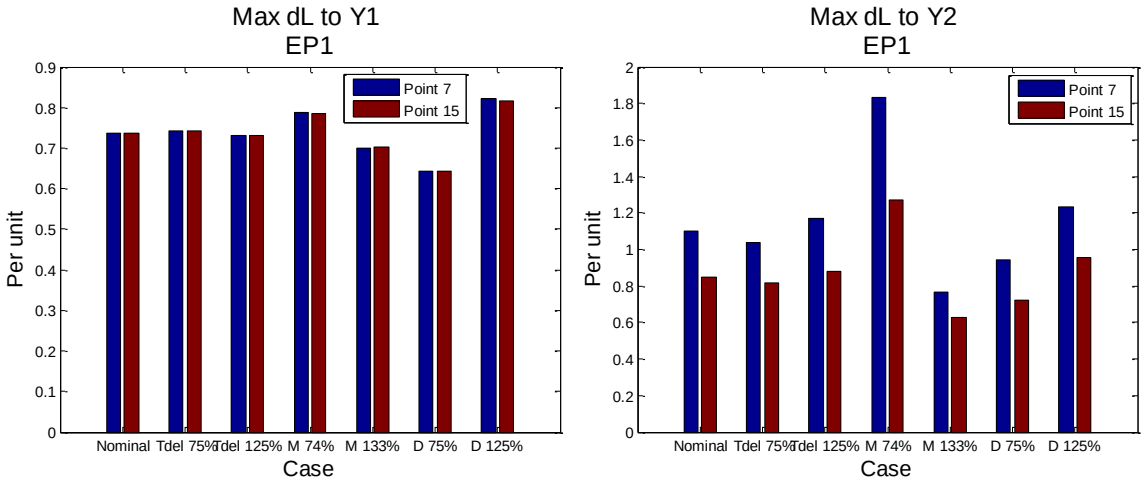


Figure E-4: Max gain from load disturbance to conventional control signal Y_1, left plot, and to modified control signal Y_2, right plot. Values are in per unit.

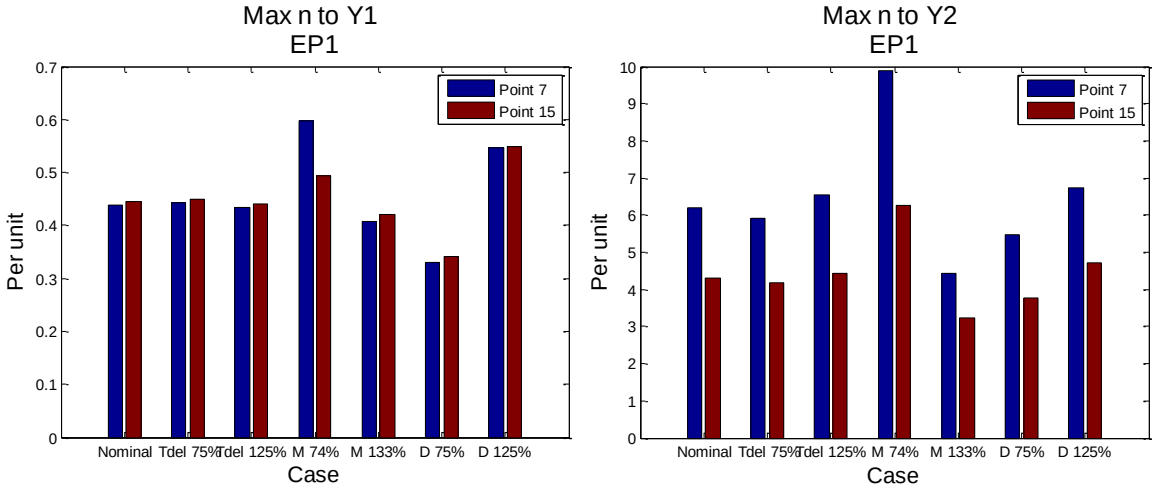


Figure E-5: Max gain from measurement noise n to conventional control signal Y_1, left plot, and to modified control signal Y_2, right plot. Values are in per unit.

The data used to generate the bar plots above are compiled in Table E-1 and Table E-2.

Table E-1: EP1-mode. Data according to set criteria for point 7.

Point 7 (EP1)								
Case	**Damping factor [%]**	$\omega_{B_{dL\rightarrow Y_1}}$ **[pu]**	$\omega_{B_{dL\rightarrow Y_2}}$ **[pu]**	$max_{dL\rightarrow Y_1}$ **[pu]**	$max_{dL\rightarrow Y_2}$ **[pu]**	$max_{n\rightarrow Y_1}$ **[pu]**	$max_{n\rightarrow Y_2}$ **[pu]**	φ_m **[°]**
Nominal	66.45	0.37	20.42	0.74	1.10	0.44	6.20	38.17
T_{del} **75%**	66.16	0.37	20.65	0.74	1.04	0.44	5.90	40.59
T_{del} **125%**	66.75	0.37	20.20	0.73	1.17	0.43	6.53	35.93
***M* 74%**	58.58	0.32	20.84	0.79	1.83	0.60	9.90	23.16
***M* 133%**	64.52	0.42	20.05	0.70	0.76	0.41	4.42	52.98
***D* 75%**	70.36	0.37	19.67	0.64	0.94	0.33	5.47	36.38
***D* 125%**	62.46	0.38	21.37	0.82	1.24	0.55	6.73	40.04
Average	**65.04**	**0.37**	**20.46**	**0.74**	**1.16**	**0.46**	**6.45**	**38.18**

Table E-2: EP1-mode. Data according to set criteria for point 15.

Point 15 (EP1)								
Case	**Damping factor [%]**	$\omega_{B_{dL\rightarrow Y_1}}$ **[pu]**	$\omega_{B_{dL\rightarrow Y_2}}$ **[pu]**	$max_{dL\rightarrow Y_1}$ **[pu]**	$max_{dL\rightarrow Y_2}$ **[pu]**	$max_{n\rightarrow Y_1}$ **[pu]**	$max_{n\rightarrow Y_2}$ **[pu]**	φ_m **[°]**
Nominal	63.30	0.41	18.37	0.74	0.85	0.44	4.31	49.29
T_{del} **75%**	62.98	0.41	18.56	0.74	0.82	0.45	4.19	51.29
T_{del} **125%**	63.62	0.41	18.18	0.73	0.88	0.44	4.43	47.36
***M* 74%**	64.97	0.36	18.76	0.78	1.27	0.49	6.25	33.95
***M* 133%**	60.81	0.46	18.00	0.70	0.63	0.42	3.25	64.60
***D* 75%**	68.02	0.41	17.70	0.64	0.72	0.34	3.77	47.11
***D* 125%**	59.20	0.41	19.22	0.82	0.95	0.55	4.71	51.53
Average	**63.27**	**0.41**	**18.40**	**0.74**	**0.87**	**0.45**	**4.42**	**49.30**

Weighing all the data together it was decided that point 15 was a more appropriate choice. The frequencies of point 15 and corresponding leadlag-parameters are presented in Table E-3.

Table E-3: EP1-mode. Leadlag-parameter settings of selected point.

Parameter (EP1)	**Point 15**
ω_1	0.01
ω_2	0.15
ω_3	0.5
K	0.6470
β	0.0667
τ_D	100
τ_I	0.2061
γ	0.1030

Time domain EP1

Time simulated plots with a sinusoidal disturbance signal of amplitude 50 MW and frequencies 1/30 Hz, 1/60 Hz, respectively 1/90 Hz. The upper plot displays the grid frequency response and the lower plot displays generated power, solid lines left axis, and control signals, dashed lines right axis.

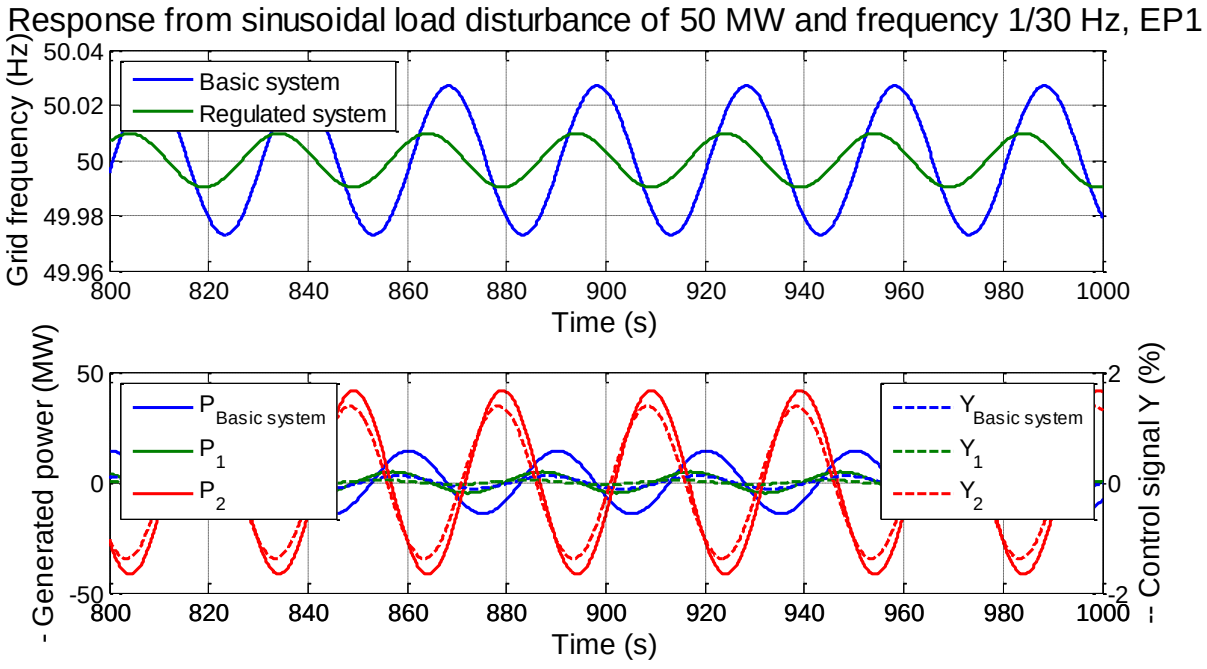


Figure E-6: Time simulation response when system excited with load disturbance of amplitude 50 MW and frequency 1/30 Hz. The upper plot displays the grid frequency response and the lower plot the generated power, solid line left axis, and control signals, dashed lines right axis.

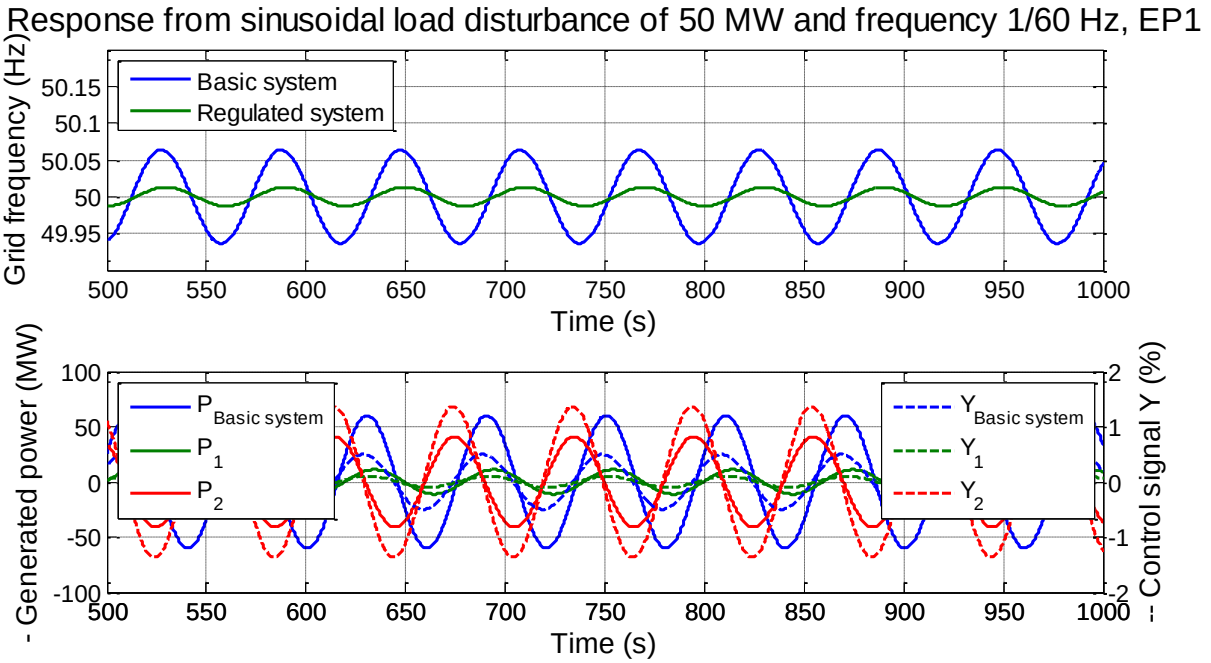


Figure E-7: Time simulation response when system excited with load disturbance of amplitude 50 MW and frequency 1/60 Hz. The upper plot displays the grid frequency response and the lower plot the generated power, solid line left axis, and control signals, dashed lines right axis.

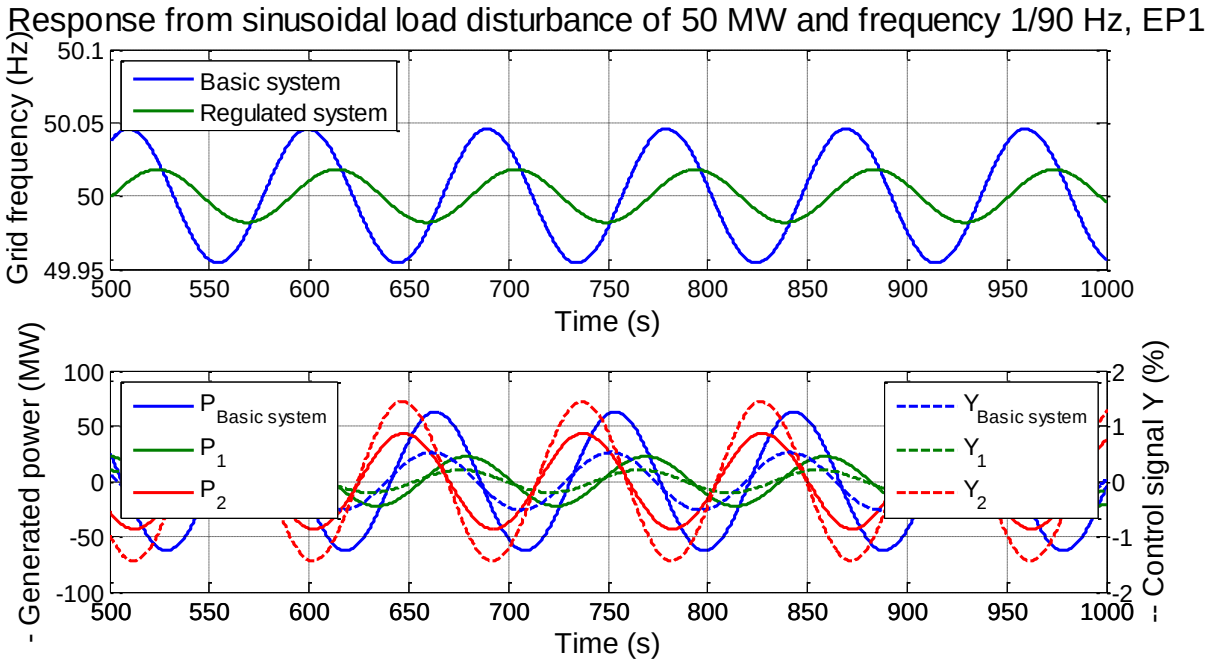


Figure E-8: Time simulation response when system excited with load disturbance of amplitude 50 MW and frequency 1/90 Hz. The upper plot displays the grid frequency response and the lower plot the generated power, solid line left axis, and control signals, dashed lines right axis.

APPENDIX F: Analysis Results EP2

Frequency domain EP2

Figure F-1 shows the results for the EP2-mode, where the upper plot in the figure displays the damping factor, solid line, and the bandwidth from d_L to Y_2, dashed line. The lower plot displays the graphs for max peaks from d_L to Y_2, solid line, and maximum peaks from the measurement noise n to Y_2, dashed lines. Note that the lower plot has two y-axes.

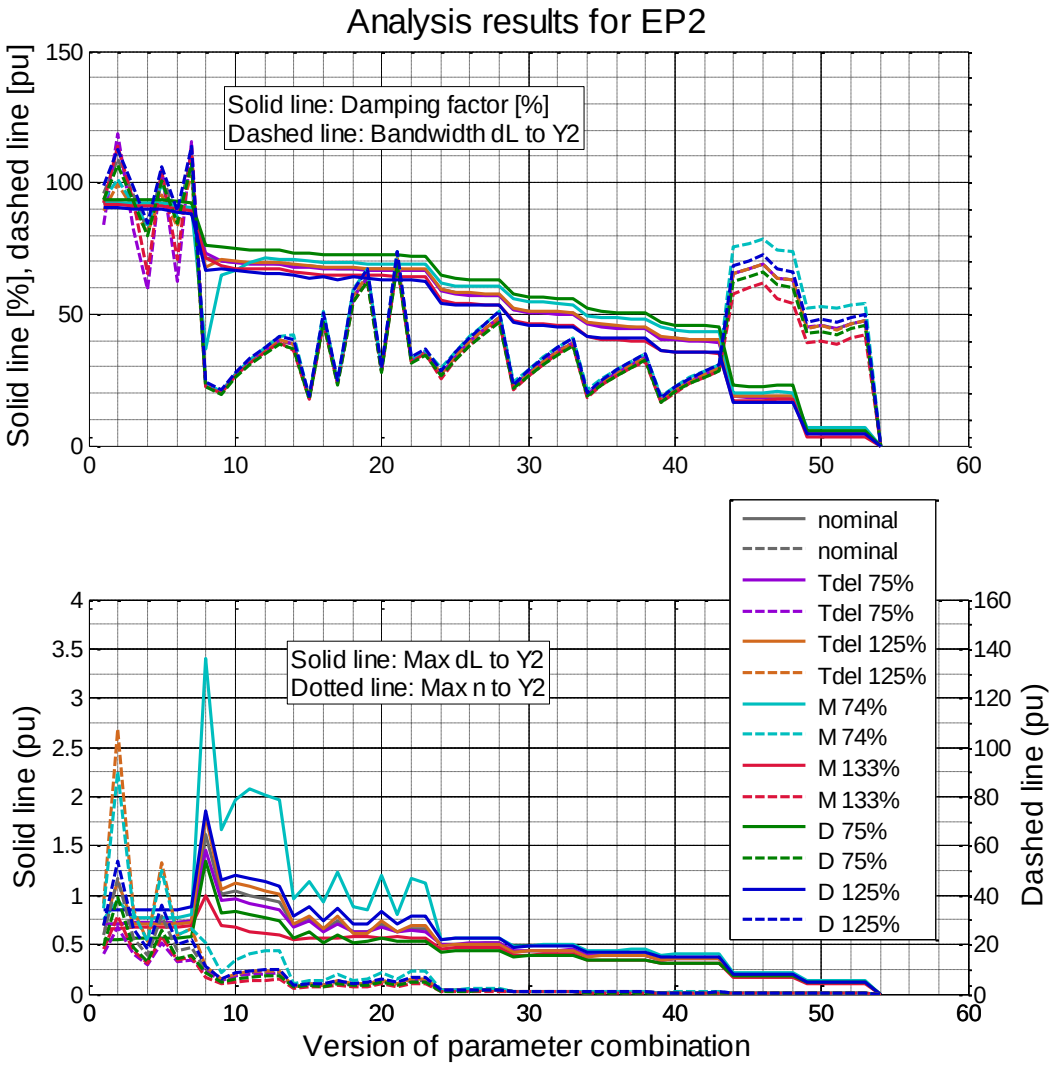


Figure F-1: Results from simulations using EP-mode EP2. The solid lines in the upper subplot are graphs of the damping factor and the dashed lines are graphs of the bandwidth from the load disturbance d_L to the control signal Y_2 from the leadlag-controller.

The solid lines in the lower subplot are related to the left y-axis and are graphs of the max peaks from d_L to Y_2. The dashed lines are related to the right y-axis and are graphs of maximum peaks from the measurement noise n to Y_2. The legend belongs to both subplots and what case the different line colors represents.

To maximize the damping factor and minimize the other criteria two sets of leadlag-parameters were chosen for the example with EP-mode 2, point 9 and point 15.

The complete individual data of point 7 and 15 are presented in Figure F-2 to Figure F-5 respectively Table F-1 and Table F-2.

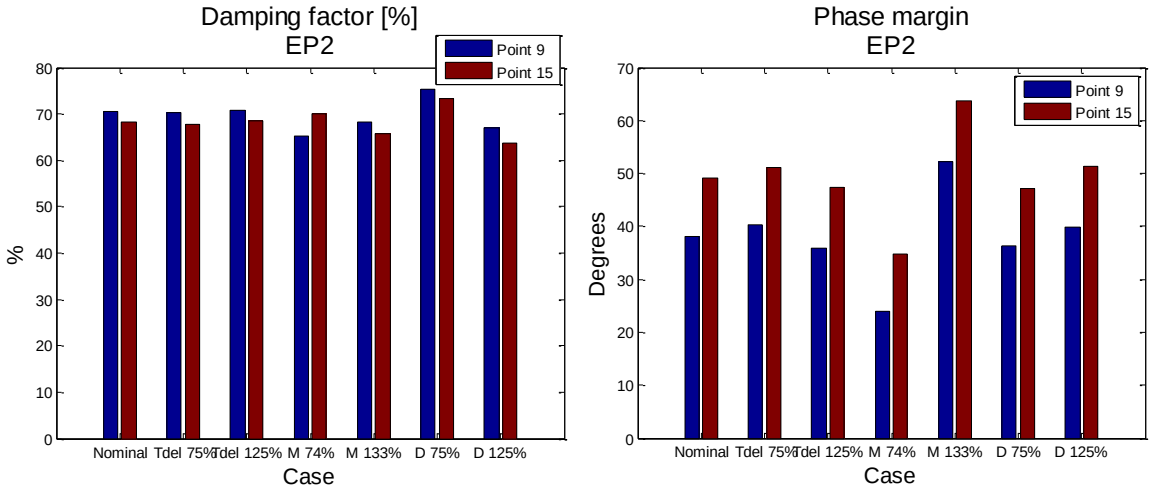


Figure F-2: Damping factor and phase margin for the two selected points for EP2.

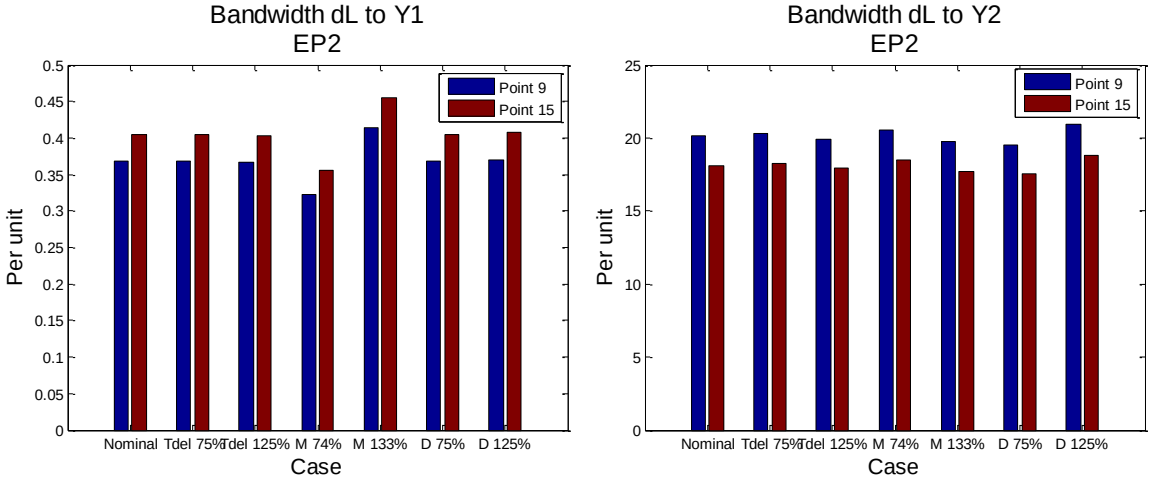


Figure F-3: Bandwidth from load disturbance to conventional control signal Y_1, left plot, and to modified control signal Y_2, right plot. Values are in per unit.

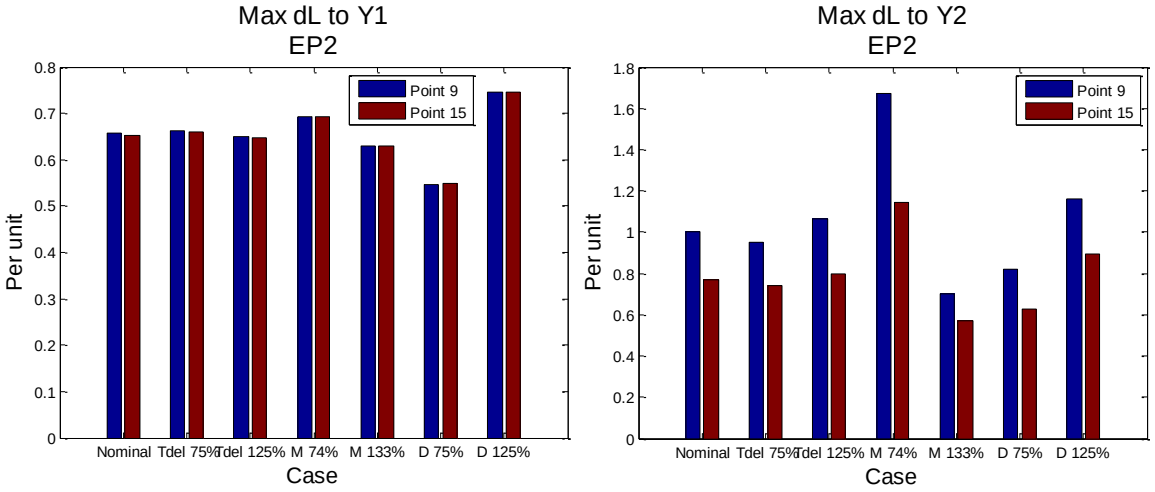


Figure F-4: Max gain from load disturbance to conventional control signal Y_1, left plot, and to modified control signal Y_2, right plot. Values are in per unit.

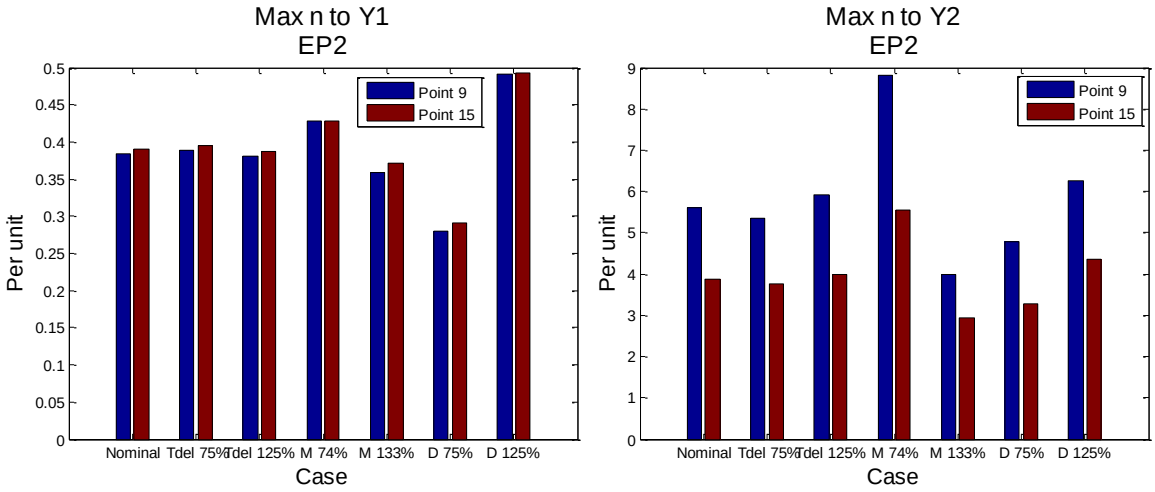


Figure F-5: Max gain from measurement noise n to conventional control signal Y_1, left plot, and to modified control signal Y_2, right plot. Values are in per unit.

The data used to generate the bar plots above are compiled in Table F-1 and Table F-2.

Table F-1: EP2-mode. Data according to set criteria for point 9.

Point 9 (EP2)								
Case	**Damping factor [%]**	$\omega_{B_{dL\rightarrow Y_1}}$ **[pu]**	$\omega_{B_{dL\rightarrow Y_2}}$ **[pu]**	$max_{dL\rightarrow Y_1}$ **[pu]**	$max_{dL\rightarrow Y_2}$ **[pu]**	$max_{n\rightarrow Y_1}$ **[pu]**	$max_{n\rightarrow Y_2}$ **[pu]**	φ_m **[°]**
Nominal	70.51	0.37	20.13	0.66	1.00	0.38	5.62	38.07
T_{del} **75%**	70.19	0.37	20.33	0.66	0.95	0.39	5.35	40.23
T_{del} **125%**	70.83	0.37	19.93	0.65	1.07	0.38	5.93	35.91
***M* 74%**	65.13	0.32	20.55	0.69	1.67	0.43	8.83	23.89
***M* 133%**	68.21	0.41	19.75	0.63	0.70	0.36	4.00	52.22
***D* 75%**	75.39	0.37	19.50	0.55	0.82	0.28	4.77	36.33
***D* 125%**	67.00	0.37	20.95	0.75	1.16	0.49	6.27	39.85
Average	**69.61**	**0.37**	**20.16**	**0.66**	**1.05**	**0.39**	**5.82**	**38.07**

Table F-2: EP2-mode. Data according to set criteria for point 15.

Point 15 (EP2)								
Case	**Damping factor [%]**	$\omega_{B_{dL\rightarrow Y_1}}$ **[pu]**	$\omega_{B_{dL\rightarrow Y_2}}$ **[pu]**	$max_{dL\rightarrow Y_1}$ **[pu]**	$max_{dL\rightarrow Y_2}$ **[pu]**	$max_{n\rightarrow Y_1}$ **[pu]**	$max_{n\rightarrow Y_2}$ **[pu]**	φ_m **[°]**
Nominal	68.18	0.40	18.10	0.65	0.77	0.39	3.88	49.16
T_{del} **75%**	67.85	0.40	18.27	0.66	0.74	0.40	3.77	51.03
T_{del} **125%**	68.51	0.40	17.94	0.65	0.80	0.39	4.00	47.30
***M* 74%**	70.12	0.36	18.50	0.69	1.15	0.43	5.56	34.75
***M* 133%**	65.65	0.45	17.74	0.63	0.57	0.37	2.95	63.76
***D* 75%**	73.27	0.41	17.54	0.55	0.63	0.29	3.27	47.07
***D* 125%**	63.71	0.41	18.84	0.75	0.89	0.49	4.36	51.32
Average	**68.19**	**0.41**	**18.13**	**0.65**	**0.79**	**0.39**	**3.97**	**49.20**

Weighing all the data together it was decided that point 15 was a more appropriate choice. The frequencies of point 15 and corresponding leadlag-parameters are presented in Table F-3.

Table F-3: EP2-mode. Leadlag-parameter settings for selected point.

Parameter (EP2)	**Point 15**
ω_1	0.01
ω_2	0.15
ω_3	0.5
K	0.6638
β	0.0667
τ_D	100
τ_I	0.2009
γ	0.1004

Time domain EP2

Time simulated plots with a sinusoidal disturbance signal of amplitude 50 MW and frequencies 1/30 Hz, 1/60 Hz, respectively 1/90 Hz. The upper plot displays the grid frequency response and the lower plot displays generated power, solid lines left axis, and control signals, dashed lines right axis.

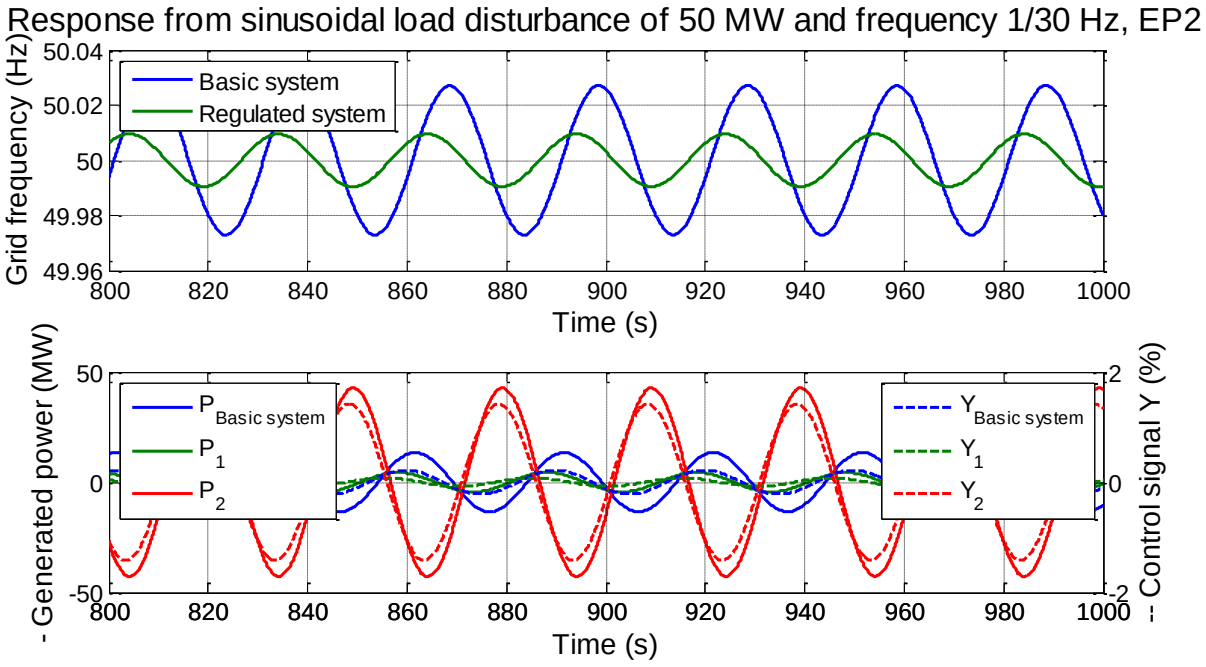


Figure F-6: Time simulation response when system excited with load disturbance of amplitude 50 MW and frequency 1/30 Hz. The upper plot displays the grid frequency response and the lower plot the generated power, solid line left axis, and control signals, dashed lines right axis.

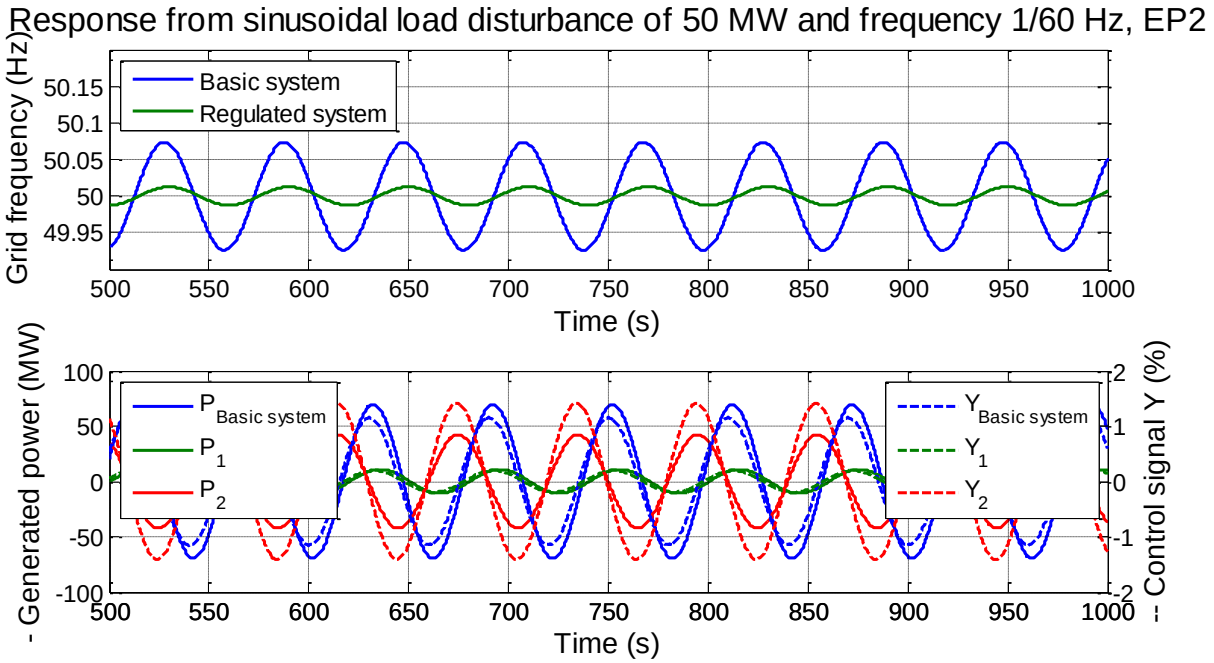


Figure F-7: Time simulation response when system excited with load disturbance of amplitude 50 MW and frequency 1/60 Hz. The upper plot displays the grid frequency response and the lower plot the generated power, solid line left axis, and control signals, dashed lines right axis.

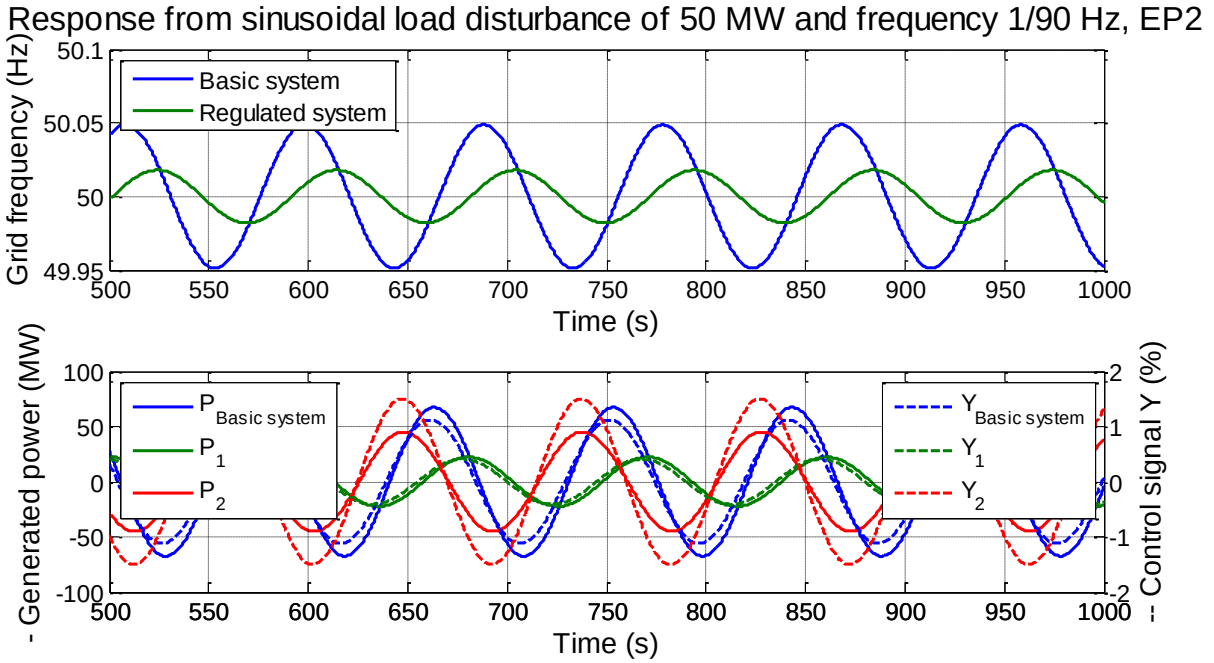


Figure F-8: Time simulation response when system excited with load disturbance of amplitude 50 MW and frequency 1/90 Hz. The upper plot displays the grid frequency response and the lower plot the generated power, solid line left axis, and control signals, dashed lines right axis.

APPENDIX G: Analysis Results EP3

Frequency domain EP3

Figure G-1 shows the results for the EP3-mode, where the upper plot in the figure displays the damping factor, solid line, and the bandwidth from d_L to Y_2, dashed line. The lower plot displays the graphs for max peaks from d_L to Y_2, solid line, and maximum peaks from the measurement noise n to Y_2, dashed lines. Note that the lower plot has two y-axes.

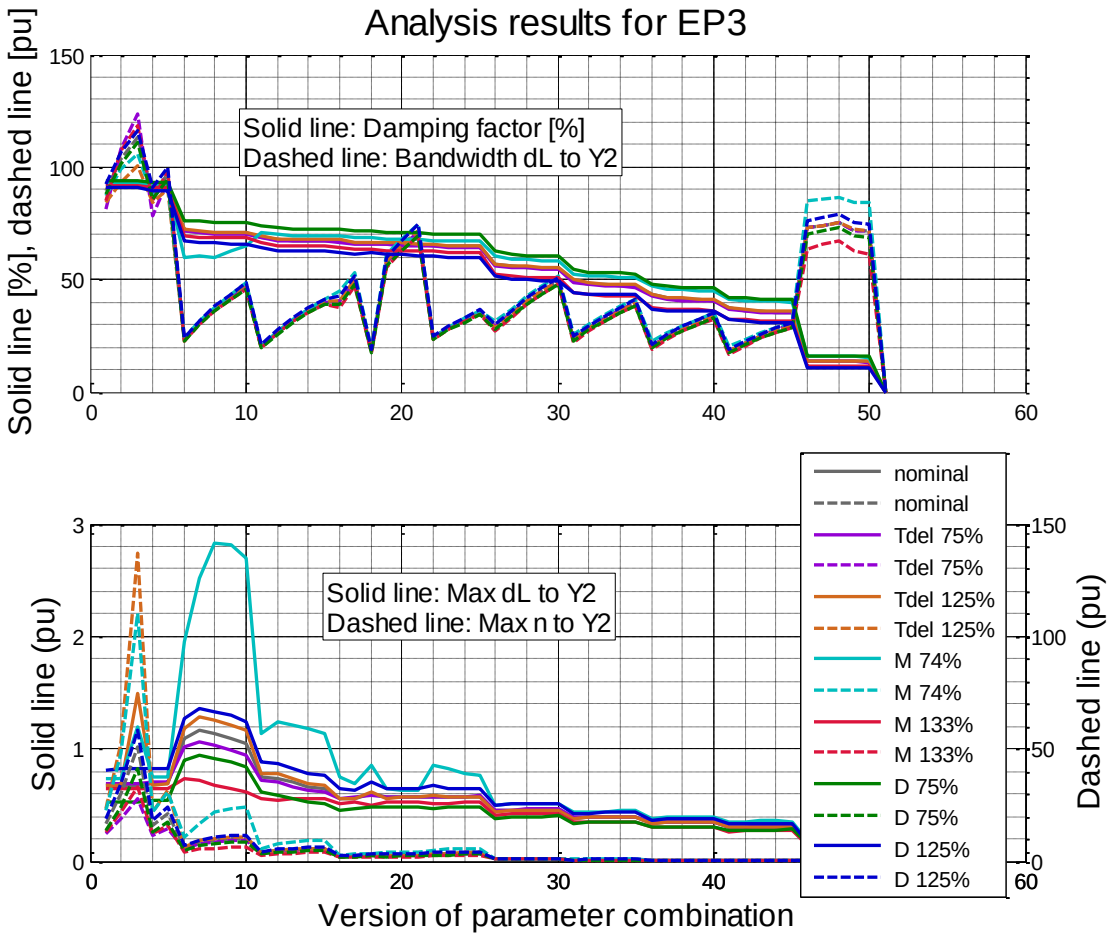


Figure G-1: Results from simulations using EP-mode EP3. The solid lines in the upper subplot are graphs of the damping factor and the dashed lines are graphs of the bandwidth from the load disturbance d_L to the control signal Y_2 from the leadlag-controller.

The solid lines in the lower subplot are related to the left y-axis and are graphs of the max peaks from d_L to Y_2. The dashed lines are related to the right y-axis and are graphs of maximum peaks from the measurement noise n to Y_2. The legend belongs to both subplots and what case the different line colors represents.

To maximize the damping factor and minimize the other criteria two sets of leadlag-parameters were chosen for the example with EP-mode 3, point 11 and point 18.

The complete individual data of point 11 and 18 are presented in Figure G-2 to Figure G-3 respectively Table G-1 and Table G-2.

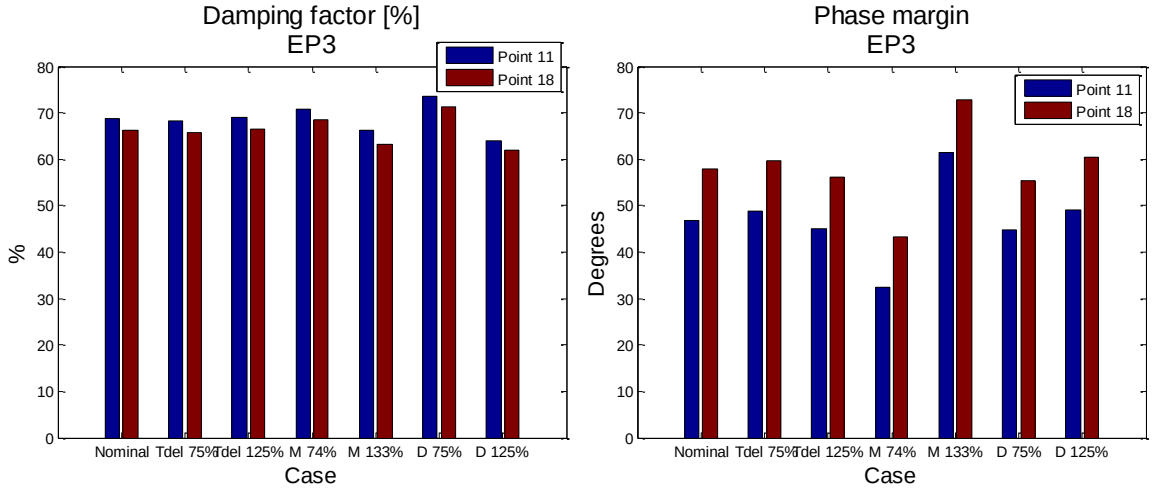


Figure G-2: Damping factor and phase margin for the two selected points for EP3.

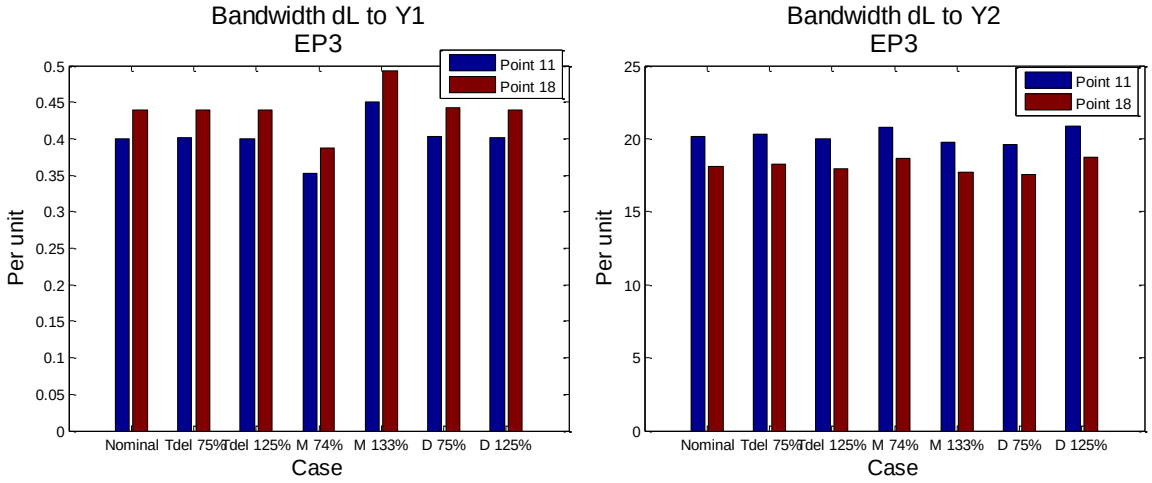


Figure G-3: Bandwidth from load disturbance to conventional control signal Y_1, left plot, and to modified control signal Y_2, right plot. Values are in per unit.

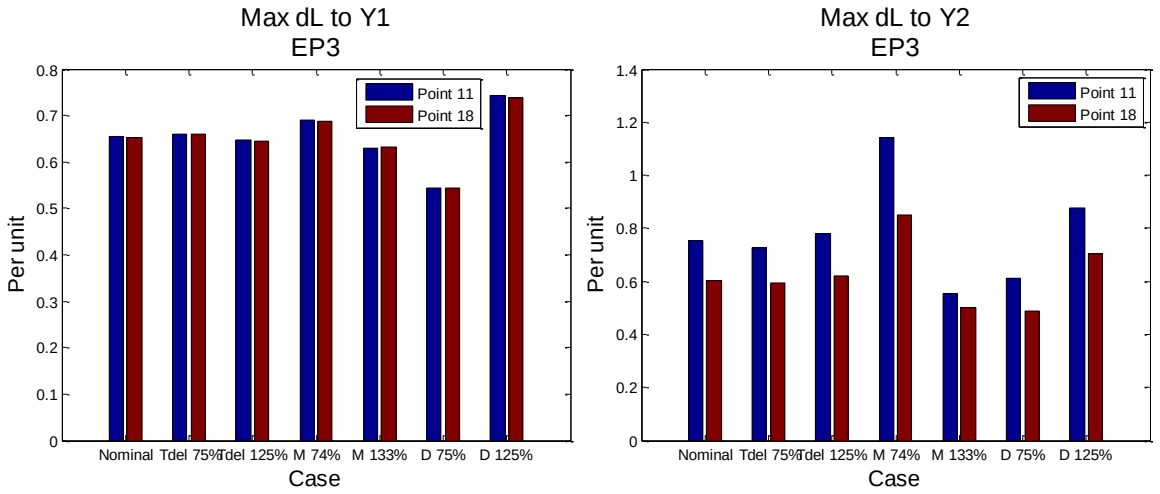


Figure G-4: Max gain from load disturbance to conventional control signal Y_1, left plot, and to modified control signal Y_2, right plot. Values are in per unit.

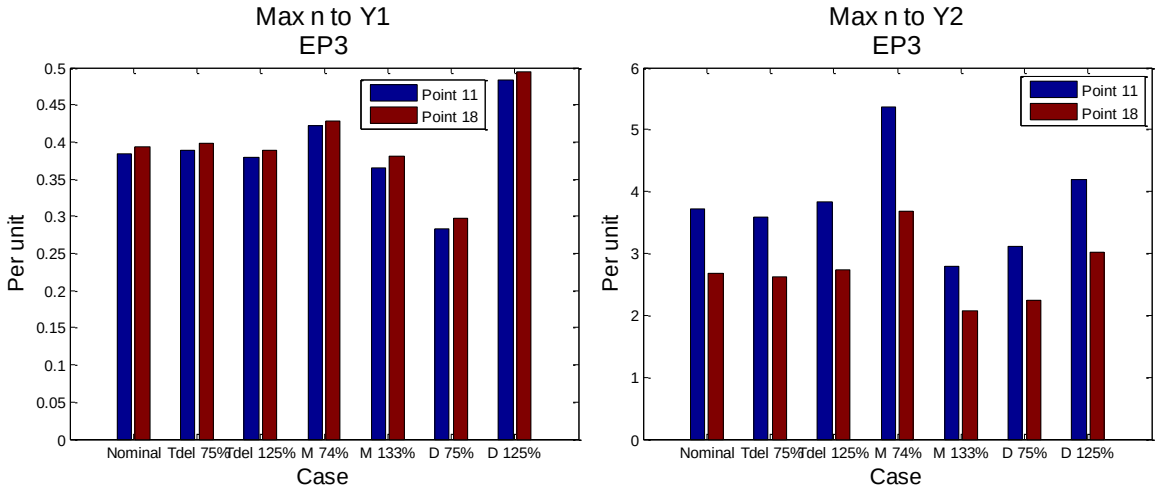


Figure G-5: Max gain from measurement noise n to conventional control signal Y_1, left plot, and to modified control signal Y_2, right plot. Values are in per unit.

The data used to generate the bar plots above are compiled in Table G-1 and Table G-2.

Table G-1: EP3-mode. Data according to set criteria for point 11.

Point 11 (EP3)								
Case	**Damping factor [%]**	$\omega_{B_{dL\rightarrow Y_1}}$ **[pu]**	$\omega_{B_{dL\rightarrow Y_2}}$ **[pu]**	$max_{dL\rightarrow Y_1}$ **[pu]**	$max_{dL\rightarrow Y_2}$ **[pu]**	$max_{n\rightarrow Y_1}$ **[pu]**	$max_{n\rightarrow Y_2}$ **[pu]**	φ_m **[°]**
Nominal	68.71	0.40	20.12	0.65	0.75	0.38	3.72	46.93
T_{del} **75%**	68.34	0.40	20.30	0.66	0.73	0.39	3.59	48.84
T_{del} **125%**	69.08	0.40	19.95	0.65	0.78	0.38	3.84	45.01
***M* 74%**	70.79	0.35	20.77	0.69	1.14	0.42	5.36	32.49
***M* 133%**	66.14	0.45	19.74	0.63	0.55	0.37	2.79	61.46
***D* 75%**	73.65	0.40	19.56	0.54	0.61	0.28	3.11	44.89
***D* 125%**	64.02	0.40	20.86	0.74	0.88	0.48	4.19	49.01
Average	**68.68**	**0.40**	**20.19**	**0.65**	**0.78**	**0.39**	**3.80**	**46.95**

Table G-2: EP3-mode. Data according to set criteria for point 18.

Point 18 (EP3)								
Case	**Damping factor [%]**	$\omega_{B_{dL\rightarrow Y_1}}$ **[pu]**	$\omega_{B_{dL\rightarrow Y_2}}$ **[pu]**	$max_{dL\rightarrow Y_1}$ **[pu]**	$max_{dL\rightarrow Y_2}$ **[pu]**	$max_{n\rightarrow Y_1}$ **[pu]**	$max_{n\rightarrow Y_2}$ **[pu]**	φ_m **[°]**
Nominal	66.22	0.44	18.08	0.65	0.60	0.39	2.68	57.93
T_{del} **75%**	65.83	0.44	18.23	0.66	0.59	0.40	2.62	59.58
T_{del} **125%**	66.61	0.44	17.94	0.65	0.62	0.39	2.74	56.28
***M* 74%**	68.59	0.39	18.68	0.69	0.85	0.43	3.68	43.20
***M* 133%**	63.34	0.49	17.71	0.63	0.50	0.38	2.08	72.89
***D* 75%**	71.31	0.44	17.58	0.54	0.49	0.30	2.25	55.44
***D* 125%**	62.02	0.44	18.75	0.74	0.70	0.49	3.03	60.50
Average	**66.27**	**0.44**	**18.14**	**0.65**	**0.62**	**0.40**	**2.73**	**57.97**

Weighing all the data together it was decided that point 18 was a more appropriate choice. The frequencies of point 18 and corresponding leadlag-parameters are presented in Table G-3.

Table G-3: EP3-mode. Leadlag-parameter settings for selected point.

Parameter (EP3)	**Point 18**
ω_1	0.01
ω_2	0.15
ω_3	0.5
K	0.6034
β	0.0667
τ_D	100
τ_I	0.2210
γ	0.1105

Time domain EP3

Time simulated plots with a sinusoidal disturbance signal of amplitude 50 MW and frequencies 1/30 Hz, 1/60 Hz, respectively 1/90 Hz. The upper plot displays the grid frequency response and the lower plot displays generated power, solid lines left axis, and control signals, dashed lines right axis.

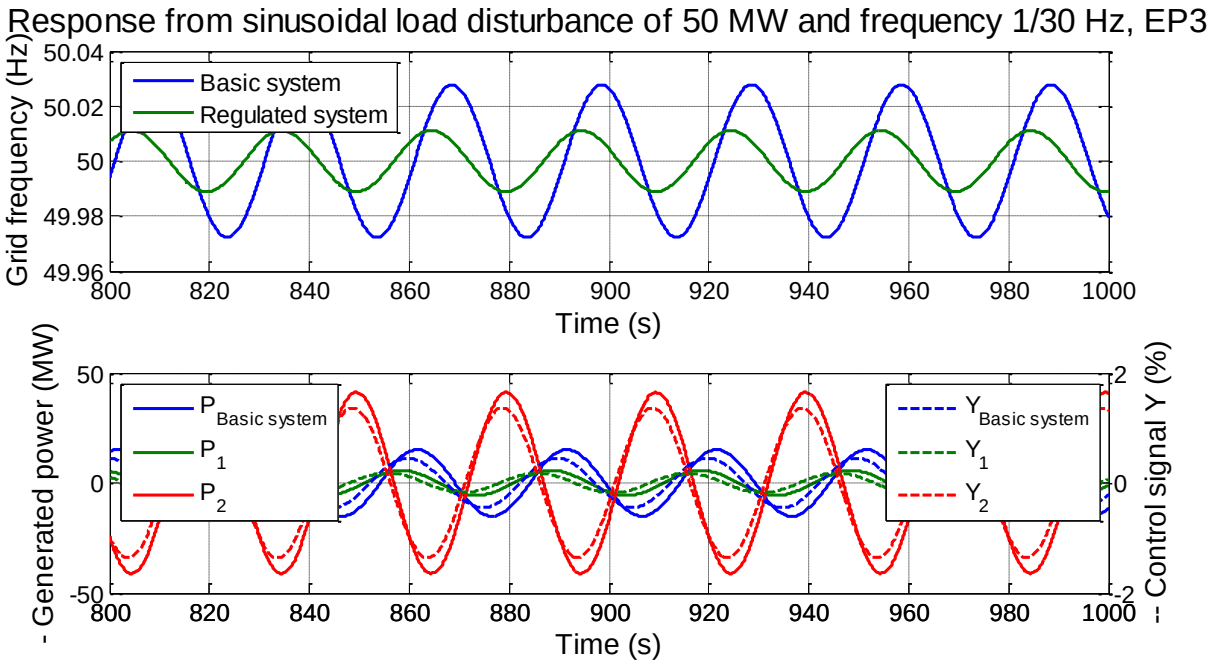


Figure G-6: Time simulation response when system excited with load disturbance of amplitude 50 MW and frequency 1/30 Hz. The upper plot displays the grid frequency response and the lower plot the generated power, solid line left axis, and control signals, dashed lines right axis.

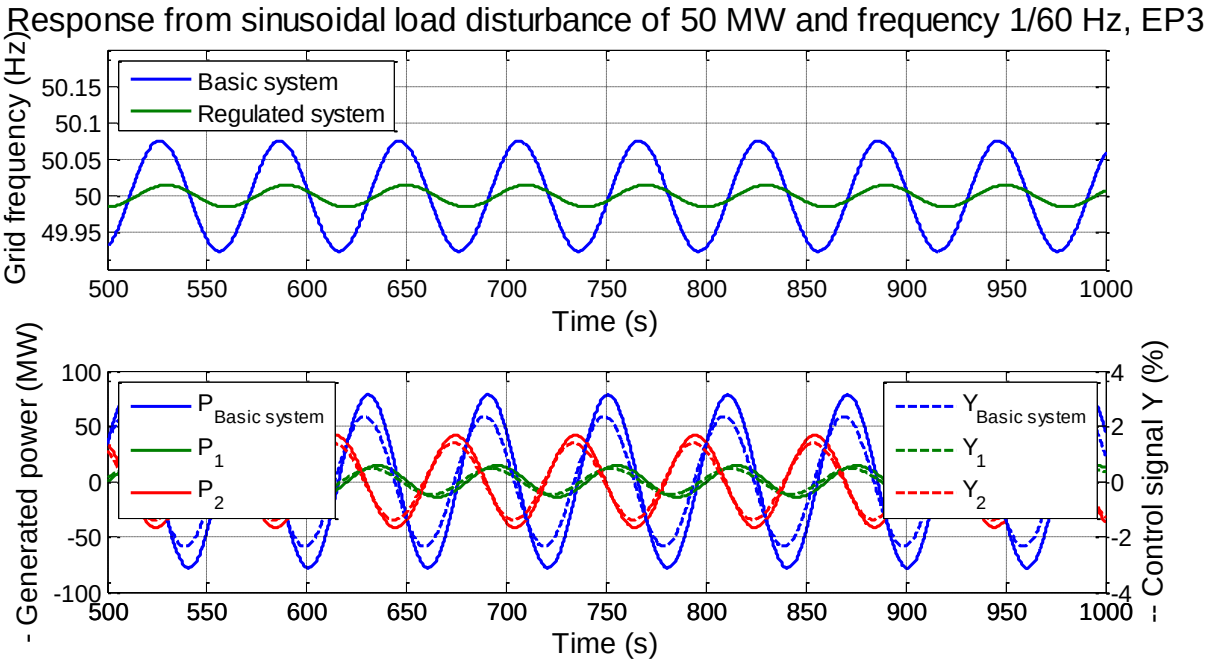


Figure G-7: Time simulation response when system excited with load disturbance of amplitude 50 MW and frequency 1/60 Hz. The upper plot displays the grid frequency response and the lower plot the generated power, solid line left axis, and control signals, dashed lines right axis.

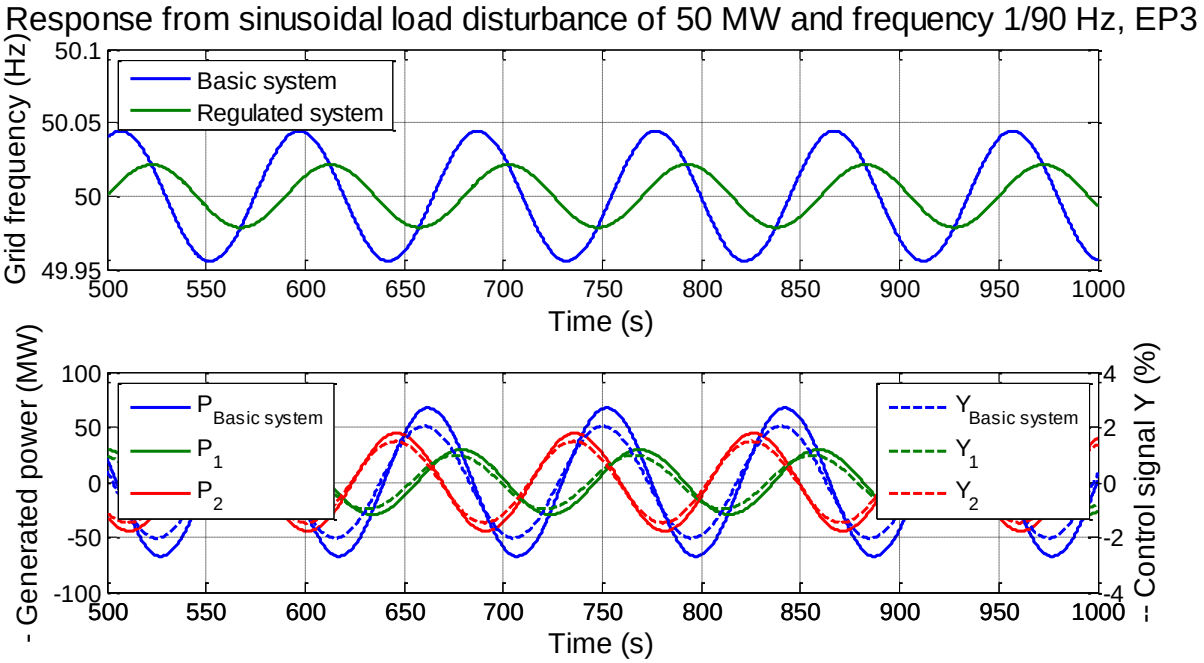


Figure G-8: Time simulation response when system excited with load disturbance of amplitude 50 MW and frequency 1/90 Hz. The upper plot displays the grid frequency response and the lower plot the generated power, solid line left axis, and control signals, dashed lines right axis.